

Review

Open Access



# Boosting VOCs elimination by coupling different techniques

Rebecca El Khawaja<sup>1</sup>, Savita Kaliya Perumal Veerapandian<sup>6</sup>, Rim Bitar<sup>6</sup>, Nathalie De Geyter<sup>6</sup>, Rino Morent<sup>6</sup>, Nicolas Heymans<sup>4</sup>, Guy De Weireld<sup>4</sup>, Tarek Barakat<sup>3</sup>, Yang Ding<sup>3</sup>, Grèce Abdallah<sup>2,6</sup>, Shilpa Sonar<sup>2,6</sup>, Axel Löfberg<sup>2</sup>, Jean-Marc Giraudon<sup>2</sup>, Christophe Poupin<sup>1</sup>, Renaud Cousin<sup>1</sup>, Fabrice Cazier<sup>5</sup>, Dorothée Dewaele<sup>5</sup>, Paul Genevray<sup>5</sup>, Yann Landkocz<sup>1</sup>, Clémence Méausoone<sup>1</sup>, Nour Jaber<sup>1</sup>, Dominique Courcot<sup>1</sup>, Sylvain Billet<sup>1</sup>, Jean-François Lamonier<sup>2,\*</sup> , Bao-Lian Su<sup>3,\*</sup> , Stéphane Siffert<sup>1,\*</sup>

<sup>1</sup>Univ. Littoral Côte d'Opale, U.R. 4492, Unit of Environmental Chemistry and Interactions with Living Organisms (UCEIV), SFR Condorcet FR CNRS 3417, Dunkerque F-59140, France.

<sup>2</sup>Univ. Lille, CNRS, Centrale Lille, Univ. Artois, UMR 8181, Unité de Catalyse et Chimie du Solide (UCCS), Lille F-59000, France.

<sup>3</sup>Univ. Namur, Namur Institute of Structured Matter (NISM), Laboratory of Inorganic Materials Chemistry, B-5000, Belgium.

<sup>4</sup>Univ. Mons, Thermodynamics and Mathematical Physics Unit, Mons B-7000, Belgium.

<sup>5</sup>Univ. Littoral Côte d'Opale, CCM, Centre Commun de Mesures, Dunkerque F-59140, France.

<sup>6</sup>Univ. Ghent, Research Unit Plasma Technology (RUPT), Department of Applied Physics, Ghent 9000, Belgium.

**\*Correspondence to:** Prof. Stéphane Siffert, Univ. Littoral Côte d'Opale, U.R. 4492, Unit of Environmental Chemistry and Interactions with Living Organisms (UCEIV), SFR Condorcet FR CNRS 3417, Dunkerque F-59140, France. E-mail: siffert@univ-littoral.fr; Prof. Jean-François Lamonier, Univ. Lille, CNRS, Centrale Lille, Univ. Artois, UMR 8181, Unité de Catalyse et Chimie du Solide (UCCS), Lille F-59000, France. E-mail: jean-francois.lamonier@univ-lille.fr; Prof. Bao-Lian Su, Univ. Namur, Namur Institute of Structured Matter (NISM), Laboratory of Inorganic Materials Chemistry, B-5000, Belgium. E-mail: bao-lian.su@unamur.be

**How to cite this article:** El Khawaja R, Veerapandian SKP, Bitar R, Geyter ND, Morent R, Heymans N, Weireld GD, Barakat T, Ding Y, Abdallah G, Sonar S, Löfberg A, Giraudon JM, Poupin C, Cousin R, Cazier F, Dewaele D, Genevray P, Landkocz Y, Méausoone C, Jaber N, Courcot D, Billet S, Lamonier JF, Su BL, Siffert S. Boosting VOCs elimination by coupling different techniques. *Chem Synth* 2022;2:13. <https://dx.doi.org/10.20517/cs.2022.10>

**Received:** 28 Apr 2022 **First Decision:** 25 May 2022 **Revised:** 13 Jun 2022 **Accepted:** 24 Jun 2022 **Published:** 30 Jun 2022

**Academic Editor:** Ying Wan **Copy Editor:** Peng-Juan Wen **Production Editor:** Peng-Juan Wen

## Abstract

Volatile Organic Compounds (VOCs) are known to be hazardous and harmful to human health and the environment. In mixtures or during repeated exposures, significant toxicity of these compounds in trace amounts has been revealed. *In vitro* air-liquid interface approaches underlined the interest in evaluating the impact of repeated VOC exposure and the importance of carrying out a toxicological validation of the techniques in addition to the standard chemical analyses. The difficulties in sampling and measuring VOCs in stationary source emissions are due to both the complexity of the mixture present and the wide range of concentrations. The coupling of VOC



© The Author(s) 2022. **Open Access** This article is licensed under a Creative Commons Attribution 4.0 International License (<https://creativecommons.org/licenses/by/4.0/>), which permits unrestricted use, sharing, adaptation, distribution and reproduction in any medium or format, for any purpose, even commercially, as long as you give appropriate credit to the original author(s) and the source, provide a link to the Creative Commons license, and indicate if changes were made.



treatment techniques results in efficient systems with lower operating energy consumption. Three main couplings are outlined in this review, highlighting their advantages and relevance. First, adsorption-catalysis coupling is particularly valuable by using adsorption and catalytic oxidation regeneration initiated, for example, by selective dielectric heating. Then, several key aspects of the plasma catalysis process, such as the choice of catalysts suitable for the non-thermal plasma (NTP) environment, the simultaneous removal of different VOCs, and the in situ regeneration of the catalyst by NTP exposure, are discussed. The adsorption-photocatalysis coupling technology is also one of the effective and promising methods for VOC removal. The VOC molecules strongly adsorbed on the surface of the photocatalyst can be directly oxidized by the photogenerated hole on the photocatalyst (e.g.,  $\text{TiO}_2$ ).

**Keywords:** VOC removal, adsorption materials, coupling techniques, catalysis, plasma, photocatalysis

## INTRODUCTION

According to World Health Organization (WHO), air pollution is responsible for one out of every nine premature deaths, or more than seven million deaths each year<sup>[1]</sup>. Residential, industrial, agricultural, and road transportation activities are the most important anthropogenic sources of air pollution. Many pollutants are now found in higher concentrations in indoor air than in outdoor air. This is especially concerning because humans spend over 80% of their time in enclosed spaces such as their homes, means of transportation, and workplaces. Volatile organic compounds (VOCs) are a type of gaseous air pollution. VOCs are harmful to human health and the environment, and they play a role in climate change. On an industrial level, the current policy for reducing VOC emissions prioritizes the total or partial substitution of VOCs used at the source. However, when this substitution is not possible due to technical constraints, it is required to develop alternative methods that are suitable for low VOC concentrations, have high energy efficiency, and allow for the entire treatment without the generation of by-products. To address this industrial issue, new innovative treatment methods adapted to the industry and based on the coupling of methods are required.

First, adsorption and catalytic technologies are often not very effective in removing low-level VOCs from off-gases when they are used separately. Indeed, after a period of use, an adsorbent becomes saturated and must be regenerated. The corresponding catalytic treatment results in high energy consumption at low VOC concentrations. An innovative approach combining both techniques can be proposed. The original process is based on the selective adsorption of the pollutant coupled with a catalytic oxidation process. The adsorption will remove the VOCs present in low concentrations in the air, and the final removal of the pollutant is done during the adsorbent regeneration step. Indeed, during this stage, the high concentration of VOCs in the effluent allows the catalytic oxidation process to be used under optimal conditions. Two tracks are considered: in the first one, the adsorption is done on an adsorbent and the oxidation during the desorption step is done on a catalyst (existing process). In the second, more innovative one, the same material is used successively as an adsorbent and then as a catalyst at higher temperatures.

Second, the use of non-thermal plasma (NTP) is attracting increased attention in the field of air purification, particularly for the removal of low concentration VOCs from industrial and/or indoor air. This treatment at room temperature and atmospheric pressure is very attractive because conventional technologies typically require a lot of energy to reach operating temperature. However, studies have shown that industrial implementation of this technology is hampered by three main drawbacks: (1) formation of unwanted by-products; (2) relatively poor energy efficiency; and (3) low degradation. To overcome these problems, the combination of heterogeneous catalysis with a non-thermal plasma can be proposed. By combining the advantages of the two processes, an efficient VOC removal process is expected.

Finally, photocatalysis is based on the principle of activation of a semiconductor using the energy provided by light. The adsorption of a photon forms an electron-hole pair that allows the formation of free radicals, which react with the VOCs to transform them into CO<sub>2</sub> and water. One of the main advantages of photocatalysis is being able to work at room temperature and thus be free of any thermal inertia. The photocatalytic reactor consists of a UV lamp surrounded by transparent substrates coated with a thin layer of the selected photocatalyst and allowing the passage and treatment of the gas flow. To optimize the operation of the reactor, it is preceded by adsorption, which traps and concentrates the VOCs. The VOCs are then periodically desorbed by heating and directed to the photocatalytic reactor, thus regenerating the adsorption column.

Some conditions need to be taken into consideration when working on a large industrial scale. The process needs to be studied from physical, legal, and economical points of view. The implemented process should be optimized while considering the feasibility of scaling it from the laboratory scale. In addition, the physicochemical properties of the materials should be deeply studied in harsh conditions. The regeneration of the materials is also thought through to keep a highly efficient and eco-friendly process. Despite being emitted at low concentrations, a mixture of VOCs is expected to be found in industrial emissions. Hence, the catalytic activity of the materials is important; more precisely, it needs to selectively convert the VOC into H<sub>2</sub>O and CO<sub>2</sub>, without leading to new problems such as the formation of by-products, adding to the maintenance cost.

In this review, we devote part of this paper to the toxicology of these VOCs, followed by a section on their measurement, which is often difficult, especially when they are in complex mixtures (industrial emissions). We also discuss how these VOCs are really measured on industrial sites. The treatment techniques are presented next, using the combinations of adsorption-catalysis, plasma catalysis, and adsorption-photocatalysis.

## TOXICITY AND MEASUREMENTS OF VOCs

### Volatile organic compounds

Before starting, it is important to know that the physico-chemical characteristics that define VOCs depend on the organisms, and there are several definitions of this family of chemicals. However, most definitions agree on the presence of the molecule in vapor form under standard conditions of temperature and pressure.

According to the United States Environmental Protection Agency (US-EPA), volatile organic compounds are any compound of carbon, excluding carbon monoxide, carbon dioxide, carbonic acid, metallic carbides, or carbonates and ammonium carbonate, which participates in atmospheric photochemical reactions, except those designated by US-EPA as having negligible photochemical reactivity. VOCs are organic chemical compounds whose composition makes it possible for them to evaporate under normal indoor atmospheric conditions of temperature and pressure. This is the general definition of VOCs that is used in the scientific literature and is consistent with the definition used for indoor air quality. Since the volatility of a compound is generally higher the lower its boiling point temperature, the volatility of organic compounds is sometimes defined and classified by their boiling points. For its part, the European Union uses the boiling point, rather than its volatility, in its definition of VOCs. A VOC is any organic compound, excluding methane, having an initial boiling point less than or equal to 250 °C measured at a standard atmospheric pressure of 101.3 kPa. VOCs are sometimes categorized by the ease of their emission. Finally, the World Health Organization (WHO) categorizes indoor organic pollutants as very volatile organic compounds (VVOCs), VOCs, or semi-volatile organic compounds (SVOs).

The higher the volatility (the lower the boiling point), the more likely the compound will be emitted from a product or surface into the air. VOCs are so volatile that they are difficult to measure and are found almost entirely as gases in the air rather than in materials or on surfaces. The least volatile compounds found in air constitute a far smaller fraction of the total present indoors, while the majority will be in solids or liquids that contain them or on surfaces including furnishings and building materials.

VOCs are widely used and produced at home or by industry. VOCs form families of pollutants, including the series of aromatic hydrocarbons that are higher homologs of benzene, known as BTEX (benzene, toluene, ethylbenzene, and m/p/o-xylene), aldehydes (such as formaldehyde, acrolein, and crotonaldehyde), and chloride compounds (such as trichloroethylene). VOCs represent a class of pollutants of interest due to their abundance in the ambient and indoor atmospheres, deleterious effects on public health, and function in atmospheric chemistry<sup>[2]</sup>. Sources are numerous and include vehicle exhaust, petrol stations, industrial activity, landfills and waste treatment plants, and combustion for domestic heating<sup>[2]</sup>. In addition, VOCs are widely used in many consumer products such as paints, varnishes, permanent felts, correction products (Tipp-Ex), glues, shoe polish, leather cleaners, solvents, and detergents. They can also be emitted by the use of other products, such as printers, photocopiers, *etc.*<sup>[3,4]</sup>. Smoking is also an important source of VOCs such as BTEX, trimethylbenzene, and naphthalene, as shown by several metrological studies conducted in Spain and Texas, before and after the ban on smoking in public places<sup>[5,6]</sup>.

#### *Health effects of VOCs*

Air pollution constitutes a mixture that exposes the respiratory system where gas exchanges with the body take place. Since they evaporate easily at room temperature, human exposure to airborne VOCs is inevitable. Early studies reported associations between respiratory symptoms and sources of indoor air pollution. Then, with the development of specific instruments to better quantify indoor air quality, researchers were able to analyze the association between respiratory symptoms and direct measurements of pollutants. The first indoor pollutants associated with respiratory effects were dust allergens, NO<sub>2</sub>, and fine particles. More recently, VOCs, emitted from various sources and suspected of being irritants, have been independently associated with short- and long-term respiratory symptoms. They have a short half-life in the body, but their exposure is recurrent and ubiquitous. Numerous VOCs are individually known to be toxic. Some are classified as carcinogenic or reprotoxic at the European level or by the WHO. Since 1993, benzene has been classified as a Group 1 carcinogen by the International Agency for Research on Cancer (IARC) and has been linked to non-malignant hematological disorders (thrombocytopenia, leucopenia, or anemia), and it has a role in the occurrence of leukemia and/or non-Hodgkin's lymphoma<sup>[7]</sup>. Formaldehyde causes cancer of the nasopharynx and leukemia (Group 1)<sup>[8]</sup>. Trichloroethylene causes cancer in the kidney (Group 1)<sup>[9]</sup>. Acrolein is probably carcinogenic to humans (Group 2A)<sup>[10]</sup>. Ethylbenzene and crotonaldehyde are possibly carcinogenic to humans (Group 2B). Xylenes are not classifiable (Group 3)<sup>[10]</sup>. Toluene is likely to harm the fetus (H304) and is classified as a Category 2 reproductive toxicant by the EU following studies showing effects on fetal development in animals, in particular delayed growth and skeletal development. In humans, the intentional inhalation of large quantities of toluene is thought to harm the fertility of female drug users, embryonic development<sup>[11]</sup>, and the regulatory mechanisms of the endocrine system<sup>[12]</sup>.

The health effects attributed to VOCs mainly concern the respiratory tract and the lungs, which are preferential target organs for gases and aerosols, but also the central nervous system (CNS)<sup>[3,13,14]</sup>. Indeed, some VOCs, such as BTEX, easily cross the blood-brain barrier<sup>[15]</sup>. Furthermore, a review of the literature on BTEX suggests the presence of endocrine mechanisms underlying many effects related to BTEX exposure, while they have generally only been assessed as potential carcinogens<sup>[16]</sup>.

Concerning respiratory effects, epidemiological investigations have shown in children aged 6 months to 3 years and 5 to 11 years a significant relationship between pulmonary exposure to benzene and an increase in certain inflammatory diseases such as asthma, bronchitis, and morning cough after adjustment for other pollutants<sup>[17,18]</sup>. Exposure to a benzene concentration of 10  $\mu\text{g}/\text{m}^3$  would triple the risk of developing asthma in children. The significant impact of a 10  $\mu\text{g}/\text{m}^3$  increase in exposure to toluene, ethylbenzene, and *m*-xylene on the development of asthma has also been shown, with odds ratios of 1.84, 2.54, and 1.61, respectively, after adjustment for co-exposures<sup>[18]</sup>. A French case-control study found that toluene exposure was significantly associated with the induction of asthma in urban and rural children<sup>[19]</sup>. In Portugal, increased levels of individual and mixed endocrine disruptors were found in classrooms with more children with respiratory symptoms<sup>[20]</sup>. In this study, the authors concluded that even low levels of exposure can increase the risk of asthma and respiratory symptoms. Regarding VOCs in mixtures, in a cross-sectional survey of 490 French dwellings, the Indoor Air Quality Observatory (OQAI) showed that co-exposure to the BTEX + styrene mixture and exposure to undecane and trimethylbenzene were associated with asthma risk<sup>[21]</sup>. In America, the association between exposure to BTEX and asthma prevalence was previously observed in adults ( $\text{OR} = 1.63$ )<sup>[22]</sup> and in children ( $\text{OR} = 1.27$ )<sup>[23]</sup>. The latter study also showed a significant association between exposure to pollutants including BTEX and the frequency of the following symptoms: cough and chronic phlegm, bronchitis, persistent wheezing, and shortness of breath<sup>[23]</sup>. Respiratory symptoms include the occurrence of rhinitis associated with ethylbenzene, *o*-xylene, and trichloroethylene<sup>[21]</sup>.

### *Toxicity of VOCs*

#### Experimental methods for studying toxicity

When identifying the mechanisms of action of a toxic agent, one of the first questions to ask is the choice of study model. Obviously, even if most studies are conducted in experimental models, the purpose of all toxicological research is to protect humans from the effects of the toxic substances that surround them. Consequently, this research must not be limited to the consideration and sometimes the inactivation of pathophysiological mechanisms in cell cultures or laboratory animals. The toxicologist must, therefore, constantly be confronted with the validation of their study model and the demonstration of its relevance, particularly when the general public asks him, sometimes naively, if their observations can be extrapolated to humans.

According to the classic hypothesis of the complementarity of study models, the predictability of measured effects decreases proportionally with the scale of observation. Exposed human populations, such as those presented in the previous paragraph, would thus be the models of choice, as their predictability for the whole species is almost absolute. This assertion can be verified when individuals potentially sensitive to the harmfulness of xenobiotics are included in the exposed population groups for reasons of age, pregnancy, or pre-existing pathology. Several ethical, moral, and scientific considerations obviously prevent their use in identifying mechanisms of toxicity, although humans are not necessarily excluded from toxicological studies. By way of illustration, the development of a drug escapes these limitations and notably includes tests on a limited number of healthy volunteers during the first phase of clinical trials. In this way, not only is the distribution of the product in the body assessed, but also its toxicity, via the search for possible negative reactions. In environmental and occupational toxicology, recourse to human exposure remains rare. One of the main challenges scientists face in understanding the toxicity of pollution is the complexity of actual exposure. People are not exposed to one or two pollutants but a mixture of very different molecules present in varying doses.



To individualize the mechanisms of action of each of the pollutants, several experimental methods can be used. The strong point of experimentation is to have complete control of the exposure parameters in terms of toxicant, dose, and duration of exposure on the one hand and homogeneity of the exposed living model on the other hand. Among these methods, the oldest are animal experiments. These methods are called *in vivo*. Healthy animals of the same age and sex are divided into groups and subjected to various exposure conditions. Homogeneity is important, and exposure to the pollutant should be the only difference between the groups. These methods allow the acute and chronic toxicity of pollutants to be assessed for extrapolation to humans. The advantage of *in vivo* models is that they integrate all the potential effects of a toxicant and its metabolites in a physiological context. Thus, for example, the interactions between organs are preserved. However, many precautions must be taken in the transposition of cross-species data. Several parameters, such as the choice of species, the mode of administration, and the exposure window, must be taken into consideration when using data from *in vivo* studies. The selection of an animal model can thus lead to under- or overestimations of the dangers for humans. These studies provide a wealth of information (see, e.g., the reviews on the toxicity of trichloroethylene, dichloroethane, benzene, toluene, xylenes, and formaldehyde<sup>[24-30]</sup>). However, these studies have their limitations, including the cost, the number of animals sacrificed, and the difficulty of transferring the effects of the animal model to humans.

### Non-animal methods

Once the cells have been selected, they must be exposed, i.e., brought into contact with the toxicant. The emergence of alternative models such as *in vitro* toxicology, which are becoming more and more efficient, makes it possible to fill certain gaps and particularly to test more exposure conditions. More than a century after the beginnings of cell culture, there is now a large number of cell lines or primary cultures that can be acquired from cell banks. Faced with this variety, it is necessary to choose the right cell strain to carry out one's research. Researching the mechanisms of action of atmospheric pollutants needs to focus on cells from the human respiratory system.

In the literature, two main methods of exposing cell culture to a gas mixture exist: the cells can either be immersed in the culture medium in which the mixture bubbles or grown on an insert<sup>[31]</sup>. In a submerged exposure system, cells are placed in the growth medium. This method simplifies the experimental procedure and is less expensive than the system using inserts<sup>[32]</sup>. However, this system may generate inaccuracies in the assessment of the toxicity of gas mixtures as it allows interactions between the tested chemicals and the components of the medium. Moreover, the actual exposure concentration is difficult to assess. The relevance of this system is limited to compounds soluble in the medium, which restricts its use. The physiology of respiratory cells is not respected. It is important to maintain the lung cells at the interface between air, representing the alveolar lumen, and a liquid, corresponding to the lung tissue. *In vitro* exposure methods to gas mixtures should allow the closest possible contact between the cells and the compounds being tested. In addition, a humidified atmosphere must be maintained to avoid drying out the cells<sup>[33]</sup>. These requirements are met by air-liquid interface (ALI) exposure systems. Grown on inserts, cells are fed and hydrated by the culture medium on the basolateral side and exposed on the apical side<sup>[34]</sup>. ALI insert culture models promote the differentiation of epithelial cells. The cell layer produced by this method is very similar to the epithelial morphology of the airway *in vivo*<sup>[35]</sup>. Although these systems are expensive in terms of equipment, they have the advantage of eliminating any direct interaction between the tested toxicants and the components of the culture medium.

Direct and dynamic exposure of human cells to chemicals in the atmosphere can be achieved using the ALI exposure device Vitrocell<sup>®</sup><sup>[36]</sup>. We have set up this system in the laboratory to test the toxicity of single and

mixed VOCs, such as benzene, toluene, ethylbenzene, xylene, trimethylbenzene, and formaldehyde, as well as the products formed during the catalytic degradation of these VOCs.

Catalytic oxidation is indeed an effective technique to remediate industrial VOC emissions. Catalysis aims at degrading pollutants, but under certain conditions, it can lead to the formation of by-products. These by-products can be toxic and sometimes even more toxic than the VOCs to be removed. For example, the catalytic degradation of toluene can lead to the formation of benzene, a known carcinogen [Figure 1]<sup>[37]</sup>.

However, the performance of the catalyst is assessed by measuring VOC conversion or CO<sub>2</sub> emissions, but rarely according to by-product formation. The combination of an ALI exposure device and the catalyst test gives us the opportunity to realize an untargeted toxicological validation of the catalyst. Moreover, the use of a biological system allows the consideration of synergies and competition between the toxic effects of VOCs and emitted by-products.

### Toxicity of acute exposure to VOCs

In the various projects, the objective of the toxicology part was, first of all, to know the toxicity of the VOCs measured in an industrial environment, and then to characterize the potential impact on human health of the emissions of various catalytic systems designed for the oxidation of these VOCs. As toluene is one of the model solvents, most studies have then focused on the assessment of its toxicity and that of its products formed by catalytic oxidation. In this way, we firstly assessed the toxicity of toluene and particularly the activation of the mechanisms involved in its biotransformation by cytochromes P450<sup>[37]</sup>. We were then able to couple the cell exposure system to the Pd/ $\gamma$ -Al<sub>2</sub>O<sub>3</sub> catalyst formulated for the catalytic degradation of toluene [Figure 2]<sup>[38]</sup>. This allowed us to test the degradation efficiency of this catalytic system. Indeed, the development of catalysts relies on the measurement of some known products, such as water and carbon dioxide, plus benzene in the case of toluene degradation. However, the formation of by-products is rarely studied. Besides, it is important that these by-products should not have higher toxicity than the initial VOCs.

After exposing the cell cultures for 1 h to the more or less diluted catalyst effluent, different toxicity markers were measured. Firstly, we did not identify any impact in terms of cell death. Secondly, the measurement of gene expression in the exposed cells showed an induction of xenobiotic metabolizing enzymes (XME) such as cytochromes P450. These enzymes have a certain substrate specificity, and the results show that the effluents of the tested catalysts contained small amounts of polycyclic organic compounds of the PAH type. By measuring the activation of XMEs classically induced by polycyclic organic compounds, as well as the activation of AhR, in lung cells exposed to emissions from the catalytic degradation of toluene, we could thus suggest the formation of high molecular weight compounds that may confer residual toxicity to the catalyst emissions [Figure 3]<sup>[39]</sup>. These compounds were not detected in the routine micro-GC analysis used in the chemical optimization of catalyst systems. This hypothesis supports the scientific relevance of using toxicological evaluation in the development of chemically and toxicologically efficient catalysts. Using dedicated by-product identification analyses, four- and five-ring PAHs were identified.

### Toxicity of repeated exposure to VOCs

The VOC toxicity study was conducted after acute and repeated exposure, i.e., human lung cell cultures were exposed to diluted VOCs for 1 h per day for 1-5 consecutive days<sup>[40]</sup>. Our study was the first to carry out repeated exposure to VOCs. Only this repeated exposure allowed the detection of CYP1A1 gene

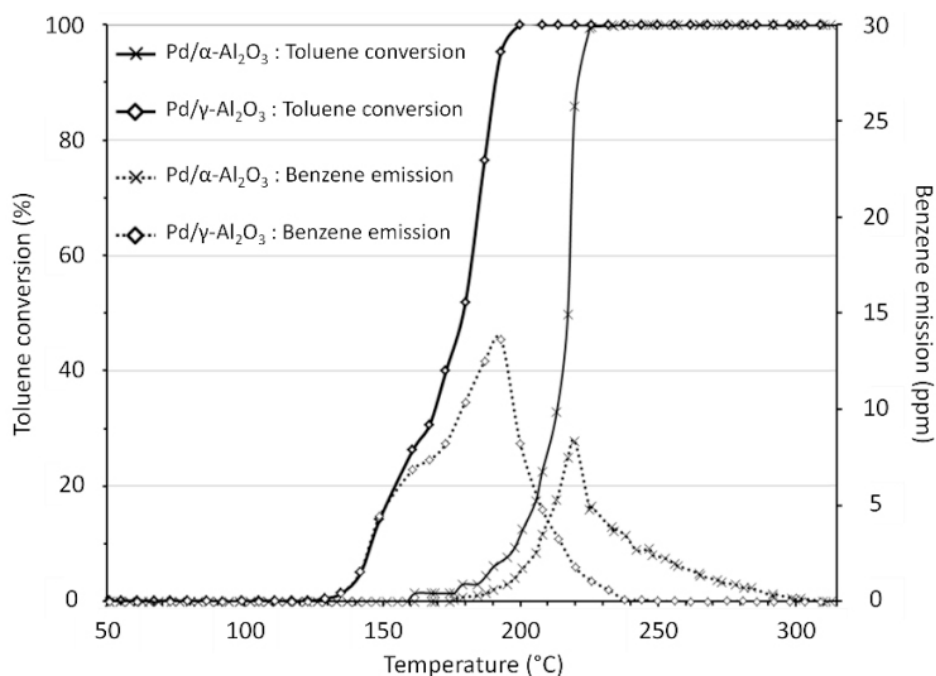


**Figure 1.** Light-off curves of  $\text{Al}_2\text{O}_3$  catalysts impregnated by Pd and production of benzene versus temperature. The dotted lines correspond to the benzene production (in ppm) as a function of the toluene light-off curve<sup>[37]</sup>.

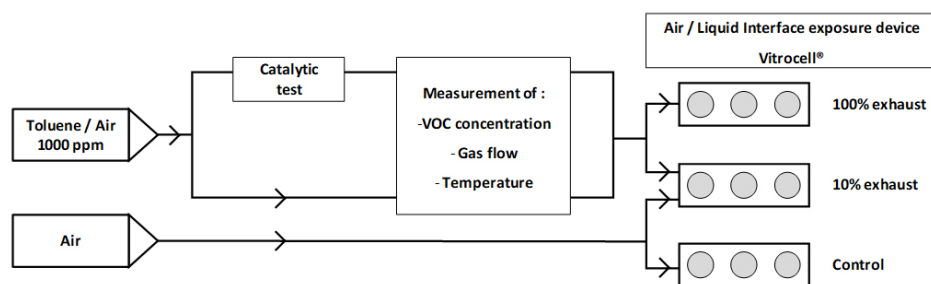


**Figure 2.** Experimental setup of the coupling of the cell exposure system to the catalyst formulated for the catalytic degradation of toluene<sup>[38]</sup>.

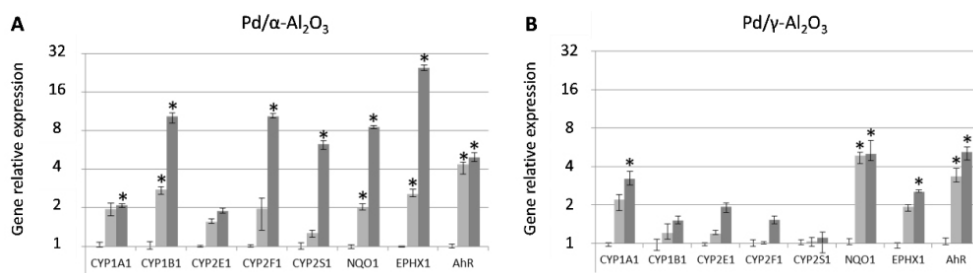


**Figure 3.** XMEs (CYP1A1, CYP1B1, CYP2E1, CYP2F1, CYP2S1, NQO1, and EPHX1) and AhR receptor in A549 cells exposed for 1 h to the emission of the catalytic degradation of toluene by  $\text{Pd}/\alpha\text{Al}_2\text{O}_3$  (A) and  $\text{Pd}/\gamma\text{Al}_2\text{O}_3$  (B) at 10% (100 ppm, light grey) or 100% (1000 ppm, dark grey). Gene induction was measured by RT-qPCR ( $n = 3$ ) and analyzed by  $\Delta\Delta\text{Ct}$  method<sup>[39]</sup> using air-exposed cells as reference and 18S as a normalization gene. Data are shown as median RQ values vs. controls and interquartile range. Significant up- or down-expression was considered if RQ was  $> 2.0$  or  $< 0.5$ , respectively.



induction, which was not previously shown in the acute studies. The studied VOCs are among the most detected chemicals in the industrial partners of the project. The toxicity of toluene homologs was studied to evaluate their substitution in industrial processes. The cellular exposure concentrations retained correspond to the regulatory doses (8 h and 15 min French Occupational Exposure Limit Values, i.e., 20 and 100 ppm). Toxic effects were assessed through parameters of cytotoxicity, inflammatory response, and gene expression of XMEs. Exposure of BEAS-2B cells to toluene and its higher homologs revealed the involvement of compound-specific metabolic pathways. Therefore, we were able to identify the different expression profiles of these four molecules despite their structural homology [Table 1]. As expected, CYP2E1 gene expression was significantly induced after cell exposure to benzene, with significant expression from Day 3 onwards. This induction corresponds to the known mechanism by which benzene is oxidized to its first metabolite, 1,2-epoxybenzene<sup>[41-43]</sup>. This ring oxidation is characteristic of benzene. This transformation was expected for its higher homologs. However, a decrease in CYP2E1 expression over time upon exposure to toluene and *m*-xylene may be related to the activation of secondary biotransformation pathways in BEAS-2B cells. A significant induction of IL-6 was also observed, with a higher concentration for xylene than for the other molecules. Using a proteomic analysis of bronchial cells exposed to toluene at 20 ppm, 3325 proteins were analyzed, of which 2423 were quantified. The statistical analysis allowed the identification of overexpressed proteins involved in metabolism pathways, amino acid and antibiotic biosynthesis, cell-cell adhesion, and defense against oxidative stress.

Non-cancerous human bronchial cells were also exposed to the by-products of the catalytic degradation of toluene under subacute conditions to assess the repeated exposure of people. The cellular response to toluene exposure was evaluated at the cytotoxic, gene expression, and protein levels, highlighting the advantages of applying repeated exposure protocols compared to classic toxicology approaches<sup>[44]</sup>. These results provide a reference for the assessment of cellular exposures to products of catalyst operation.

In addition, the toxicology study again suggested the identification of chemically undetected by-products. The measured XME gene induction was not only due to the presence of unconverted toluene and benzene by-product. It also revealed the presence of other by-products of catalytic oxidation, such as PAHs, not detected by the standard analytical method used for catalyst development. The repeated exposure mode allowed us to reveal the presence of very low levels of by-products due to the delayed expression of genes, such as those of the CYP1A1 and ALDH families. Consequently, this ALI *in vitro* approach underlined, on the one hand, the value of assessing the impact of repeated exposure to VOCs and, on the other hand, the relevance of performing toxicological validation of catalysts in addition to standard chemical analysis. This approach was therefore also followed to assess the toxicity of formaldehyde and the products of its treatment by photocatalysis. This showed an alteration of the aldehyde metabolism pathways even at very low concentrations of exposure.

### VOCs emission measurements

The difficulties in the measurement of VOCs in industrial emissions are due to the complexity of the mixtures and the extent of the ranges of concentrations encountered. Emitted VOC mixtures can contain saturated or unsaturated hydrocarbons, benzene rings, chlorinated hydrocarbons, esters, ketones, alcohols, and amines, as shown in Table 2<sup>[45]</sup>. The quantity emitted can range from ppb to whole percentages, which means that major and trace compounds may have to be measured simultaneously. To these difficulties are added the conditions of temperature, pressure, humidity, and dustiness to which VOCs will be subjected during their emission. All these conditions and difficulties lead to sampling trains and/or analyses, which are described below. We also focus on the so-called channeled emissions.

**Table 1. Relative expression of XME-encoding genes after exposure of BEAS-2B cells to benzene, toluene, m-xylene, or mesitylene for 1 h/day for five days**

| Days    | Benzene<br>20 ppm |   |   | Benzene<br>100 ppm |   |   | Toluene<br>20 ppm |   |   | Toluene<br>100 ppm |   |   | m-Xylene<br>20 ppm |   |    | m-Xylene<br>100 ppm |   |    | Mesitylene<br>20 ppm |   |   | Mesitylene<br>100 ppm |   |    |
|---------|-------------------|---|---|--------------------|---|---|-------------------|---|---|--------------------|---|---|--------------------|---|----|---------------------|---|----|----------------------|---|---|-----------------------|---|----|
|         | 1                 | 3 | 5 | 1                  | 3 | 5 | 1                 | 3 | 5 | 1                  | 3 | 5 | 1                  | 3 | 5  | 1                   | 3 | 5  | 1                    | 3 | 5 | 1                     | 3 | 5  |
| CYP1A1  | =                 | = | = | =                  | + | = | =                 | = | = | =                  | = | + | =                  | = | =  | =                   | = | =  | =                    | = | = | =                     | + | =  |
| CYP1B1  | =                 | = | = | =                  | = | = | =                 | = | = | =                  | = | = | =                  | = | =  | =                   | = | =  | =                    | = | = | =                     | = | =  |
| CYP2E1  | =                 | + | + | =                  | + | + | +                 | + | = | +                  | + | + | =                  | = | =  | +                   | + | =  | =                    | + | + | =                     | + | +  |
| CYP2S1  | =                 | = | = | =                  | = | = | =                 | = | = | =                  | = | = | =                  | + | =  | =                   | + | =  | =                    | = | = | =                     | = | =  |
| CYP2F1  | =                 | = | = | =                  | = | = | =                 | = | = | =                  | = | = | =                  | = | =  | =                   | = | =  | =                    | = | = | =                     | = | =  |
| EPHX1   | =                 | + | = | =                  | + | = | =                 | = | = | =                  | = | = | =                  | = | +  | =                   | = | +  | =                    | = | = | =                     | = | +  |
| NQO1    | =                 | = | = | =                  | = | = | =                 | = | = | =                  | = | = | =                  | = | =  | =                   | = | =  | =                    | = | = | =                     | = | =  |
| GSTM1   | =                 | = | = | =                  | = | = | =                 | = | = | =                  | = | = | =                  | = | =  | =                   | = | =  | =                    | = | = | =                     | = | =  |
| DHHDH   | =                 | = | = | =                  | = | = | =                 | = | = | =                  | = | = | =                  | = | =  | =                   | = | =  | =                    | + | = | =                     | + | =  |
| ADH1A   | =                 | = | = | =                  | = | + | =                 | = | = | =                  | = | = | =                  | = | =  | =                   | = | =  | =                    | = | = | =                     | = | =  |
| ALDH2   | =                 | = | = | =                  | = | = | =                 | = | = | =                  | = | = | =                  | + | +  | =                   | + | +  | =                    | = | = | =                     | = | +  |
| ALDH3B1 | =                 | = | = | =                  | = | = | =                 | = | = | =                  | = | = | =                  | = | ++ | =                   | = | ++ | =                    | = | + | =                     | = | ++ |

Expression of the 12 genes was measured by RT-qPCR ( $n = 3$ ) and analyzed by the  $\Delta\Delta C_t$  method<sup>[39]</sup> using cells exposed to filtered air as a reference and the geometric mean  $C_t$  of 18S, GAPDH, and B2M as normalization genes (=, no significant gene expression change; -,  $RQ < 0.5$ ; +,  $RQ > 2$ ; ++,  $RQ > 4$ ).

In general, successive steps of filtration, gaseous effluent transfer via an inert line (heated or not according to the studied processes), and abatement of moisture are necessary before the actual sampling phase of the VOC, which can imply a supplementary concentration step depending on the emission levels.

Moreover, two different analytical approaches can be chosen to characterize as well as possible the compounds emitted by the process studied, depending on the target of the study and the feasibility of on-site implementation. In the first approach used, for example, to evaluate emission levels, sampling on site can be carried out, and deferred analyses will be conducted in the laboratory. The difficulty is to be representative of the process during the sampling. This will also create additional problems with packaging, transport, and conservation (conditions and duration) of the samples. In the second approach used, for example, to understand the correlation between VOC emissions and production phases, samples and analyses on-site and/or on-line can be carried out.

Before on-site measurement, documentary preparation work is necessary with at least a study of the process and the safety data sheets (SDS) of the chemicals handled, examination of the analytical reports and previous results if available, and, if relevant, the legal requirements concerning the emissions. A preliminary laboratory phase may also be conducted on raw materials (i.e., chemicals handled) in conditions close to the process to anticipate their possible discharges and

**Table 2. VOCs detected in stacks emissions of several industrial activities**

| Industrial activity   | Compounds  | Detected compounds   |
|---|--|--|
| Production of components with formophenolic resin                                   | Aldehydes<br>Phenols<br>Aromatics<br>Furans                                    | <u>Aldehydes</u> : formaldehyde, hydroxybenzaldehyde, benzaldehyde<br><u>Phenols</u> : phenol and derivated compounds<br><u>Furans</u> : benzofuran, methyl and dimethylfuran<br><u>Aromatics</u> : methylethylbenzene<br>Toluene, xylene<br>Propylbenzene<br>Trimethylbenzene<br>Tetramethylbenzene   |
| Fabrication of surfactants and detergents   | Amines<br>Oxides   | Methylamine, dimethylamine, trimethylamine<br>Ethylene and propylene oxides  |
| Synthesis of organic compounds  | Alcohols<br>Halogenated compounds<br>Aromatics                                 | <u>Alcohols</u> : methanol, ethanol<br><u>Chlorides</u> : chloromethane, dichloromethane, chloroform<br>chlorobenzene<br><u>Aromatics</u> : ethylbenzene, toluene<br>Dimethylbenzene<br>Methylethylbenzene<br>Propylbenzene  |
| Collection of biogas from buried waste (exhaust of the thermic treatment technique) | Aromatics<br>Cyclical compounds<br>Alkanes<br>Halogenated and sulfur compounds | Limonene, -pinene, cyclohexane<br>Chlorobenzene, dichlorobenzene<br>Thiophene  |
| Varnishing of metal supports (food industry, automobile)                            | Alcohols<br>Aromatics<br>Ketones   | <u>Alcohols</u> : methanol, ethanol, butanol, butoxyethanol, butoxyethoxyethanol, butylglycol acetate, methoxypropanol<br><u>Ketones</u> : methylethylketone, methylisobutylketone<br><u>Aromatics</u> : xylene<br>Methylethylbenzene<br>Propylbenzene<br>Trimethylbenzene<br>Diethylbenzene<br>Methylpropylbenzene<br>Ethylidimethylbenzene<br>Tetramethylbenzene |
| Agri-industry (odour problems)  | Sulfur compounds<br>Esters<br>Aldehydes<br>Ketones                             | <u>Sulfur compounds</u> : dimethylsulfide, dimethyldisulfide, dimethyltrisulfide, thiophene derivated compounds  |

identify relevant VOCs not announced in the SDS. This is consistent with the definition of VOCs given by the European Directive 1999/13/EC concerning the reduction of the emissions of volatile organic compounds (VOCs), which states that a “volatile organic compound” is any organic compound, excluding methane, having a vapor pressure of 0.01 kPa or more at a temperature of 293.15 K or having corresponding volatility under specific conditions of use. For our diagnosis, it concerns, in particular, the operating temperatures encountered in the process. These preliminary steps are strongly recommended based on our experience in this field. Our approach is described in [Figure 4](#).

#### Raw material analysis

To simulate the process “specific conditions of use” of VOCs, a relevant technique can be static headspace coupled to gas chromatography (GC). The detector coupled to GC can be mass spectrometry (HS-GC/MS) in the case of a complex matrix or flame ionization detector (HS-GC/FID) when the matrix contains few compounds. The basic principle of the static headspace technique (HS) is to encapsulate the matrix to analyze in a vial. As an example, a small droplet (~10-20 µL) of raw materials is sealed in a 20 mL headspace vial. The vial is then heated at a selected temperature (close to the process one or around 80 °C if the matrix is water-based), and the gas phase formed over the matrix is injected in GC. The volume injected is, for example, 1 mL. The different VOCs present in the sample are then separated by GC, and the retention time of each compound is used for their identification. In HS-GC/FID, compounds are only identified by their retention time. In HS-GC/MS, the VOCs are also analyzed by mass spectrometry, and the identification of each molecule is made by comparison between the experimental mass spectrum and the reference spectra of the NIST Library (US National Institute of Standards and Technology). The HS method has the advantage of being quite easy to implement, requiring little handling and no solvent. Its main limitation is related to the small volume of gas injected, which implies a low sensitivity. Care must be taken with the temperatures

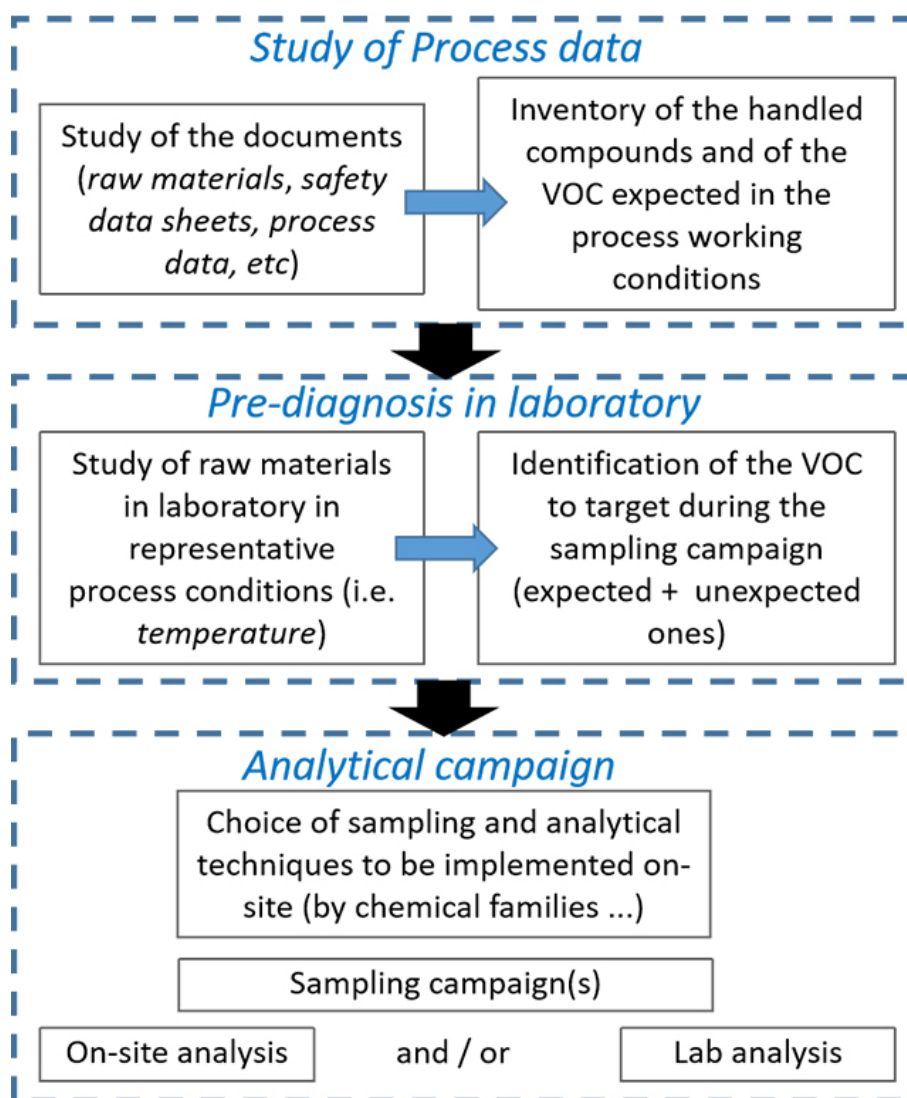


**Figure 4.** Analytical approach to perform for on-site VOCs analysis. VOCs: Volatile organic compounds.

of the HS-GC technique (vial heating, injector temperature, *etc.*) if the targeted VOCs present a risk of thermal degradation. Caution also has to be taken for VOC quantification as the gas phase can be saturated by the most volatile VOC, thus masking the less volatile ones. This phenomenon is linked to the fact that the vial is hermetically sealed which limits the volume available for the formation of the gas phase; this is not the case in the “open” operating conditions encountered in most industrial processes.

It should be noticed that HS-GC analysis does not represent the composition of the raw sample, which may contain water or non-volatile compounds, but simulates the volatile part likely to be found in the gaseous effluent. Table 3 gives an example HS-GC analysis of some raw materials analyzed at a temperature close to the process one in a metallic can production industry. Data in brackets indicate the concentration announced in the SDS.

The dynamic headspace technique may partly solve these limitations since an additional step of condensation of the extracted volatile compounds on a trap is added, which concentrates the VOC. The trap

**Table 3. Comparison of HS-GC analysis results and SDS data**

| Compounds (%)            | Varnish A     | Varnish B     | Lacquer C |
|--------------------------|---------------|---------------|-----------|
| Ethanol                  | 5 [2,5 - 10]  |               |           |
| Methyl ethyl ketone      | 91 [50 - 100] |               |           |
| Butanol                  | 2 [0 - 2,5]   | 47 [2,5 - 10] | 6         |
| Methyl isobutyl ketone   | Trace         |               |           |
| Ethyl benzene            | Trace         |               | Trace     |
| m,p-xylene               | 1             |               | Trace     |
| O-xylene                 | Trace         |               | Trace     |
| 2-butoxy ethanol         |               | 52 [2,5 - 10] | 11 [< 5]  |
| Trimethyl benzene        |               |               | 11        |
| Ethyl methyl benzene     |               |               | 1         |
| Di-isobutyl ketone       | Trace         |               |           |
| Tetramethylbenzene       |               |               | 47        |
| Indane                   |               |               | 1         |
| Diethyl benzene          |               |               | 7         |
| Dimethyl ethenyl benzene |               |               | 1         |
| Naphtalene               |               |               | 2         |
| Methyl naphtalene        |               |               | Trace     |
| 2-diméthyl-aminoéthanol  |               | [0,1 - 2,5]   |           |

can either be adsorbent or temperature-based using cryogenic fluids or “Pelletier” effect. Trace amounts of VOCs can thus be determined. The choice of the sorbent used for the trap has to be carefully considered as its selectivity among some VOCs families may become a disadvantage (untrapped types of VOCs that are thus not detected). Caution also has to be taken to avoid pollution of the trap.

#### *Choice of sampling and analytical techniques*

After the study of process data and pre-diagnosis in the laboratory by raw material analysis, the selection of the relevant sampling and analytical techniques can be made. This selection has to take into account the constraint of the site to be investigated (for example, accessibility of sampling points) and the technical capacities of the laboratory, such as the ability to perform on-site diagnosis. The range of concentrations to measure and the type of process to be investigated also have to be considered: continuous, discontinuous or cyclic phenomenon, batch production, *etc.* Moreover, the gaseous effluents to be investigated (working area, diffuse, or stack emissions) and the associated conditions (temperature, humidity, dust level, and pressure) will condition the technical choices that will be relevant for sampling and analysis.

For stack emissions, a precious help to guide the specific VOCs sampling conditions (relevant period, volume to collect, *etc.*) is to use continuous monitoring of parameters such as total hydrocarbon or combustion gases ( $O_2$ ,  $CO/CO_2$ ,  $NO_x$ , and  $SO_2$ ). Some industrial stacks are equipped with these analyzers, but they can also be implemented specially for a sampling campaign. Total organic content is measured by a flame ionization detector (FID), which often allows measuring methane hydrocarbons (MHC), non-methane hydrocarbons (NMHC), and total hydrocarbons [THC, or total organic carbon (TOC)]. This analyzer can be calibrated with methane ( $CH_4$ ) or propane ( $C_3H_8$ ) standard. Concentrations can thus be determined in methane (or propane) equivalent and then converted to carbon equivalent. Combustion gases are measured by specific analyzers based on the technique, such as paramagnetism ( $O_2$ ), IR, or UV for the other gases. The use of the data provided by these continuous monitors allows better monitoring and/or understanding of the process as one can follow in real time the emission levels. It is then possible to decide what are the relevant periods for sampling. A significant change in THC and/or combustion gas levels is

generally associated with a change in the VOC mixture composition. High levels of THC (and NMHC) will allow short samplings of VOCs to avoid, for example, saturation of absorbent or adsorbent media. Oppositely, low NMHC levels will require sampling of larger volumes of gaseous effluents to increase the concentration factors on the selected sampling media and thus improve the detection limits of the specific VOC targeted.

## Sampling

The sampling techniques can be divided into two categories: non-selective sampling with or without preconcentration (containers) and selective sampling with preconcentration using adsorbent, absorbent, impingers, *etc.* The first one has the advantage of bringing back the whole air sample to the laboratory, whereas the second one is selective and adapted to targeted compounds.

Non-selective sampling without preconcentration in containers (gasbags, canisters, ampoules, *etc.*) allows non-selective sampling, requires less equipment, and is fast and easy to perform. Gas bags allow taking 1-200 L gas samples, and a pump is used to fill the bag with the gas. Some cautions must be taken as the bag composition must be adapted to the gaseous compounds targeted: inert materials such as Tedlar® or Teflon® are often used as they do not generate a retention phenomenon or reaction on the walls of the bag. They are valid for all ambient gases or common solvents (H.C. and chlorinated solvents). Another wall composition exists for specific VOCs. Gas bags can be cleaned (nitrogen flushing) and used several times. Their normal operating temperature is between -73 and 105 °C. Canisters are metallic containers that are placed under vacuum. When opening the closing valve, the gaseous effluent is sucked into the container. Canisters can be equipped with a flow control kit, and sampling times from instantaneous to 24 h can be obtained. The stability of the container content depends on the gaseous effluent composition, and thus they have to be analyzed as soon as possible. Direct analysis of the various container types' content is possible if the VOC levels of the effluent collected are compatible with the detection limits of the analytical system used. Injection into GC is carried out by gas syringe, gas loop, or pumping. If the VOC level is too low for direct analysis, preconcentration on adsorbent tubes or other media can be performed.

Non-selective sampling using condensation of VOCs at low temperature using dry ice or liquid nitrogen is possible but is very constraining on-site in terms of implementation, conservation, and transport of samples and can be impacted by simultaneous trapping of water. Other techniques are thus often preferred.

Sampling with preconcentration using sorbent tubes or impingers allows more or less selective collection of VOCs at quite low concentrations. Caution must be taken to avoid the saturation of the sampling media which would lead to an underestimation of the VOC concentrations. To overcome this risk, two sampling units are often placed in series, the second one serving as a guard: the absence or presence of low VOC content on the second unit (< 10% of the first one) ensures that the first one was not saturated.

The impinger technique consists in bubbling gaseous effluents in an appropriate solution for trapping the VOC family targeted by absorption in a liquid. The liquid used for trapping can be aqueous solutions adjusted to a suitable pH (amines, phenols, carboxylic acids, *etc.*), solvents for dissolution of VOCs, or reagents that transform by chemical reaction the VOC targeted in less volatile compounds [e.g., dinitrophenylhydrazine (DNPH) to trap aldehydes and ketones]. Impingers allow managing the sampling of higher concentrations than sorbent tubes as their volume (and thus of the trapping solution used) can be adjusted, keeping in mind that high volume may impair the detection limit. The evolution of the volume of the solution in the impingers has to be checked (e.g., by weighting) between the beginning and the end of



sampling in order to check if no evaporation or loss has occurred. As a quite large volume of solution is available for analysis, it allows multiple injections in GC or HPLC.

The adsorbent tubes allow the trapping of most gases and vapors. Their use has been widely studied since the 1990s<sup>[46-49]</sup>, with higher attention on VOCs and their impact on health and the environment. Numerous reference documents describe sampling and analytical conditions for VOC characterization in stationary sources<sup>[50]</sup> or working areas<sup>[51]</sup> using sorbent tubes. Adsorption of VOCs on a solid support is based on the physisorption or chemisorption phenomenon. Depending on the type of tube, a conditioning step may be done before use (e.g., nitrogen flushing and solvent elution); preconditioned tubes can be purchased. For each batch of tubes employed, an unsampled one must be used as a blank to check the absence of contamination during the storage, transport, and implementation on-site. At the end of the sampling process, the tubes are closed with sealed caps to prevent any external contamination before the extraction step and analysis. Ideally, the tubes should be analyzed as soon as possible. To extend the storage time before analysis to several weeks, the tubes can be stored in a dark and cold place (minimum 4 °C, ideally -18 °C). The maximum storage delay depends on the sorbent tube type and the kind of VOC trapped.

The determining factors for the choice of a solid support can be thermal stability, porosity, selectivity of adsorption [Figure 5], sensitivity to water, ease of use, *etc.*

Solid adsorbents are divided into three categories: porous polymers (Porapak®, Chromosorb®, XAD®, PUF, Tenax®, *etc.*), carbonaceous adsorbents (graphitized carbons (carbotrap® and carbopack®) and molecular sieves (carboxen® and carbosieve®), and inorganic adsorbents (alumina, silica, thermotrap®, florisis®, and other inorganic sieves). Other tubes containing silica grafted or impregnated with a chemical reagent are also available (e.g., DNPH tubes).

The properties of some common adsorbents are given in Table 4. Commercial tubes containing multibed adsorbents to get them more polyvalent are available.

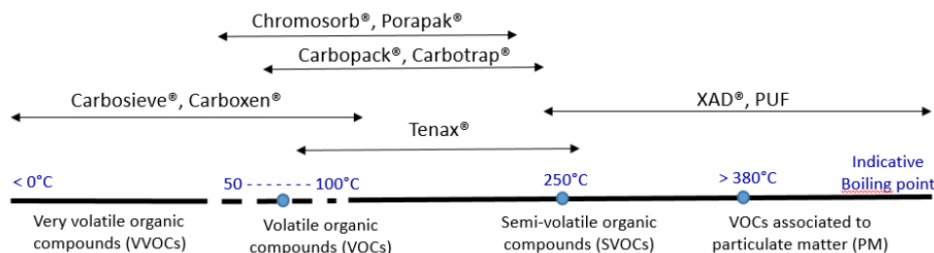
Hydrophilic sorbents (e.g., activated carbons) require the removal of water at the beginning of the sampling line. However, if polar compounds are targeted, the use of desiccants (calcium chloride, magnesium perchlorate, calcium carbon, silica gel, and Nafion® membrane) upstream of the adsorbent cartridges should be avoided, as they tend to retain polar compounds such as alcohols, ketones, acids, *etc.* Nafion® tube may be used in some cases.

Schematically, in the case of sampling on sorbent tubes, the gaseous effluent to be analyzed is drawn by means of a pump through the tube containing the adsorbent used to trap the organic compounds targeted. The various elements that can be integrated into a VOC sampling train are as follows, if sampling is performed in a stack: (1) pitot tube for flow measurement, temperature, and pressure sensors; (2) glass fiber filter for particulate matter trapping (to be maintained above 130 °C to avoid water condensation and light VOC adsorption); (3) transfer line (heated at 130 °C if the emitted gases are not at ambient temperature), which should be as short as possible; (4) water trapping system if the sampling tubes used are hydrophilic; (5) module containing the adsorbent tubes and/or the impingers (this module may be refrigerated); (6) condensate collection system; (7) flow meter to control the volume of gas sampled; and (8) pumping unit. Dynamic or static dilution systems can be integrated into the sampling train if the gas concentrations are too high or in order to limit water condensation. This solution should be considered if polar compounds are targeted, as in this case, a water trapping system (4) should be avoided. The sampling system should be made of materials that are physically and chemically inert to the gas constituents (stainless steel, glass,

**Table 4. Properties of some common adsorbents**

| Commercial name                 | Type  | Volatility range (carbon & BP) °C | Water affinity | Desorption                                   | Note  |
|---------------------------------|-------|-----------------------------------|----------------|--|---|
| TENAX® TA                       | PP    | C6-C26; 100-400 °C                | Hydrophobic    | Thermal (max desorption temperature: 250 °C) | Degradation giving benzene derivatives<br>Regeneration only a few times<br>Quite polyvalent |
| TENAX® GR                       | PP    | C7-C30; 100-450 °C                | Hydrophobic    | Thermal                                      | Alkyls benzene, PAH, PCB, heavy alcohols  |
| Chromosorb® 102 & 106           | PP    | C5-C12; 50-200 °C                 | Hydrophobic    | Thermal (stab. max: 250 °C)                  | Chlorinated, oxygenated, organometallic compounds   |
| Porapak® Q/HayeSep® Q           | PP    | C5-C12; 50-200 °C                 | Hydrophobic    | Thermal                                      | Polar compounds   |
| Carbosieve® II                  | CA    | C1-C2                             | Hydrophilic    | Thermal (High thermal stability)             | High specific surface   |
| Carbosieve® III                 | (CMS) | C2-C4; -60-80 °C                  |                |  |   |
| Carboxen® 563                   | CA    | C3-C5; 50-200 °C                  | Hydrophobic    | Solvent                                      | Sampling of low volumes & VVOC  |
| Carboxen® 564, 569              | (CMS) | C2-C5                             |                |  |   |
| Carbopack® B/Carbotrap®         | CA    | C5-C12                            | Hydrophobic    | Thermal (High thermal stability) or solvent  | High adsorption capacity  |
| B/Anasorb® GCB1/Carbograph® 1TD | (GCB) | > 75 °C                           |                |  | Polar compounds   |
| Carbopack® C/Carbotrap®         |       |                                   |                |  |   |
| C/Anasorb® GCB2/Carbograph® 2TD |       | C8-C20                            |                |  |   |
| Amberlite XAD-2                 | PP    | specific                          | Slight         | Solvent                                      | Apolar compounds, PAH, PCB, dioxins   |
| Coconut charcoal                | CA    | C2-C5                             | Hydrophilic    | Solvent (CS <sub>2</sub> )                   | VVOC  |
| Petroleum charcoal              |       | -80-50 °C                         |                |  |   |
| Silica gel                      | IA    | C2-C5                             | Hydrophilic    | Solvent                                      | Polar compounds   |

PP: Porous polymer; CA: carbonaceous adsorbent; IA: inorganic adsorbent; CMS: carbon molecular sieves; GCB: graphitized carbon black; VVOC: very volatile organic compounds.

**Figure 5.** Adsorbent use and properties.

PTFE, and polypropylene fluoride are reliable materials).

Depending on the situation encountered, the different elements of the chain should be specifically selected. For example, if the gaseous effluents contain no or few solid particles, the use of filters may be unnecessary. If a water vapor trapping system is used upstream of the tubes (hydrophilic adsorbents), the condensate collection system downstream of the tube is not necessary. Oppositely, hydrophobic adsorbents (e.g., Tenax) do not require a water vapor trapping system upstream. In this case, a condensate collection system may still be necessary downstream of the tubes to protect the flow meter and pump. If the sampling train includes impingers and their efficiency may be affected by dilution of the trapping solutions that they contain, a water vapor trapping system should be used.

As a caution, it may be interesting if feasible to duplicate samplings or to vary the sampling flow or sampling volume.

#### Delayed analysis in laboratory

Identification and quantification can then be performed by GC/MS (VOC, PAH, PCB, and other persistent compounds) or HPLC/UV (aldehydes, phenols, *etc.*).

Samples collected in impingers may need specific preparation (pH adjustment) before analysis and can be analyzed several times with different chromatographic conditions or diluted if needed to improve the analytical conditions. Sampling tubes must be either eluted with a solvent or desorbed thermally to release the trapped VOCs. When eluted by solvent (CS<sub>2</sub>, methanol, acetone, or acetonitrile), they can be analyzed by HPLC or GC depending on the VOC to be detected, and injection can be repeated if necessary as the injection volume is low (1 µL) compared to the elution volume (milliliters). The drawback is that the presence of the solvent can mask the most volatile products during the GC analysis as a solvent delay must be applied. Solvent elution also decreases the detection sensitivity because of the dilution of the sample in the solvent. Thermal desorption concerns only GC analysis, as the VOCs are released in the gas phase<sup>[52]</sup>. The tube is heated at high temperatures in order to desorb the molecules by thermal agitation. The carrier gas carries the molecules to the GC. No solvent has to be used, and the GC method does not require a solvent delay, allowing the detection of VVOCs. Thermal desorption gives maximum sensitivity, but in most equipment configurations, the analysis cannot be repeated. Duplicate sampling can thus be interesting.

Figure 6 shows the coupling of a thermodesorber and a GC. If needed, a split can be applied to dilute the desorbed VOCs. The use of an on-line preconcentrator using a trap at -15 °C (Peltier cooled trap) followed by a flash thermal desorption focuses the VOCs before injection in the GC, which improves peak resolution and chromatographic separation.

Table 5 presents the possible analytical techniques for specific VOCs targeted by the French legislation concerning industrial emissions (Arrêté intégré of the 2nd of February 1998).

Some of these techniques are described in the documentary booklet FD X43-319 (2010) concerning the “Stationary source emissions - Guide for sampling and analyzing VOC” established by the French standardization organization Afnor.

On-line analysis: example of a detailed process characterization used for treatment test evaluation at laboratory pilot scale

Sampling on-site followed by analyses in the laboratory is the classical configuration. However, on-site analysis can also be performed with specific analyzers.

An on-site campaign for detailed characterization of the VOC composition of industrial gaseous effluents is described hereafter. This campaign aimed to collect data on a real industrial process to gain information for the development of treatment technology at the laboratory pilot scale. The species-by-species knowledge of VOCs, or even by family, is essential for developing an efficient catalytic oxidation process. This requires the use of semi-continuous analytical techniques and adsorbent tube sampling to identify the VOCs present in the effluents. The process studied is a car production industry and, more specifically, the car painting process. The measurements were performed in the painting booth air extractors stacks on three consecutive days.

**Table 5. Sampling and analytical techniques proposed for specific VOCs**

| VOC concerned   | Sampling   | Extraction/Analysis                |
|---|--|------------------------------------|
| Acetaldehyde, formaldehyde, 2-furaldehyde, acroleine, chloroacetaldehyde  | DNPH (impingers or silica impregnated tubes)           | Elution/HPLC-UV                    |
| Chloroform, chloromethane, dichloromethane, 1,2-dichloroethane, 1,1,2,2-tetrachloroethane, tetrachloroethylene, Tetrachloromethane, 1,2-dichloroethylene, 1,1,2-trichloroethane, 1,2-dibromoethane, 2-dibromo 3-chloropropane | Activated carbon tube                                  | Thermal desorption/GC-FID or GC-MS |
| Vinyl chloride, acrylonitrile, methyl acrylate, pyridine, 1,4-dioxane, 1,2- $\epsilon$ poxypropane, epichlorhydrine, 1,3-butadiene  | Activated carbon tube                                  | Thermal desorption/GC-FID or GC-MS |
| Biphenyls, chlorotoluene, 1,2-dichlorobenzene, benzene  | Tenax tube   | Thermal desorption/GC-MS           |
| Benzo(a)pyrene, dibenzo(a,h)anthracene  | Filter (VOC adsorbed on particles) and XAD (gaseous)   | Solvent extraction/GC-MS           |
| 2-naphtylamine, diethylamine, dimethylamine, ethylamine, trimethylamine, aniline  | Silicagel tubes or impingers filled with acid solution | Elution (tube)/GC-FID, HPLC-UV     |
| Nitrobenzene, nitrotoluene, o-toluidine, benzidine  | Silicagel tubes  | GC-FID or GC-MS                    |
| Phenol, 2,4,5-trichlorophenol, 2,4,6-trichlorophenol, 2,4-dichlorophenol  | Impingers filled with basic solution                   | HPLC-UV                            |

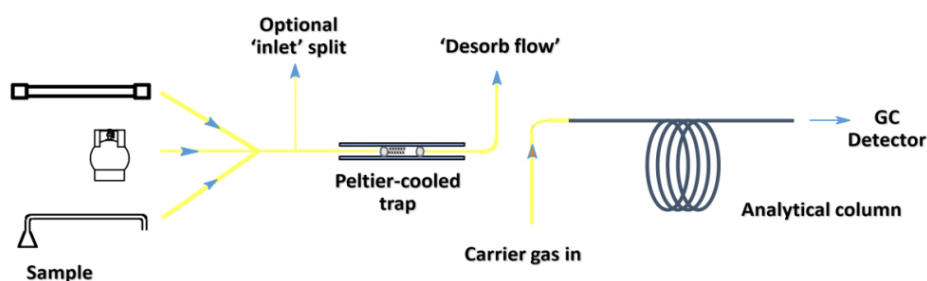
**Figure 6.** Principal of thermal desorber coupled to GC. GC: Gas chromatography.

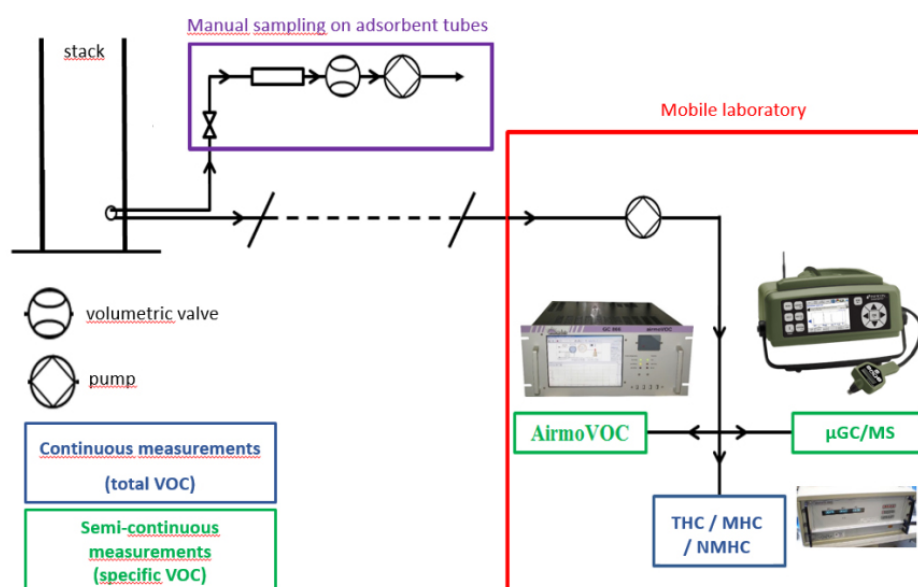
Figure 7 describes the different measurement devices that were used during the campaign to characterize the effluents in the stacks. A mobile laboratory was placed near the studied point and a PTFE sampling line at ambient temperature was drawn between the stacks located on the roof of the production building and the mobile laboratory. A volumetric pump ensures the transfer of the effluents towards the various continuous and semi-continuous measurement devices (THC/NMHC/MHC analyzer, mobile  $\mu$ -GC, and GC-FID), which are placed in parallel. These analyzers sample the amount of flue gas they require, thanks to their internal pump. A cooler is located between the sampling point and the pump to avoid the condensation of moisture in the sampling train. At the same time, a short sampling line is used to perform, on the roof directly in the stacks, sampling on adsorbent tubes with a portable system that includes a volumetric pump, a flow meter, and a needle valve to regulate the pumping rate.

Thus, the characterization of the effluents was divided into three types of complementary analyses or measurements [Table 6].

First, the measurement of physical parameters such as temperature, flow rate, and hygrometry was performed at each stack. These parameters are important for the dimensioning of a treatment unit since they will influence the working conditions and the size of the unit. They are also used to convert the concentrations into  $\text{mg}/\text{Nm}^3$  and calculate the emission rate.

**Table 6. Mobile equipment used**

| Measurement type    | Mode            | VOC targeted                    | Equipment used                               | Model   | Use        |
|---------------------|-----------------|---------------------------------|--|---|------------|
| Physical parameters | Manual          | -                               | T, RH% and flow measurement probes           | AMI 300 (Kimo Sauermann)                                | on-site    |
| Total VOC           | Continuous      | C <sub>x</sub>                  | THC/NMHC/MHC analyzer                        | Graphite 655 (COSMA)                                    |            |
| Specific VOC        | Semi-continuous | C <sub>2</sub> -C <sub>12</sub> | μGC/MS                                       | Hapsite® (Inficon)                                      |            |
|                     |                 | C <sub>6</sub> -C <sub>12</sub> | GC/FID                                       | AirmoVOC® (Chromatotec)                                 |            |
|                     | Manual          | C <sub>2</sub> -C <sub>5</sub>  | "AirToxic®" sampling tubes analyzed by GC/MS | TurboMass TD/GC Clarus 680/MS Clarus 600S (PerkinElmer) | laboratory |
|                     |                 | C <sub>6</sub> -C <sub>12</sub> | "Tenax®" sampling tubes analyzed by GC/MS    |   |            |

**Figure 7.** On-site equipment.

Then, continuous monitoring of total organic content of the effluents was performed with a total hydrocarbon analyzer (COSMA Graphite 655) equipped with a FID. The analyzer is calibrated every day thanks to a methane (CH<sub>4</sub>) standard at 3000 ppm. Concentrations are thus determined in methane equivalent and then converted to carbon equivalent. This step consists of monitoring the emissions from the stacks and thus highlighting the production steps or cycles. This analysis allows following the evolution and concentration level of non-methane hydrocarbons (NMHC) over time. It is, therefore, a global measurement that does not allow the identification of the species present in the effluents but is complementary to the specific analyses.

Finally, specific VOC analyzers were used to identify and quantify the VOC contributing to the NMHC signal. Two different micro-chromatograph analyzers were used to identify and quantify the specific VOCs present in the flue gas:

- μGC coupled with a FID (μGC/FID; AirmoVOC® C6-C12, Chromatotec): an air sample is automatically trapped on Tenax resin over 2 min and analyzed every 15 min.

- $\mu$ GC coupled with a mass spectrometer ( $\mu$ GC/MS; Hapsite, Inficon): analyses are performed in parallel with the  $\mu$ GC/FID to help identify the VOCs.

The two systems allow monitoring, identifying, and quantifying the specific VOCs emitted by the process lines. Calibration of the  $\mu$ GC/FID for the VOCs detected in the raw materials was performed in the lab before the on-site measurement campaign. Identifications of the molecules were confirmed by the  $\mu$ GC/MS. These semi-continuous measurements were completed by samplings on adsorbent tubes.

## SORPTION-CATALYSIS COUPLING FOR VOC ABATEMENT

Adsorption and catalytic oxidation are both efficient ways of environmental remediation of VOCs. However, these techniques are sometimes not sufficient or adequate for some industrial applications, which produce low concentrated VOC emissions. In this context, it is interesting to develop integrated methods where the individual techniques are combined to overcome their respective drawbacks, leading to more efficient, cost-effective, and selective technologies. These methods permit concentrating and then oxidizing VOCs from contaminated industrial emissions, based on the fine relation between adsorption and catalysis since the activity of catalysts results from their adsorption capacity and the effective activity of their active phase. The following section provides a brief overview of the adsorption and catalysis systems for VOC removal, while presenting the most common materials used for each process. We also review the trend of hybrid treatments in laboratory research with new adsorbents and catalytic active phases.

### Thermal oxidation vs. catalytic oxidation

Thermal oxidation, also known as incineration, is commonly used in industry as a removal technique of VOCs with 95%-99% efficiency. Thermal oxidation possesses a high operating cost since high temperatures ( $> 800\text{ }^{\circ}\text{C}$ ) are required to achieve complete elimination of VOCs. Three conditions referred to as the “3T rule” for an optimal thermal reaction should be taken into consideration: sufficient temperature, retention time, and turbulence level are necessary for a good conversion yield. Using oxygen from the air, this conventional process converts polluting molecules into  $\text{CO}_2$  and  $\text{H}_2\text{O}$ , which are less dangerous to the environment. Emissions with high VOC concentrations ( $> 5000\text{ ppm}$ ) can be efficiently treated, since the reaction is self-maintaining through the energy released by the oxidation reaction. However, this system is not suitable in the presence of heteroatoms such as sulfur, nitrogen, or halogens in the gas flow. In this case, oxidation would lead to the formation of by-products  $\text{SO}_2$  and  $\text{NO}_x$ , as well as acid vapor from halogenated compounds. These undesirable compounds are more toxic than the starting reagent. Catalytic combustion is an alternative way of eliminating VOCs, which considerably reduces energy costs and the formation of harmful by-products. The presence of a catalyst, which increases the speed of the oxidation reaction, allows the reaction to take place at lower temperatures ( $200\text{--}500\text{ }^{\circ}\text{C}$ ), thus resulting in energy cost savings. Catalytic systems are well adapted to treat dilute gaseous streams of VOCs ( $> 1\%$ ). Various catalysts can be used for this reaction, which should present high activity, high selectivity, good mechanical and thermal properties, and low cost<sup>[53]</sup>.

Many studies are carried out on the synthesis and design of efficient catalysts for catalytic oxidation. The choice of the catalytic material depends on many factors related to the catalytic conditions, especially the nature and concentration of VOCs. The lifetime of the catalysts is also an important parameter to consider. Catalysts can be divided into two categories: supported noble metal catalysts (Pt, Pd, Au, *etc.*) and simple/mixed transition metal oxides (Cu, Mn, Ce, Fe, Co, *etc.*). Noble metals are widely used for VOC oxidation because of their high catalytic performance despite their high cost and low resistance to sintering and poisoning. Noble metals are found as active phases carried on porous materials (zeolites,  $\text{SiO}_2$ ,  $\text{Al}_2\text{O}_3$ , *etc.*), ensuring their dispersion on the surface and inside the pores. The catalytic performance of noble



metals depends on several parameters, such as the physicochemical properties of the active metal and/or the support, the interaction between the active phase and the support, the preparation method, and the state of the active phase particles (dispersion and size). In the literature, there is a strong use of palladium and platinum as active noble metals for oxidation reactions<sup>[54-56]</sup>. These are part of some industrial commercial catalyst formulations. However, transition metal catalysts are a cheaper alternative to noble metal catalysts and are recognized for their low cost, excellent reducibility, good thermal stability, and resistance to poisoning<sup>[57-59]</sup>.

### VOCs adsorption

VOC adsorption is a process that refers to the migration of a compound in the gas phase to a solid phase by the surface reaction. The compound will bind to the outer and inner surfaces of the porous material, the so-called adsorbent. Adsorbents are usually divided into organic (polymer) and inorganic (carbons, zeolites, silica gels, and clays) adsorbents. Natural materials or some industrial and agricultural wastes can also be used directly or as a resource needed for the elaboration of adsorbents. Adsorption properties may change from one adsorbent to another. Different behaviors may be noticed depending on the type of the adsorbent, its nature, its porosity, or even the type of VOC and its concentration. According to the functional group of VOCs, different interactions can be generated, such as unspecific interactions (van der Waals force) or specific ones (pi-complexation, H-bonding, electrostatic interaction, *etc.*). To choose the adequate adsorbent for VOC removal, the adsorbent should present:

- Good textural properties (surface area, pore size distribution, pore volume, *etc.*).
- Good surface chemical properties (acidity/basic properties and affinity with polar or non-polar compounds).
- Mechanical strength (to avoid the decrease in the performance and the loss of material during adsorption-desorption cycles).
- High thermal and hydrothermal stability (to ensure the cyclic adsorption-regeneration usage).
- High selectivity for VOCs compared to other adsorbable species (such as water vapor).
- High adsorption capacity.
- High hydrophobicity (to overcome the competitive adsorption from water vapor commonly present in the flue gas).
- Insensitivity to the permanent gases constituting the effluent (such as N<sub>2</sub>, O<sub>2</sub>, CO<sub>2</sub>, *etc.*).

Therefore, the adsorption capacity is strongly dependent on the physicochemical properties of the materials, especially their textural ones<sup>[60]</sup>. The adsorbent can act as a solid catalyst, can be used as a support for a catalytic phase ensuring a high dispersion of the active species, and can be used prior to the catalytic set to eliminate organic or inorganic compounds (H<sub>2</sub>S, VOCs, *etc.*). In the following section, we outline the most common types of adsorbents for the removal of VOCs: activated carbons, biochar, and zeolites.

### *Most used adsorbents for VOC removal*

#### Activated carbons

Activated carbons (ACs) have shown high adsorption potential for VOC removal. Known to be earth-abundant and inexpensive, ACs have been extensively used on an industrial scale. The high capacity of adsorption of activated carbons is linked to their highly developed porous structures, their large accessible surfaces, and the very particular interactions that they have with many organic and inorganic compounds<sup>[61-63]</sup>. The high degree of microporosity of AC is responsible for the high surface area, which can reach 2700-3600 m<sup>2</sup>/g<sup>[64]</sup>. Then, varying the porous structure of AC, the pore size distribution and connectivity can highly influence the capacity of adsorption of VOCs.

ACs can be found in the form of pellets, granular, spheres, powder, or fibers. The most common raw materials used to produce activated carbon are wood, coal, petroleum pitch, willow peat, lignite, polymers, nutshell flour, or coconut shells. Depending on the precursor and the activation method, the prepared AC will have very different physical and chemical properties. Physical, chemical, or combined activation can be used for the preparation of AC samples in bi- or trimodal porosity. Alkali treatments by KOH activation revealed the capacity to add pores network and increase the pore volume<sup>[63,65-67]</sup>. Five types of ACs synthesized from different raw materials (wood, coal, and coconut shell) were studied by Yang *et al.*<sup>[62]</sup>. They showed that the surface area, pore volume, and pore structure controlled the capacity of ACs for toluene adsorption. With wood precursors, the ACs showed the highest surface area and the largest mesopores volume, favoring the better adsorption of toluene<sup>[62]</sup>. Besides, studies showed that, even when the surface area is higher than 2000 m<sup>2</sup>/g, the adsorption capacity of ACs can be reduced by the lack of mesopores in the structure<sup>[68]</sup>.

However, some critical problems can restrict the widespread application of ACs for VOC removal:

- High pressure drop problems when used as traditional packed beds.
- Limited applicability for low molecular weight VOCs (e.g., formaldehyde).
- High hygroscopicity (strong competitive adsorption of water vapor through the capillary condensation of water vapor in the micropores).
- High transmission resistance.
- Pore blocking.
- Promoting polymerization and/or oxidation of some toxic compounds.
- Flammability (fire risk, particularly during the exothermic adsorption process)<sup>[61,69]</sup>.

In addition to the above, the main limitation of AC usage is their regeneration process. Due to their carbonaceous structure, thermal regeneration in a gas stream containing oxygen is not suitable. The fixation of oxygen groups on its surface will reduce the pore volume, thus affecting the adsorption capacity afterward<sup>[70,71]</sup>. Normally, regeneration should cause the least damage possible to the material while maintaining most of the initial textural properties of the adsorbent, including the surface area and porosity.

Considering the strong adsorption force inside the micropores, chemical and/or thermal treatments can be used to eliminate the adsorbed compounds and regenerate the ACs.

## Biochar

Biochar is a key member of the carbonaceous materials that can be used as sorbents. It is produced by slow pyrolysis of biomass in an anaerobic atmosphere at relatively low temperatures (< 700 °C). Biochar is considered a low-cost material and a very promising substitute for AC for the capture of atmospheric pollutants<sup>[72]</sup> due to the feedstock availability and the moderate pyrolytic conditions. The latter control the structural (surface area, pore size, and bulk properties) and molecular (carbonized or non-carbonized fractions) characteristics of the biochar<sup>[73]</sup>. Biochars can undergo physical or chemical activation in order to increase the surface area and, thus, the adsorption capacity of the sorbents. At high temperatures, physical activation takes place in the presence of oxidizing gases (steam, CO<sub>2</sub>, air, *etc.*). Many authors have established that thermal activation under CO<sub>2</sub> atmosphere produces more microporous char, whereas steam favors the formation of mesopores<sup>[74,75]</sup>. Some authors clarified the efficacy of the structure-activity relationship on the adsorption capacity of VOCs. Their results show that the hierarchization and functionalization promoted the adsorption of phenol over biochars. The incorporation of a mesoporous network facilitated the intraparticle diffusion of the VOC and overcame the steric hindrance<sup>[76]</sup>. Han *et al.*, on the other hand, proved that biochar's adsorption capacity is related to the micropore volume<sup>[77]</sup>. Carbonization and chemical activation can be accomplished in one single process by treating biochar at 300-800 °C in the presence of activating agents such as acid, KOH, alkali, metal salt, *etc.*<sup>[78,79]</sup>. The choice of the pyrolysis temperature is also essential since it controls both the non-carbonized organic matter content and the surface morphology<sup>[80]</sup>. In general, the surface area increases with the increase of the pyrolysis temperature, favoring the adsorption capacity of the biochar<sup>[72]</sup>.

Vikrant *et al.* evaluated the adsorption performances of 12 standard biochars made of six different raw materials (Miscanthus straw pellets, oil seed rape straw pellets, rice husk, sewage sludge, softwood pellets, and wheat straw pellets)<sup>[81]</sup>. Two temperatures were selected for the pyrolysis (500 and 700 °C). These non-activated adsorbents were tested against gaseous benzene, xylene, methylethylketone (MEK), and other VOCs. They reported that the preparation method can highly influence the structure morphology, especially the textural properties of the material<sup>[81]</sup>. Besides, it can also control the oxygenated groups, which are responsible for surface acidity and increasing the adsorption of hydrophilic VOCs<sup>[80]</sup>. According to Rawal *et al.*, the acidity and polarity (hydrophilic/hydrophobic) of the surface are determined by the surface oxygen- and nitrogen-containing functional groups of activated biochar<sup>[82]</sup>, which present some distribution properties. Basic functional groups, including nitrogen, are usually found in micropores. However, oxygen-containing acidic (polar) groups are primarily present in meso/macropores, while oxygen-containing non-polar ones are broadly dispersed on the multilayer's surface<sup>[76]</sup>. Yang *et al.* revealed the increase of phenol adsorption over aminated materials, which shows the strong connection to the nitrogen-functional groups on the biochar's surface<sup>[83]</sup>.

## Zeolites

For many years, natural and synthetic zeolites have been the material of choice for various applications and industrial uses. Zeolites are crystalline aluminosilicates with a structural formula  $M_{x/n}(AlO_2)_x(SiO_2)_y(H_2O)_z$  (M: charge compensating cation). Their three-dimensional (3D) microporous structure is formed by a regular succession of TO<sub>4</sub> tetrahedra (SiO<sub>4</sub> or AlO<sub>4</sub><sup>-</sup>) interconnected by oxygen atoms. These are considered primary building units (PBU) that lead first to the formation of secondary building units (SBU) and then to

composite building units (CBU). The crystalline structure of zeolite is therefore the result of the periodic assembly of CBU and SBU<sup>[84,85]</sup>. Zeolites are divided into four categories defined by the number of T atoms in the pore apertures:

- Small pore size zeolites: apertures with eight T-atoms, with pore diameters from 0.3 to 0.45 nm (LTA, CHA, GIS, *etc.*).
- Intermediate pore size zeolites: 10 T-atom apertures, with pore diameters between 0.45 and 0.6 nm (MFI, FER, MWW, *etc.*).
- Wide pore zeolites: 12 T-atom diameter pore size ranging from 0.6 to 0.8 nm (FAU, MOR, BEA\*, *etc.*).
- Very large pore zeolites: apertures of  $\geq 14$  T atoms, with pore diameters  $\geq 0.9$  nm (CLO, VFI, AET, *etc.*).

Conventional zeolites are recognized for distinct properties, including their high surface area (up to 900 m<sup>2</sup>/g), large pore volume (up to 0.5 cm<sup>3</sup>/g), uniform pore size, high thermal stability (that can exceed 1000 °C), and low cost. Zeolites thus present remarkable adsorption capacity for a wide variety of VOCs. The influence of the channel size and pore structure was investigated in toluene adsorption for three hydrophobic zeolites (mordenite, ZSM-5, and faujasite). This study showed that toluene could be efficiently adsorbed by FAU zeolite. However, the adsorption capacity was reduced when ZSM-5 or MOR was used, indicating a fine relation between the molecular size of the VOC and the pore and channel structure<sup>[86]</sup>. In addition, Kim *et al.* carried out some experiments to study the adsorption behavior of mordenite and faujasite for VOCs<sup>[87]</sup>. They showed that mesopore volumes of zeolites played a key role in VOC adsorption by the faujasite zeolites (X and Y), whereas the adsorption performance of the mordenite was more related to its crystal structure. Aromatics (benzene, toluene, *etc.*) were more easily adsorbed into the faujasite structure than mordenite due to their large sizes. This was not the case for non-aromatic compounds (methanol, ethanol, *etc.*), where mordenite showed good adsorption capacity. In addition, the authors pointed out that the adsorption capacity did not seem to be linked to Si/Al ratio or acidic properties since the more performant catalyst in the mentioned work (HY901 and MS13X) consists of higher and lower Si/Al ratios and similar acid sites<sup>[87]</sup>. Those results do not concur with the study of Li *et al.* who found that increasing the Si/Al ratio helped increase the adsorption capacity of p-xylene over commercial zeolites by more than 25%<sup>[88]</sup>.

The surface polarity of the zeolite is highly considered during the adsorption process since it controls the competition between water molecules and VOCs. Water will interact more with the hydrophilic framework of the zeolite compared to relatively hydrophobic VOCs. Research pointed out the efficacy of high-temperature hydrothermal treatment for hydrophobic zeolite synthesis. The nature of the cation was reported to influence the ease of this modification. For example, it has been observed that sodium ions stabilize the framework structure of NaY zeolite, thus influencing the rate of the dealumination process<sup>[89]</sup>. Researchers are showing more interest in the development of a hydrophobic adsorbent with rapid regeneration, with more advantages at an industrial scale. Lv *et al.* investigated the adsorption of VOC over hydrophobic AC combined with zeolite<sup>[90]</sup>. First, NaY zeolite underwent pretreatment (hydrothermal dealumination, acid treatment, and salinization) and was added physically to 30% of AC. The composite materials gained in adsorption capacity (from 46 to 97 mg/g) and regeneration rate. Therefore, complete regeneration was assured in 30 min under microwave irradiation. The fire-resistant characteristic of the zeolite permitted overcoming the flammability of AC along with the discharge<sup>[90]</sup>. As reported in many studies, the most effective way to improve the hydrophobicity of the zeolite is to increase Si/Al ratio by

removing Al or adding Si to the framework of the zeolite<sup>[91,92]</sup>. The more dealuminated the zeolite is, the more hydrophobic the sample will be. As reported in the literature, pressure swing, temperature swing, purge gas stripping, reactive regeneration, and microwave heating<sup>[91-93]</sup> have all been considered effective ways for zeolite regeneration.

### Coupling adsorption and catalysis for VOC removal

Over the last decade, developments in the adsorption process have focused on the improvement of adsorbents (functionalization, hierarchization, *etc.*) as well as coupling the adsorptive removal with the catalytic oxidation. Adsorption and catalysis technologies are not very effective in removing VOCs present in low concentrations (< 100 ppm) in flue gas when used separately. Many hybrid systems based on the adsorption-catalysis pathway have been introduced to the industrial market in this context. Those original processes are based on selective adsorption of the pollutant coupled with a catalytic oxidation process. The first step of the process is the adsorption of the VOC on the surface of the adsorbent or the catalyst. In fact, the VOCs condense on the surface, and when most of the surface is saturated with VOCs, they start to desorb as part of the regeneration process of the material. Therefore, the molecular dissociation and surface diffusion ensure the contact between the active phase and the VOCs, which are oxidized and destroyed. The final elimination of the pollutant takes place during the regeneration stage of the adsorbent. During this stage, the high concentration of VOCs (> 1000 ppm) in the effluent allows the catalytic oxidation process to be used under optimal conditions. In bifunctional systems, the advantages of adsorption (high adsorption selectivity and large adsorption capability) and oxidation (complete and cost-effective decomposition) are combined in the hybrid adsorption-catalytic technology, which exhibits high adsorption capacity, catalytic activity, and selectivity to totally convert VOCs into H<sub>2</sub>O and CO<sub>2</sub>. These systems are provided as a new practical, efficient, and economical alternative to conventional VOC removal treatments. Small concentrations of VOCs in industrial emissions will thus be easier to control and treat.

In the following section, recent hybrid treatments at a laboratory scale are reviewed. Two approaches are considered: (1) adsorption is first carried out on an adsorbent followed by catalytic oxidation carried out on a catalyst; and (2) the same material is used successively as an adsorbent and as a catalyst at a higher temperature.

#### *Sequential treatments*

Sequential treatments are conventional techniques where the VOC is first captured by an adsorbent and then delivered to a reactor system for its catalytic oxidation. In this case, both parts are usually tested alone to determine their adsorption and catalytic activity. The bifunctional systems should aim for total oxidation of the adsorbed VOCs into CO<sub>2</sub> and H<sub>2</sub>O while avoiding the formation of toxic by-products during the process. The preconcentration of VOCs on the adsorbent seems to be a potentially cost-effective way to reduce VOC emissions [Figure 8].

Guillemot *et al.* focused on the elimination of MEK via a bifunctional system based on adsorption and catalysis<sup>[94]</sup>. The experiment was done over HFAU-Pt/FAU systems, where the adsorbent (HFAU) and the catalyst (Pt/HFAU) were carried out in the same reactor, but in two different beds. The study revealed three essential points concerning this type of VOC removal system:

- The adsorbent should present a high catalytic adsorption capacity. However, the capacity before a breakthrough is a factor that needs to be taken into consideration, especially when the experiment will eventually be scaled up to an industrial level.

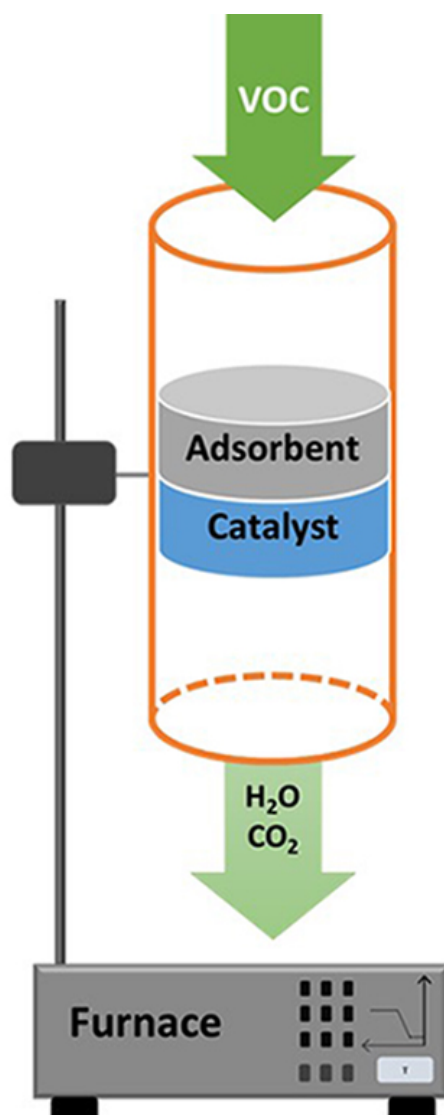


**Figure 8.** Experimental setup of sequential treatments of VOCs. VOCs: Volatile organic compounds.

- In industrial conditions, the inhibiting effect of water is highlighted; the competition between  $\text{H}_2\text{O}$  and the VOC causes a faster breakthrough, and the  $C/\text{Co}$  can be higher than 1.
- Coke formation is an important factor to consider since, depending on its nature, it can cause the deactivation of either the adsorbent (thus influencing its adsorption capacity by blocking the pores and adsorption sites) or the catalysts by deactivating the active phase and limiting the accessibility to them. As evidenced in the presented work, protonic zeolites are more likely to be deactivated via the formation of large molecules after isomerization reactions by hydrogen spillover. As for the catalyst, the rate of deactivation is related to its synthesis method and the dispersion of the metallic particles.

This hybrid system was stable for three adsorption-desorption cycles. The formation of carbon does not increase from one cycle to the next. Overall, 5.58 and 0.49 wt% of carbon were detected on the adsorbent and the catalysts, respectively. Therefore, it was presented as a promising system for the adsorption-catalysis approach.



Another heterogeneous catalytic system was studied by Urbutis *et al.* CuO-CeO<sub>2</sub>/NaX was tested for the removal of toluene based on the recognized activity of copper and ceria oxides, also on the adsorption capacity of NaX zeolite materials<sup>[95]</sup>. The adsorption of the VOCs from the effluent gas flow was the initial step of the adsorption-catalysis process. Secondly, the desorption was induced with thermal treatment by increasing the temperature of the reactor. Carbon monoxide and benzene were detected during the oxidation but were totally converted into CO<sub>2</sub> and H<sub>2</sub>O at higher temperatures (~250 °C). Urbutis *et al.* also investigated the influence of the operating parameters of this bifunctional system<sup>[95]</sup>. The efficiency of the system was related to the saturation level of CuOCeO<sub>2</sub>/NaX (toluene conversion is reduced with a high saturation degree) and the flow rate of the regenerative air (longer contact time between the oxygen of the airflow and the catalytic system). The same tendency was demonstrated for another VOC: o-xylene. However, this study showed that higher temperatures are required to totally desorb this VOC. It is worth mentioning that benzene was not a by-product of this reaction. Finally, this dual system presents some complications that involve competing effects between the endothermic reaction of desorption and the exothermic reaction of the catalytic oxidation. Overall, the VOC is first adsorbed at room temperature into the internal surface of the material. A source of energy is then required to heat the catalytic bed to the catalytic temperature and ensure the desorption process of the adsorbed VOC<sup>[95]</sup>. Wang *et al.* reported that Ru loaded on hierarchical HZSM-5 zeolite may be a promising material for the removal of bulky VOCs such as toluene, o-xylene, and TMB<sup>[96]</sup>. A fine relationship between the textural properties and the catalytic ones was established. Depending on the type of VOC treated, the adsorption capacity of the hierarchical Ru/HZSM-5 samples was almost 2, 7.5, and 35 times higher after the incorporation of the mesoporous network into HZSM-5. The latter also improved the low-temperature reducibility of Ru, which enhanced its catalytic performance. The adsorption-catalysis process was held in two reactors. The Ru/HZSM-5 catalyst was first used as an adsorbent at room temperature. After the breakthrough, VOC flow was replaced by air while increasing the temperature to desorb the VOC. The desorbed species passed through a second reactor where the bifunctional catalyst was kept at 300 °C for the catalytic oxidation step. No by-products were noticed, and the carbon balance remained stable (> 95%) during three cycles. The test conditions allowed a self-regeneration of the hybrid system<sup>[96]</sup>.

Nigar *et al.* compared the catalytic activity of a catalyst PtY placed in a single bed reactor to another combined system where a double fixed bed reactor was used<sup>[97]</sup>. In the double bed configuration, DAY zeolite was used for the adsorptive bed, while Pt/NaY zeolite was used for the single and double catalytic bed configurations. MW-assisted desorption was experienced. The microwave heating procedure helps produce a concentrated VOC flow that is then eliminated by catalytic oxidation. This approach is essential when the VOC emission sources contain only a few ppm of volatile compounds (< 1000 ppm). Once the MW is on, the catalytic bed is heated, promoting the adsorption of n-hexane on DAY. The authors established that the double bed configuration was very promising since only half of the catalytic load was used for approximately the same activity towards the total oxidation of n-hexane. To study the stability of this system, 11 cycles were achieved given almost total oxidation of n-hexane (99% conversion)<sup>[97]</sup>.

Other alternative heating technologies were developed, showing even more interest in elaborating efficient systems with lower operating energy consumption. Desorption and regeneration processes can be established by thermal treatment. Depending on the thermal conductivity of the reactor, external heating might induce significant temperature gradients between the catalytic bed and the reactors walls. New regeneration-desorption methods are then introduced to the literature to overcome this drawback. They reflect the possibility of using techniques assisted by MW or other irradiations. Some authors proposed a new concept for hybrid bifunctional systems: adsorption and regeneration by catalytic oxidation-initiated selective dielectric heating. Radio-frequency energy was used during this experiment, studying NaY and

Pt/NaY zeolite-based materials for the total oxidation of toluene. The regeneration was ensured regularly with scheduled pulses (every 20 min). This continuous process ensures homogeneity of heating, leading to a sequence of purification phases of VOCs<sup>[98]</sup>.

#### *Successive adsorbent-catalytic systems*

The combination of adsorption and catalysis processes in a single reactor has the advantage of increasing efficiency, improving catalyst productivity, and reducing capital investment and the need for external energy supply. The adsorbent is regenerated in an energy-supplied system by taking benefits of the exothermic nature of the oxidation reaction.

Hybrid systems based on successive adsorbent-catalytic systems occur in two steps [Figure 9]. First, the VOC flow is introduced into the reactor, where the bifunctional material is deposited. This is progressively saturated with VOCs. In the second step, the VOCs are desorbed during the regeneration process. An oxygen flow is sent to the reactor as a supply for the oxidation reactor or as a purge gas. The endothermic aspect of the desorption of VOCs is overcome by the heat and energy provided by its combustion. In some cases, the regeneration stream is heated upstream of the reactor, allowing the necessary heat transfer to initiate the destruction of the VOCs.

As reported in the literature, the adsorption capacity and the catalytic performance are directly related to the material in the first place. The adsorbent-catalyst configuration is recently being improved to obtain a higher surface area and a more porous network. Some authors focused their research on the configuration of monoliths, foams, honeycomb structures, laminate structures, *etc.* to favor the good dispersion of the active phases. Joung *et al.* worked on a novel Pt/carbon nanotube (CNT) for the catalytic oxidation of BTEX<sup>[99]</sup>. Based on the characterization techniques, they showed that the multi-walled carbon nanotube configuration resulted in not only a hydrophobic material but also a larger VOC adsorption surface. The material is therefore more convenient for industrial use, resistant to water vapor, and ensures strong adsorption of BTEX. The latter is oxidized by the active phase, which is very well dispersed on the support, thus also enhancing the catalytic performance of the material<sup>[99]</sup>. Hybrid systems consisting of nanogold/FeO<sub>2</sub> and nano-Au/CeO<sub>2</sub> supported on granular activated carbon were studied for the removal of toluene. These systems showed a good efficiency for this reaction (76%). The Mars Van Krevelen mechanism was used to explain the process and the different steps leading to the total oxidation of VOCs. First, the presence of metal oxides (FeO<sub>2</sub> and CeO<sub>2</sub>) was proven responsible for the good dispersion of Au nanoparticles, which caused the weakening of the metal-O bonds. The active oxygen species (lattice oxygen) thus gained better mobility. In this study, the conversion of the support with and without the metal oxide was investigated to compare and determine the essential role of gold nanoparticles. Even though the granular activated carbon showed high adsorption capacity, no conversion at low temperatures of toluene was noticed for FeO<sub>2</sub>/GAC or CeO<sub>2</sub>/GAC. The oxidation starts only at higher temperatures of 175-480 °C. This was mainly related to the low mobility of oxygen species, thus influencing the reducibility of the active species. In addition, this study tested the efficiency of toluene removal as a function of the temperature. After 30 min at 75, 100, 125, 150, and 200 °C, a decrease in the adsorption capacity was noticeable. Kim *et al.* showed that the toluene desorption temperature is 150 °C, which explained why the hybrid systems tested were no more efficient at higher temperatures, with a decrease in the removal efficiency by 13%<sup>[100]</sup>. In fact, since the first step of the catalytic system is adsorption, the more the VOC is desorbed at reactive sites, the less is the conversion of toluene. In the fixed bed reactor used in this study, the toluene is adsorbed on two types of sites: (i) adsorption sites (which are first saturated); and (ii) catalytic sites<sup>[101]</sup>.

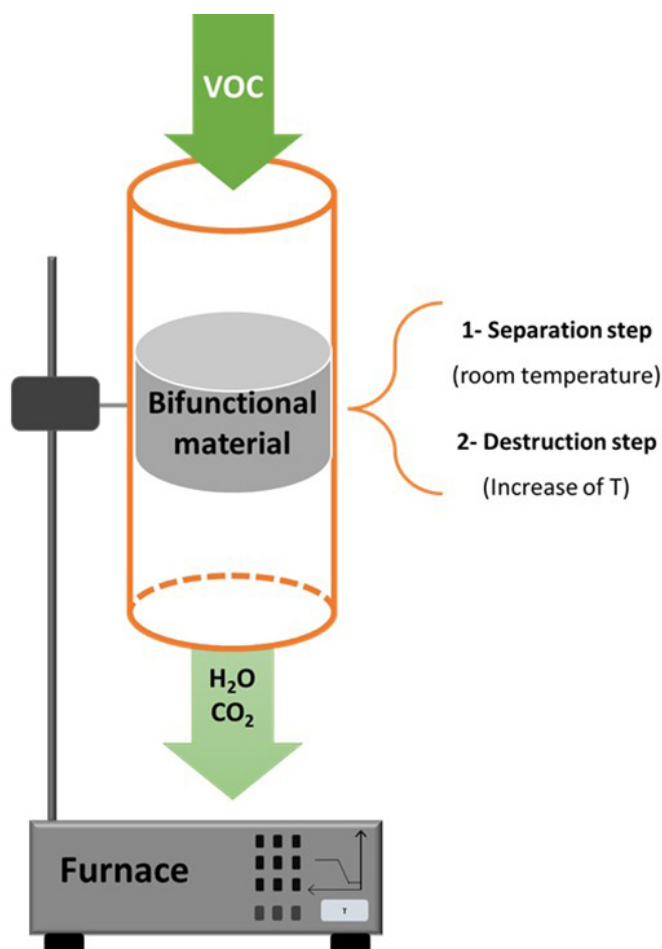


**Figure 9.** Experimental setup of successive adsorbent-catalytic systems.

The efficient performance of a zeolite-based catalyst is ensured by two essential factors: (i) the accessibility of active sites within the zeolite crystals; and (ii) the diffusion of reactants and products through the pores. The small pore sizes (< 2 nm) of microporous zeolites can inhibit the diffusion of molecules within the structure, implying a loss in adsorption and catalytic activity while increasing the possibility of deactivation by coking. This porosity limits the use of zeolites for large VOCs and explains why the use of carbonaceous adsorbents or polymers is sometimes favored for industrial applications. The latter present a broad range of pore sizes and are therefore more suitable for the adsorption of large VOCs.

The literature reveals the existence of several strategies for reducing the constraints on the transport of molecules within the zeolite structure. Modifying the porosity of the zeolite is one of the most interesting ways to overcome this major drawback by incorporating a new pore network with a different porosity range. Conventional microporous zeolites are now bi- or trimodal inorganic materials after what is called the “hierarchization process”. Two approaches can be considered: (i) bottom-up modification via the addition of hard or soft templates during the hydrothermal synthesis of zeolite; and (ii) top-down modification that consists of post-synthetic treatments such as desilication, dealumination, acid washing, *etc.* Through this process, many authors revealed the importance of the dealumination. As zeolite is initially hydrophilic (having a high affinity to water and polar molecules), dealumination allows an increase in the hydrophobic character of zeolite by chemically replacing the Al with Si without modifying the zeolite

structure. Hierarchical zeolites showed interesting advantages as heterogeneous catalysts for the removal of VOCs due to the shorter diffusion path and the greater accessibility of the active sites compared to conventional zeolites. Research is underway to further exploit these advantages by developing bifunctional catalysts with high adsorption capacity as well as catalytic efficiency.

After acid and alkaline treatment, hierarchical mordenite was used as sorbent support for platinum metallic particles. With a mesoporous volume of  $0.16 \text{ cm}^3/\text{g}$  and a pore size of 8.5 nm, these Pt/MOR catalysts showed interesting performance for toluene oxidation. The hierarchization favored the dispersion of the Pt particles on the support. The diffusion of toluene was eased, and its interaction with the Pt particles was favored. On the other hand, the improvement of the catalytic oxidation was also related to the medium adsorption strength and high adsorption capacity of the hierarchical mordenite. These two parameters play a key role in the diffusion of VOCs in the porous structure of the zeolite, particularly the internal one. The adsorption capacity was also compared to Pt/ $\text{Al}_2\text{O}_3$ , which revealed a peak at  $700^\circ\text{C}$  in toluene adsorption-desorption profiles. This peak was assigned to strong adsorption strength and, thus, a delay in desorption and a more complicated regeneration. Using XPS analysis, it was demonstrated that the improvement of Pt dispersion on hierarchical mordenite led to an increase of the active oxygen species (an increase of  $\text{O}_{\text{ads}}/\text{O}_{\text{lat}}$ )<sup>[102]</sup>. Yao *et al.* evaluated the catalytic performance of the  $\text{Rh}_1\text{Cu}_y/\text{ZSM-5}$  materials with different copper content ( $y = 1, 3, 5, 10$ ) for the total oxidation of toluene using a Langmuir-Hinshelwood model<sup>[103]</sup>. They found that the strong adsorption of the toluene on the support is crucial for a good catalytic performance. This study showed that 3 wt% of Cu was adequate content to obtain a performant bimetallic catalyst from a catalytic (50% of toluene was converted into  $\text{CO}_2$  at  $253^\circ\text{C}$ ) or adsorption (higher adsorption capacity) point of view. First, this result was mainly related to the surface area of  $\text{Rh}_1\text{Cu}_3/\text{ZSM-5}$ , which promoted the toluene adsorption. It also relied on the better interactions between Rh and Cu oxides, leading to an increase in the chemisorbed oxygen species in the lattice layer of the catalyst. Based on the L-H model, the catalytic activity was then enhanced. The stability of  $\text{Rh}_1\text{Cu}_3/\text{ZSM-5}$  was also studied and showed that it can be stable for 100 h, compared to monometallic catalysts or ZSM-5 alone<sup>[103]</sup>. Aziz *et al.* studied the impact of the synthesis method on the catalytic and absorptive capacity of Co supported on ZSM-5 materials<sup>[104]</sup>. Their adsorption-catalysis performance was tested for cyclic VOCs (BTX) in air. The results show that, depending on the synthesis methods, the adsorption capacity was related to the micropore volume. However, the adsorption capacity is strongly related to the characteristics of the VOC such as molecular size and interaction with the surface depending on the groups attached to it<sup>[104]</sup>. Beauchet *et al.* showed that the catalytic performance followed the order:  $\text{CsX} > \text{NaX} > \text{HY}$ <sup>[105]</sup>. It appears that the conversion ratio of the VOC is strongly dependent on the acidic/basic sites of zeolite since better adsorption is detected for basic zeolites, which showed better catalytic conversion. It is also related to the functional group of the VOCs, which can control the strength of the adsorption. For example, unlike isopropanol, o-xylene does not possess a functional group, and thus, the adsorption capacity will be weaker<sup>[105]</sup>. Baek *et al.* studied a variety of transition metal catalysts (Ag, Mn, Co, Zn, Fe, Ni, and Cu) loaded on HY zeolite<sup>[106]</sup>. Ag/HY catalyst revealed the lowest temperatures for the total oxidation of toluene and MEK ( $310$  and  $310^\circ\text{C}$ , respectively). These results show another dual functional adsorbent/catalyst system for the reduction of VOCs at low concentrations<sup>[106]</sup>.

Nevertheless, the hybrid system may risk deactivation due to the sintering of the metals at the high temperatures of the reaction. Therefore, some researchers are trying to fix the metals inside the framework of the zeolite in order to overcome this disadvantage that can influence the catalytic performance and the regeneration of the zeolite. The confinement of the metallic particles inside the zeolite's structure helps the size control and the active phase site adjustment<sup>[107]</sup>. For example, this sinter-resistance strategy was effective for the oxidation of toluene by Pt@ZSM-5 nanosheets. The support demonstrates good pore diffusion

properties related to its ultrashort diffusion path and rich interlayer mesopores, leading to higher adsorption capacity<sup>[108]</sup>. In fact, there are three typical ways of producing metal-containing zeolites<sup>[109]</sup>. First, a simple impregnation method is usually required for metal/zeolite preparation. During thermal treatments (calcination and reduction), metallic particles might migrate and tend to form aggregates and clusters. Conversely, the crystalline frameworks and the microporous network can produce strong confinement effects, limiting the sintering of the particles at higher temperatures in the case of metal@zeolite materials. However, the diffusion of the VOCs might be limited and the accessibility to the active phase will be affected. In this case, and depending on the type of the VOC, the shape selectivity of the zeolite will be highlighted. Finally, in metal-zeolite samples, metallic particles are incorporated into the framework of the zeolite as cations. After extraction and reduction procedures, the catalyst will turn into one of the forms mentioned above depending on the experimental conditions<sup>[109]</sup>.

Chen *et al.* studied the total oxidation of toluene based on the adsorption-catalysis pathway. They worked on a series of Pt nanoparticles in the range between 1.3 and 2.3 nm on MFI zeolite. The best catalytic performance was evaluated depending on the highest Pt dispersion and the Pt<sup>0</sup> particles. Thus, it was concluded that 1.9Pt/MFI was the optimal bifunctional catalyst<sup>[110]</sup>. A bifunctional catalyst was developed on hierarchical silicalite-1 enveloping Pd-CeO<sub>2</sub> nanowires for the oxidation of propane. After a “one-pot two-step strategy”, the synthesized materials appeared to have high catalytic activity, thermal/hydrothermal stability, and recyclability. The support trapped the low alkane VOC concentration at low temperature, and then the hydrocarbons were converted into CO<sub>2</sub> and H<sub>2</sub>O via catalytic oxidation<sup>[111]</sup>. Mono- and bimetallic based in NaY or NaY<sub>nano</sub> catalysts were tested for the total oxidation of ethyl acetate. The samples with different amounts of metal (Cu, Pd, Ag, and Zn) were prepared by ion exchange on both microporous and nanoporous NaY. The better catalytic performance was related to the surface area of the samples and the quantity of metals deposited<sup>[112]</sup>.

Composite-based materials: Shi *et al.* compared the efficiency of noble metal catalysts (Ag/HZSM-5) and nonmetal catalysts (Ag-MnOx-CeO<sub>2</sub>) for the removal of formaldehyde<sup>[113]</sup>. Both catalysts performed both HCHO adsorption and catalytic total oxidation into H<sub>2</sub>O and CO<sub>2</sub>. No by-product was detected. In this study, Ag-MnOx-CeO<sub>2</sub> was found to be more active for both functions since the mixed oxides ensured a better dispersion of the Ag clusters, inducing better redox properties of Ag. Interestingly, the presence of H<sub>2</sub>O promoted the adsorption capacity of formaldehyde on mixed oxide-based samples contrary to the zeolitic one. In this case, water molecules competed with VOC for accessible active sites<sup>[113]</sup>. Mixed metal oxides were studied for the total abatement of toluene by TiO<sub>2</sub>/SiO<sub>2</sub> and ZrO<sub>2</sub>/SiO<sub>2</sub> microporous-mesoporous systems. Ti-based catalysts showed more efficiency for this application due to their larger surface area and pore volume. The results were also related to the structural defects and hydroxyl groups. These materials displayed a higher adsorptive capacity (3.8 mmol/g compared to 2.9 mmol/g for Zr samples for 550 ppm of toluene at 25 °C) in a system where the flow was first adsorbed and concentrated at low temperatures (25 °C) and then oxidized at higher T (250 °C) given a conversion around 86%. This removal of VOCs was done on a lab-scale reactor where the catalytic bed is divided into two parts: an adsorptive part and an oxidizing part. First, the polluted air passes through the reactor, where the VOCs are adsorbed on the material at room temperature. After that, the reactor is heated at higher temperatures (250 °C) to activate the catalytic phase of the materials. Thus, the adsorbed VOCs are destroyed and converted into H<sub>2</sub>O and CO<sub>2</sub>. It is also important to notice that no coke formation was noticed after the process<sup>[114]</sup>.



## PLASMA CATALYSIS COUPLING FOR VOC ABATEMENT

### Plasma catalysis

NTP is a partially ionized gas consisting of ions, electrons, neutral species, and photons, where the electron temperature (10,000-250,000 K)<sup>[115]</sup> is orders of magnitude higher than the temperature of heavy constituents such as ions and neutral species<sup>[116]</sup>. Due to this non-equilibrium state, the overall temperature of NTP is maintained close to the ambient temperature, and there is no need to heat the entire treated gas<sup>[117]</sup>. Thus, a highly reactive environment is created without heating the entire gas as in the thermal process<sup>[118]</sup>. The accelerated energetic electrons generated in NTP collide with a carrier gas, which is predominantly air for environmental applications and generate highly reactive species, such as ground and excited atomic oxygen and nitrogen, and vibrationally and electronically excited oxygen and nitrogen molecules. These reactive species, in turn, react with the diluted VOCs and convert them into less toxic substances such as H<sub>2</sub>O, CO<sub>2</sub>, and other by-products. NTP contains a diverse mix of various ions and radicals, and, thus, it is difficult to control the reaction to produce a particular product with high yield and high selectivity. Although NTP has been proposed and investigated as an end-of-pipe technology for the removal of VOCs, NO<sub>x</sub>, *etc.*<sup>[119]</sup>, the formation of toxic by-products, poor energy efficiency (particularly for low VOC concentration), and mineralization efficiency still hinder the commercialization of this technique<sup>[120,121]</sup>.

To overcome the above-mentioned shortcomings and to take advantage of individual techniques such as NTP (e.g., highly reactive environment and rapid ignition/response) and heterogeneous catalysis (e.g., improved product selectivity and total VOC oxidation)<sup>[122]</sup>, researchers investigated plasma catalysis for air cleaning applications such as VOC abatement [Figure 10]<sup>[123]</sup>. The main strength of plasma catalysis lies in the synergetic effect of the two individual technologies, which enhances the mineralization efficiency and reduces the formation of unwanted by-products and intermediates<sup>[124]</sup>. Several experimental investigations showed that plasma catalysis enhances CO<sub>2</sub> selectivity and energy efficiency, in particular for low VOC concentration<sup>[125,126]</sup>. In plasma catalysis, the catalytic materials are placed either within the plasma discharge [known as in-plasma catalysis (IPC) or single-stage plasma catalysis] or in the downstream of the plasma discharge [known as post-plasma catalysis (PPC) or two-stage plasma catalysis]<sup>[127,128]</sup>. In the latter, the role of the NTP is to alter the gas composition and, thus, the reactants that encounter the catalyst surface. Therefore, the complexity of the underlying mechanism of PPC is much reduced and better understood when compared to the IPC process<sup>[129]</sup>.

Despite various advantages of plasma catalysis over the individual techniques, several problems must be resolved before practical implementation, which mainly include the high energy consumption for treating low VOC concentrations and deposition of polymeric substance on the catalyst during VOC decomposition, which deteriorates the catalyst performance. This review addresses several key aspects of the plasma catalysis process such as the choice of catalysts suitable for NTP environment, simultaneous removal of various VOCs, energy saving process through cycle operation of adsorption and NTP discharge, long-term stability of catalyst in plasma catalysis, and *in situ* regeneration of the catalyst by NTP exposure.

### Post-plasma catalysis

Several plasma process parameters, such as humidity level, initial VOC concentration, temperature, oxygen content, and gas flow rate, influence the abatement of the most common VOCs using the plasma catalysis system. In the following, we discuss the most important results and the influence of different operating parameters on the abatement processes of different VOCs for post-plasma catalytic systems.



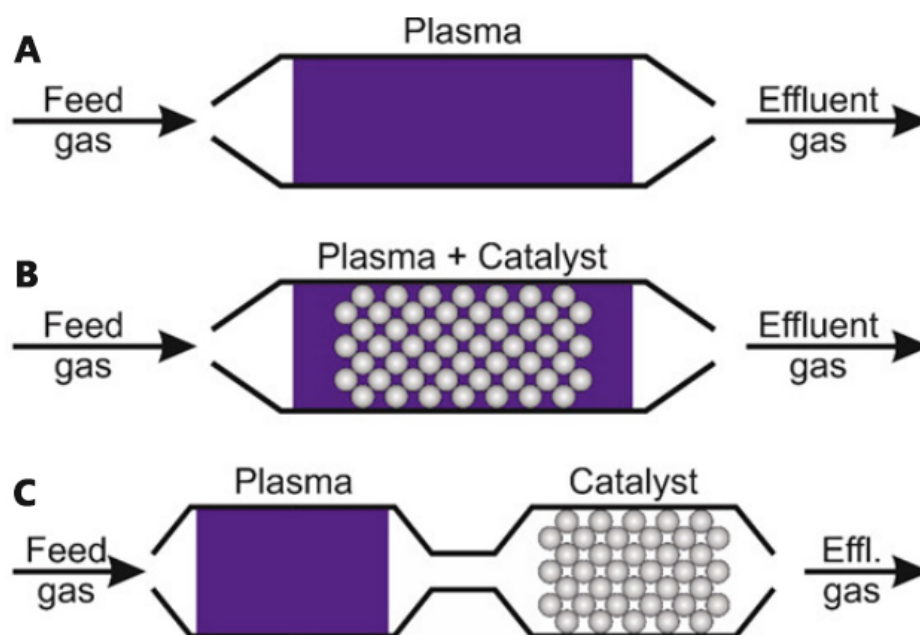


**Figure 10.** The schematic representation of plasma catalysis configurations: (A) NTP alone; (B) in-plasma catalysis; and (C) post-plasma catalysis. This figure is quoted with permission from Ollegott *et al.*<sup>[123]</sup>. NTP: Non-thermal plasma.

### BTX compounds

Benzene, toluene, and xylene (BTX) are typical volatile organic compounds and are harmful to the environment and human health<sup>[130]</sup>. Therefore, the removal of BTX for the purification of indoor air and gaseous industrial streams is very important and necessary.

### Toluene

Magureanu *et al.* investigated the toluene total oxidation in air in a plasma catalytic system formed by a dielectric barrier discharge (DBD) and Mn-based phosphate catalysts (MnPO<sub>4</sub>, Mn-APO-5, and Mn-SAPO-1), tested at 400 °C and placed downstream the plasma reactor<sup>[131]</sup>. The initial concentration of toluene (560 ppm) was decomposed by reactions with oxygen on the catalyst surface under purely catalytic conditions at an energy density range of 900-2700. The toluene removal efficiencies reached using the PPC system and the catalysts MnPO<sub>4</sub>, Mn-APO-5, and Mn-SAPO-1 were 70%, 65%, and 70%, respectively. The maximum CO<sub>2</sub> yield (33%) was obtained at 400 °C using Mn-SAPO in the PPC system.

A combination of photocatalyst with NTP was carried out by Huang *et al.*<sup>[132]</sup>. The experimental results show that the toluene removal efficiency was proportional to the ozone consumption rate in the PPC system, in which catalytic ozonation played a vital role in toluene decomposition. The dominant active species in the combined system are active oxygen species generated from ozone catalytic decomposition. Huang *et al.* showed that the toluene removal efficiency was increased by 35% and the ozone concentration present at the outlet was reduced by 70% in the PPC system, compared with the results obtained in the plasma-alone system<sup>[132]</sup>.

In addition, a system combining a DBD reactor with MnO<sub>2</sub>Co<sub>3</sub>O<sub>4</sub> catalysts was developed and tested by Chang *et al.* to decompose toluene and minimize unnecessary reaction products [Figure 11]<sup>[124]</sup>. Catalyst characterization indicated that the Mn/Co molar ratio remarkably affected the crystal structures, physico-

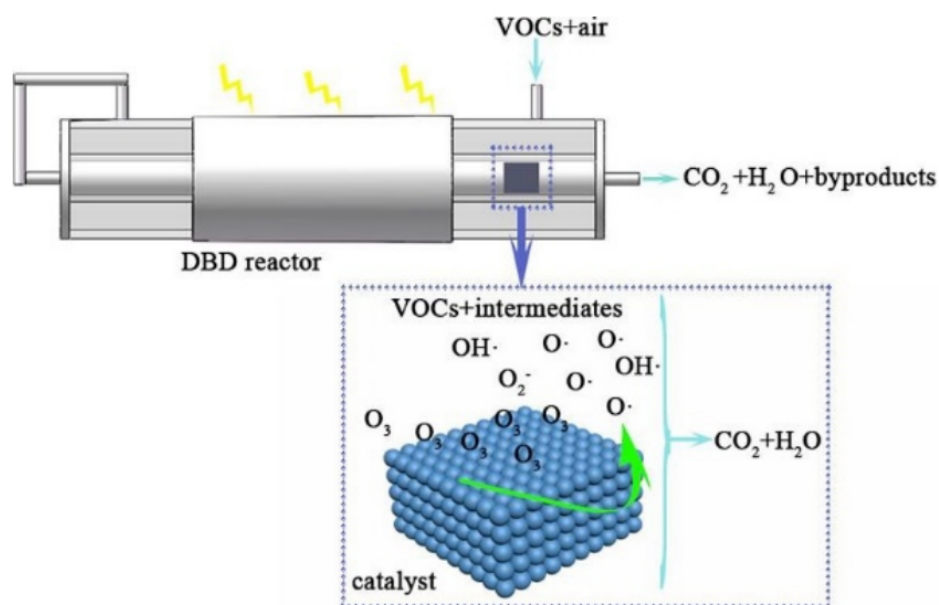


**Figure 11.** Schematic representation of the post-plasma catalytic system developed by Chang *et al.*<sup>[124]</sup>.

chemical properties of the catalyst, and subsequently influenced their catalytic activity. In particular, in the PPC system over  $\text{Mn}_1\text{Co}_1$  catalyst, the toluene removal efficiency, energy yield,  $\text{CO}_x$  yield, and  $\text{CO}_2$  yield were increased by 26.77%,  $1.76 \text{ g kWh}^{-1}$ , 25.65%, and 21.07%, respectively, compared with that in the plasma-alone system at specific energy densities of 423.58, 92.59, 456.76, and  $456.76 \text{ J/L}$ , respectively. It was shown that the synergistic effect of the Mn and Co species was the main factor in accelerating the production and transmission of active oxygen species, which in turn were responsible for the oxidation of toluene.

A similar plasma reactor system was developed by Tang *et al.* to investigate the toluene decomposition in air at atmospheric pressure<sup>[126]</sup>. Three Ag-based composite oxide catalysts, located downstream the DBD reactor, were used to recycle O radicals for the ozone decomposition and certainly the VOC decomposition. Tang *et al.* found that the toluene removal efficiencies were about 62% and 100% in the plasma-alone and PPC systems, respectively, at a specific energy density of  $60 \text{ J/L}$ <sup>[126]</sup>. In terms of ozone and/or toluene decomposition, the efficiencies of the three catalysts were in the order of: Ag-Mn-O > Ag-Co-O > Ag-Ce-O. Moreover, the Ag-Mn-O catalyst showed very good stability at room temperature.

Subrahmanyam *et al.* used a DBD system for the abatement of toluene by modifying a sintered metal fiber (SMF) filter, which acts as an inner electrode, with Mn and Co oxides<sup>[133]</sup>. Several parameters such as the VOC concentration, input energy, and the SMF modification were investigated. Figure 12 presents the influence of SMF modification and energy density on the conversion of 100 ppm of toluene. At an energy density of  $235 \text{ J/L}$ , nearly 100% conversion was achieved with both  $\text{MnO}_x/\text{SMF}$  and  $\text{CoO}_x/\text{SMF}$ . It was also observed that SMF modification with Mn and Co oxides enabled an increase in the total oxidation selectivity. All the catalytic electrodes were able to keep the same activity during almost 3 h of toluene decomposition. This result confirms that the electrodes maintained their stability during toluene destruction.

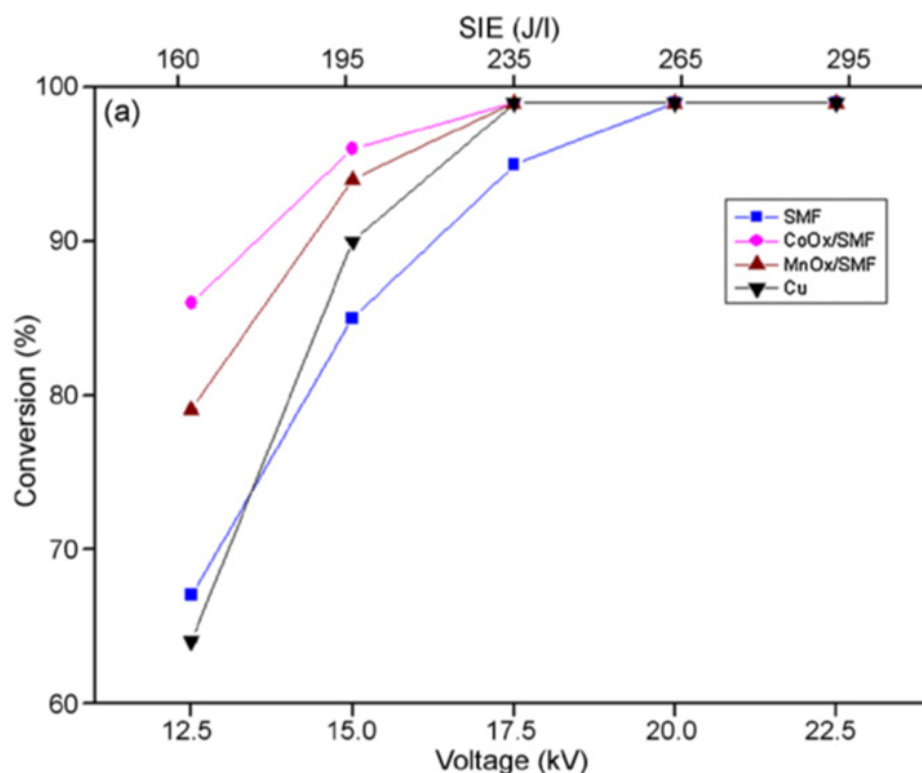


**Figure 12.** Influence of SMF modification and energy density on the conversion of 100 ppm toluene<sup>[133]</sup>. SMF: Sintered metal fiber.

In another study, Van Durme *et al.* used several catalysts that were tested downstream of a DC corona discharge<sup>[134]</sup>. In particular, the effect of relative humidity (RH) was investigated on both ozone and toluene removal. With Pd/Al<sub>2</sub>O<sub>3</sub> catalyst, it was shown that toluene removal efficiency was about > 90% and 37% in dry air and air with 74% RH (25 °C), respectively. This proved that the PPC system is less efficient when the relative humidity increases. The negative humidity effect was mostly attributed to changing van der Waals interactions.

Because extensive papers have been published on the post-plasma catalytic abatement of toluene, only a summarized discussion is given on selected papers. Several other studies that represent the abatement of toluene using a DBD reactor and a corona discharge system are not discussed in detail but are summarized in Tables 7 and 8, respectively.

## Benzene

Ge *et al.* compared a DC corona discharge system and a combined plasma-MnO<sub>2</sub> catalytic (CPMC) air cleaner for the removal of low-concentration benzene in air<sup>[145]</sup>. The catalyst MnO<sub>2</sub> was located downstream of the discharge reactor for both systems. The effects of discharge power and RH on benzene removal efficiency were investigated in a closed chamber. It was found that the benzene removal efficiency increased with discharge power in both systems by fixing the initial benzene concentration at 150 ppm. Moreover, with the increase of RH up to 20% in air, benzene removal efficiency firstly increased and then decreased in NTP, while it gradually decreased in CPMC.

**Table 7. Overview of published papers on toluene removal using catalysts placed downstream a DBD plasma reactor**

| Authors                                   | Catalyst  | T <sub>cata</sub> (°C) | Carrier gas | Flow rate (mL/min) | Concentration range (ppm) | Maximum removal efficiency (%) | Energy density (J/L) |
|---|---|------------------------|-------------|--------------------|---------------------------|--------------------------------|----------------------|
| Hayashi <i>et al.</i> <sup>[135]</sup>    | Fe <sub>2</sub> O <sub>3</sub> /MnO honeycomb   | 20                     | Dry air     | 2500               | 85                        | 65                             | 72                   |
| Ban <i>et al.</i> <sup>[136]</sup>        | Ti-MPS<br>Mn (5 wt%)-Ti-MPS<br>Mn (10 wt%)-Ti-MPS   | -                      | Air         | 200                | 1000                      | 45<br>58<br>75                 | 300                  |
| Burton <i>et al.</i> <sup>[137]</sup>     | TiO <sub>2</sub> /Al <sub>2</sub> O <sub>3</sub> /Ni foam   | -                      | Dry air     | 200                | 50                        | 95                             | 900                  |
| Harling <i>et al.</i> <sup>[138]</sup>    | MnO <sub>2</sub><br>MnO <sub>2</sub> -CuO   | -                      | Air         | 10 <sup>4</sup>    | 70                        | > 99<br>> 99                   | 340                  |
| Delagrange <i>et al.</i> <sup>[139]</sup> | N150 (MnO <sub>2</sub> -Fe <sub>2</sub> O <sub>3</sub> )<br>Al <sub>2</sub> O <sub>3</sub><br>MnO <sub>2</sub> (9 wt%)/Al <sub>2</sub> O <sub>3</sub><br>Activated carbon (AC)<br>MnO <sub>2</sub> (3 wt%)/AC | -                      | Air         | 588                | 240                       | 76<br>74<br>88<br>98.5<br>99.7 | 172                  |
| Demidyuk <i>et al.</i> <sup>[140]</sup>   | Al <sub>2</sub> O <sub>3</sub><br>Ag <sub>2</sub> O (7 wt%)/Al <sub>2</sub> O <sub>3</sub><br>MnO <sub>2</sub> (7 wt%)/Al <sub>2</sub> O <sub>3</sub>   | 425<br>300<br>330      | Dry air     | 1000               | 500                       | 78<br>> 99<br>> 99             | 60                   |
| Harling <i>et al.</i> <sup>[141]</sup>    | TiO <sub>2</sub><br>Al <sub>2</sub> O <sub>3</sub><br>Ag (0.5 wt%)/TiO <sub>2</sub><br>Ag (0.5 wt%)/Al <sub>2</sub> O <sub>3</sub>  | 600                    | Dry air     | 1000               | 500                       | 95<br>> 99<br>95-99<br>99      | 60                   |

**Table 8. Overview of published papers on toluene removal using catalysts placed downstream a corona discharge plasma reactor**

| Authors                                  | Catalyst  | T <sub>cata</sub> (°C) | Carrier gas    | Flow rate (mL/min)  | Concentration range (ppm) | Maximum removal efficiency (%) | Energy density (J/L)       |
|--|---|------------------------|----------------|---------------------|---------------------------|--------------------------------|----------------------------|
| Demidiouk <i>et al.</i> <sup>[142]</sup> | Pt-honeycomb  | 240                    | Air            | 2 × 10 <sup>4</sup> | 330                       | 90-95                          | 142                        |
| Li <i>et al.</i> <sup>[143]</sup>        | TiO <sub>2</sub>  | -                      | Air            | 1000                | 80-100                    | 70                             | 330                        |
| Van Durme <i>et al.</i> <sup>[144]</sup> | CuOMnO <sub>2</sub> /TiO <sub>2</sub>   | 20                     | Dry Air        | 10 <sup>4</sup>     | 0.5                       | 78                             | 2.5                        |
| Van Durme <i>et al.</i> <sup>[134]</sup> | Cu-Mn/TiO <sub>2</sub> (a)<br>N140<br>N150<br>Pd (0.5 wt%)/Al <sub>2</sub> O <sub>3</sub><br>Cu-Mn/TiO <sub>2</sub> (b) | 20                     | Air<br>(50%RH) | 10 <sup>4</sup>     | 0.5                       | 40<br>47<br>34<br>47<br>62     | 14<br>16<br>16<br>10<br>20 |

In another study, Jiang *et al.* combined the use of alumina-supported catalysts with a surface/packed-bed hybrid discharge reactor to degrade an initial benzene concentration of 370 mg/m<sup>3</sup><sup>[146]</sup>. The catalysts used were  $\gamma$ -Al<sub>2</sub>O<sub>3</sub> supported MO<sub>x</sub> (M = Ag, Mn, Cu, or Fe) with varying the M loading amount. The results show that the benzene degradation was enhanced and the mineralization process was strongly improved towards total oxidation when combining the plasma reactor with all MO<sub>x</sub>/γ-Al<sub>2</sub>O<sub>3</sub> catalysts. In particular, AgO<sub>x</sub>/γ-Al<sub>2</sub>O<sub>3</sub> exhibited the best catalytic activity in benzene degradation of the catalysts in the PPC system. The highest benzene degradation efficiency of 96% and CO<sub>x</sub> selectivity of 99% were obtained for the AgO<sub>x</sub>/γ-Al<sub>2</sub>O<sub>3</sub> catalyst with an optimum Ag loading amount of 15%.

Hu *et al.* developed a bipolar pulsed series surface/packed-bed discharge (SSPBD) reactor<sup>[147]</sup>. TiO<sub>2</sub>/zeolite, MnO<sub>2</sub>/zeolite, and MnO<sub>2</sub>-TiO<sub>2</sub>/zeolite catalysts, located downstream of the plasma reactor at room temperature, were tested separately for the degradation of benzene. The highest benzene degradation efficiency of 83.7% and CO<sub>2</sub> selectivity of 68.1% were obtained by the MnO<sub>2</sub>-TiO<sub>2</sub>/zeolite at 10.33 W, which were 4.9% and 5.6% higher than TiO<sub>2</sub>/zeolite. It could be attributed to the incorporation of Mn into TiO<sub>2</sub> catalyst, which was ascribed to the charge transfer between Ti<sup>4+</sup> and Mn<sup>4+</sup> on the surface of MnO<sub>2</sub>-TiO<sub>2</sub>.

/zeolite catalyst enabling the formation of hydroxyl radicals. In addition,  $\text{MnO}_2$ - $\text{TiO}_2$ /zeolite presented a better performance in ozone suppression than  $\text{TiO}_2$ /zeolite, which was mainly due to the strong ozone decomposing ability of  $\text{MnO}_2$ .

## Xylene

Extensive studies have shown that the manganese oxide ( $\text{MnO}_x$ ) catalyst, one of the most noticeable transition metal oxides, is the most appropriate catalyst for the conversion of ozone to atomic oxygen species and promotes oxidation of VOCs with atomic oxygen. This fact was demonstrated by Zhang *et al.* in performing xylene oxidation degradation in a PPC system<sup>[148]</sup>. A double plate dielectric barrier discharge (DPDBD) reactor was used in dry air at room temperature. The  $\text{MnO}_x$  catalysts were prepared using three different precursors: manganese nitrate (MN), manganese acetate (MA), and manganese sulfate (MS). Zhang *et al.* showed that  $\text{MnO}_x$  (MN) had excellent performance with strong capacity in xylene oxidation (94.1%),  $\text{CO}_2$  selectivity (80.1%),  $\text{O}_3$  suppression (76.4%), and  $\text{NO}_2$  prohibition (78.5%) compared to  $\text{MnO}_x$  (MA) and  $\text{MnO}_x$  (MS)<sup>[148]</sup>. The anions present in the precursors had an important role in the distribution of the  $\text{MnO}_x$  material on the support, which explained the excellent catalytic activity of the catalysts.

In a comparable study, Wang *et al.* introduced  $\text{Mn}/\text{Al}_2\text{O}_3$  catalysts downstream of the discharge zone of a DBD reactor for the removal of o-xylene<sup>[149]</sup>. The catalysts were prepared with different precursors: manganese acetate, manganese chloride (MC), manganese sulfate, or manganese nitrate precursor solutions. They showed that o-xylene conversion was significantly increased with the addition of  $\text{Mn}/\text{Al}_2\text{O}_3$  catalysts even at 0.2 J/L, which constitutes a very low specific energy density (SED). Among the different prepared catalysts,  $\text{Mn}/\text{Al}_2\text{O}_3$ -MA exhibited the highest catalytic activity for o-xylene removal. In particular, 6 wt% Mn loading was the optimum condition for the preparation of catalysts for high o-xylene conversion, as shown in Figure 13.

Furthermore, Piroi *et al.* investigated the decomposition of p-xylene by placing  $\text{AlAg}$  catalysts in a catalytic reactor heated up 500 °C, located downstream a DBD plasma reactor<sup>[150]</sup>. In a plasma-alone system, the conversion of p-xylene increased with increasing the specific input energy (SIE), ranging between 24% and 66% for SED between of 72 and 264 J/L, respectively. Moreover, the  $\text{CO}_2$  selectivity was below 45% for all applied SED. Under a purely catalytic system, the catalyst started to be active and allowed a conversion of 11% when reaching 500 °C. In the case of the PPC system, the p-xylene conversion efficiency was not significantly altered, although the selectivity towards  $\text{CO}_2$  was significantly improved compared to the results obtained with plasma alone. In addition, Piroi *et al.* demonstrated the importance of the catalyst temperature which has a remarkable influence on the  $\text{CO}_2$  selectivity as well. Above 300 °C the  $\text{CO}_2$  selectivity reached 65%-70%<sup>[150]</sup>.

Another important study is related to the removal of low-concentration BTX (a mixture of benzene, toluene, and p-xylene; 1.0-1.5 ppm of each compound) in air. Fan *et al.* developed a plasma-catalytic system by introducing  $\text{MnO}_x/\text{Al}_2\text{O}_3$  catalyst after the discharge zone of a link tooth wheel-cylinder plasma reactor<sup>[151]</sup>. They showed the conversion of benzene, toluene, and p-xylene reached 94%, 97%, and 95%, respectively, at a SIE of 10 J/L. In addition, this PPC system allowed a reduction in the emission of  $\text{O}_3$  and  $\text{NO}_2$  as compared to the plasma-alone system. For instance, the  $\text{O}_3$  outlet concentration decreased from 46.7 ppm for plasma-alone to 1.9 ppm for PPC, while the  $\text{NO}_2$  emission correspondingly decreased from 1380 to 40 ppb.

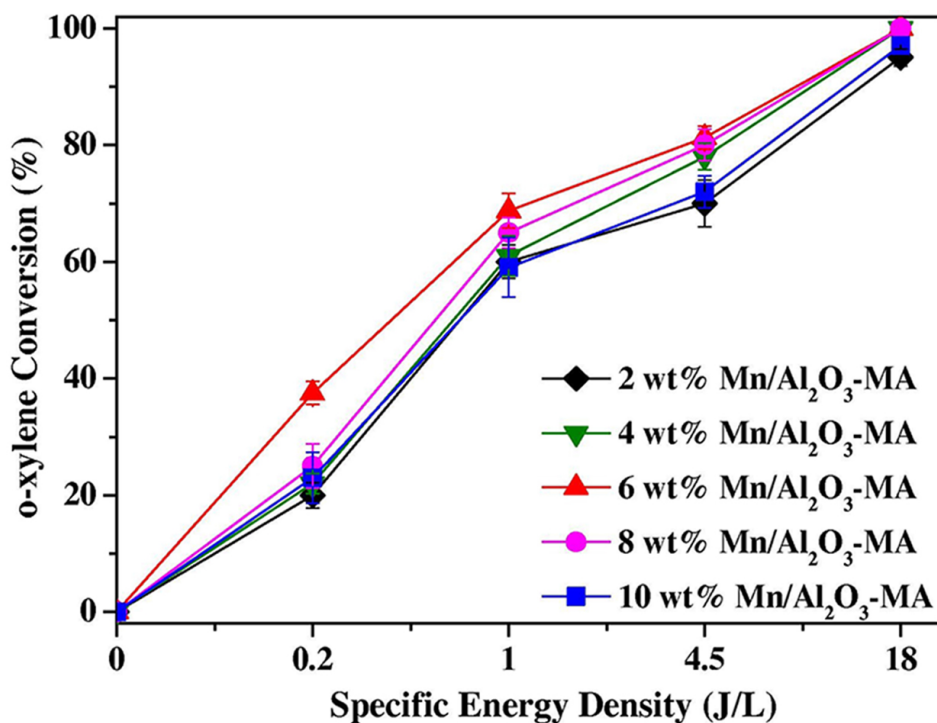


Figure 13. Effects of loading amounts of Mn/Al<sub>2</sub>O<sub>3</sub>-MA on o-xylene conversion<sup>[149]</sup>.

#### Trichloroethylene

Oda *et al.* developed a PPC system using manganese oxide (MnO<sub>2</sub>) as a catalyst in direct (contaminated air is directly processed by the plasma) and indirect processes (plasma processed clean air is mixed with the contaminated air)<sup>[152]</sup>. It was shown that MnO<sub>2</sub> catalyst was very efficient in enhancing the decomposition efficiency for both processes. For instance, when using 100 ppm as the initial TCE concentration, more than 99% of this VOC was decomposed at the discharge power of 0.5 W for both processes. The catalyst's effectiveness in dissociating ozone generated enough oxygen radicals, which are strong oxidizers for TCE removal.

In addition, Han *et al.* examined the effect of manganese dioxide on the TCE removal in similar direct and indirect processes<sup>[153]</sup> as the ones used by Oda *et al.*<sup>[152]</sup>. For the direct process, the decomposition efficiency was enhanced to about 99% at 40 J/L with passing through the catalyst. This was because the oxygen species, which were generated from collisions between excited species/electrons with O<sub>2</sub>, mainly oxidized TCE into DCAC. In addition, further oxygen species were produced during the ozone degradation at the surface of the catalyst, which led to the oxidation of the remaining TCE into trichloroacetaldehyde (CCl<sub>3</sub>-CHO, TCAA). It was also obtained that the CO<sub>x</sub> yield increased from 15% to 35% at 120 J/L when MnO<sub>2</sub> was present. When the energy density was raised to 400 J/L, a CO<sub>x</sub> yield of 98% was established. For the indirect process, similar conclusions were obtained, although the CO<sub>x</sub> yield was lower than for the direct process.

Magureanu *et al.* tested the oxidation of TCE using a plasma-catalytic DBD in the absence and presence of gold nanoparticles embedded in mesoporous silica catalysts<sup>[154]</sup>. The catalyst with the least amount of Au (0.5 wt.%) showed the most efficiency in TCE oxidation (> 99%) and the increase in the CO<sub>x</sub> selectivity at 670 J/L. As for MnO<sub>2</sub>, the Au/SBA-15 was able to dissociate the ozone generated by plasma to oxygen radicals that decompose TCE. It was also shown that the isolated gold cations were the active sites that



explained the catalytic behavior.

In a study conducted by Vandenbroucke *et al.*, a DC multi-pin-to-plate corona/glow discharge reactor was used<sup>[155]</sup>. The catalyst Pd/ $\gamma$ -Al<sub>2</sub>O<sub>3</sub>, located downstream of the plasma reactor, was set at 100 °C. The maximal removal efficiency obtained was 80% at an ED of 300 J/L and an initial TCE concentration of 600-700 ppm. The combination of plasma with a post-plasma catalyst clearly showed synergetic effects for the removal of TCE.

A similar DC glow discharge was also tested by Sultana *et al.*<sup>[127]</sup>. Fe-doped manganese oxide octahedral molecular sieves (referred to as K-OMS-2) of the cryptomelane-type structure were located downstream of the plasma reactor. It was found that both TCE conversion and CO<sub>2</sub> yield globally increased as a function of ED. Fe-K-OMS-2 showed better performance for TCE removal in moist air in comparison to the iron-free manganese oxide octahedral sieve (K-OMS-2). This result was attributed to high surface oxygen mobility and an increase of structural defects resulting from improved textural properties of the Fe-K-OMS-2 catalyst. These characteristics were responsible for enhancing O<sub>3</sub> decomposition and TCE catalytic total oxidation efficiencies. Sultana *et al.* also investigated the influence of ceria catalyst on the abatement of TCE using the same PPC reactor configuration<sup>[127]</sup>. CeO<sub>2</sub> is known as a catalyst with unique properties such as a higher oxygen storage/transport capacity. Moreover, it has a good ability to shift between reduced and oxidized states (Ce<sup>3+</sup> to Ce<sup>4+</sup>), enabling an increase in oxygen vacancies and subsequently contributing to the enhancement of the catalytic activity. When using the catalyst-alone system at high temperatures, the maximum TCE removal efficiency reached 90% at 550 °C. Meanwhile, the CO<sub>x</sub> selectivity reached a plateau (87%) at 450 °C. These results confirm the importance of high temperature in achieving both high TCE abatement and selectivity. However, in the PPC system, the TCE removal efficiency increased by around 10% (90%) at 100 °C catalyst temperature compared to the plasma-alone system (79.6%). Hence, the PPC system process had a great capability as abatement technology for low concentrated TCE air streams at a lower energy cost. An overview of several studies on TCE abatement using a PPC system is presented in Table 9.

#### Formaldehyde-acetaldehyde

Li *et al.* developed a PPC system by combining a DBD reactor and MnO<sub>2</sub> catalysts with different phase structures for acetaldehyde degradation<sup>[159]</sup>. With the introduction of  $\alpha$ -MnO<sub>2</sub>/Al<sub>2</sub>O<sub>3</sub>, the acetaldehyde removal efficiency was the highest (84.1%), which means that this catalyst exhibited the best catalytic activity among the different types of MnO<sub>2</sub>/Al<sub>2</sub>O<sub>3</sub> catalysts. This is due to the existence of OH groups, higher VOC adsorption capacity, and higher mobility of oxygen in the sample. In parallel to the PPC test for acetaldehyde removal, the degradation of benzene was also tested using similar catalysts. A lower removal efficiency, lower production of NO<sub>x</sub>, and more residual ozone were obtained.

In another study performed by Li *et al.*, other types of catalysts were located downstream of the DBD reactor to study the acetaldehyde decomposition process<sup>[160]</sup>. Metal ion-modified cryptomelane-type manganese oxide octahedral molecular sieves M'-OMS-2 (M' = Co, Ce, Cu) supported on alumina were selected for their study due to: (i) the excellent properties of the cryptomelane in catalysis reaction and easy release of lattice oxygen; and (ii) the positive effect of the metal ions on the cryptomelane catalytic activity. They showed removal efficiencies of 94.8%, 87.7%, 79.6%, and 50.2% for Cu-OMS-2/Al<sub>2</sub>O<sub>3</sub>, Ce-OMS-2/Al<sub>2</sub>O<sub>3</sub>, K-OMS-2/Al<sub>2</sub>O<sub>3</sub>, and plasma-alone, respectively, at 15.2 kV. However, a total degradation of acetaldehyde was obtained when using Co-OMS-2/Al<sub>2</sub>O<sub>3</sub> catalyst in the PPC system and under the same conditions. This can be ascribed to more substitution of manganese by cobalt on the catalyst's surface.

**Table 9. Overview of published papers on TCE removal using PPC reactors**

| Authors                           | Plasma reactor             | Catalyst                                     | T <sub>cata</sub> (°C) | Carrier gas | Flow rate (mL/min) | Concentration range (ppm) | Maximum removal efficiency (%) | Energy density (J/L) |
|-----------------------------------|----------------------------|--|------------------------|-------------|--------------------|---------------------------|--------------------------------|----------------------|
| Han <i>et al.</i> [156]           | DBD                        | MnO <sub>2</sub>                             | 20                     | Air         | 500                | 250                       | 95-99                          | 240                  |
| Vandenbroucke <i>et al.</i> [155] | DC negative glow discharge | Pd (0.05 wt%)/Al <sub>2</sub> O <sub>3</sub> | 100                    | Humid air   | 2000               | 600-700                   | 80                             | 300                  |
| Vandenbroucke <i>et al.</i> [157] | DC negative glow discharge | MnO <sub>2</sub>                             | 300                    | Dry air     | 500                | 500                       | 90                             | 240                  |
| Nguyen Dinh <i>et al.</i> [158]   | DC negative glow discharge | LaMnO <sub>3</sub> <sup>+</sup> <sub>δ</sub> | 150                    | Humid air   | 500                | 510                       | 93                             | 460                  |

Chang *et al.* investigated the formaldehyde degradation in a PPC system over a series of MnO<sub>x</sub>-Fe<sub>2</sub>O<sub>3</sub> catalysts located downstream of a DBD plasma reactor [161]. The influence of several working parameters such as gas flow rate, discharge power, and the molar ratio of Fe/Mn on formaldehyde removal were investigated using a response surface methodology (RSM). They showed that the optimal process operating conditions (discharge power of 5 W, gas flow rate of 0.5 L/min, and the molar ratio of Fe/Mn of 0.71) can be selected to reach the optimum formaldehyde removal efficiency (95.01%) and CO<sub>2</sub> selectivity (86.20%). Hence, this study confirmed that RSM is an effective tool to enhance the performance of the PPC working parameters.

### Methanol

Zhu *et al.* developed a PPC reactor for the abatement of methanol over Mn-Ce oxide catalysts with different Mn/Ce molar ratios at low temperatures [162]. The main results show that the catalyst with Mn/Ce ratio of 1:1 had the best catalytic activity in the decomposition of the methanol and led to the highest energy efficiency of the plasma-catalytic process. The use of the Mn<sub>50</sub>Ce<sub>50</sub> oxide catalyst located downstream of the DBD plasma reactor resulted in a methanol removal efficiency of 95.4% at 15 W and a gas flow rate of 1 L/min. In addition, the highest energy efficiency of the plasma-catalytic process was 47.5 g/kWh at 1.9 W.

Moreover, Norsic *et al.* investigated the decomposition of methanol at low concentration (25-150 ppm) using an NTP reactor coupled with different metal oxide based catalysts (MnO<sub>2</sub>, CeO<sub>2</sub>, CuO, MnO<sub>2</sub>-CeO<sub>2</sub>, and MnO<sub>2</sub>-CuO supported on Al<sub>2</sub>O<sub>3</sub>) [163]. They showed the effectiveness of bi-metallic oxides of MnO<sub>2</sub>/CeO<sub>2</sub>/Al<sub>2</sub>O<sub>3</sub> and MnO<sub>2</sub>/CuO/Al<sub>2</sub>O<sub>3</sub> in terms of methanol conversion, carbon oxides selectivity, and ozone utilization. In particular, for an initial concentration of methanol of 50 ppm, 4 g of MnO<sub>2</sub>/CeO<sub>2</sub>/Al<sub>2</sub>O<sub>3</sub> coupled to the DBD plasma reactor were needed to result in 100% methanol conversion with 48% and 52% selectivity to CO and CO<sub>2</sub>, respectively.

### In-plasma catalysis

An overview of the published work on IPC abatement of VOCs is given in Table 10. From the Table 10, it can be concluded that dielectric barrier discharge (DBD) is one of the widely investigated NTP reactor configurations for IPC, where at least one insulating layer is present between the high voltage (discharge) electrode and ground electrode [184]. When the voltage applied across the discharge gap exceeds the breakdown voltage, numerous microdischarges occur. The presence of the dielectric barrier limits the amount of energy and charge imparted to every microdischarge, resulting in the distribution of microdischarge over the entire electrode, which makes the DBD reactor suitable for applications such as O<sub>3</sub> generation and air cleaning [185]. In the DBD reactor, the catalyst is usually introduced as a packed bed in the form of pellets [186], powder [187], granules, or fibers. The presence of packing material in the discharge gap enhances the electric field near their contact points, increases the VOC residence time, and reduces the plasma volume, resulting in better VOC removal efficiency. The physical properties of the packing material,

**Table 10. Overview of published work on IPC for VOC abatement**

| VOC          | Reactor | Catalyst   | Carrier gas                     | Flow rate (L/min) | VOC <sub>in</sub> (ppm) | $\eta_r$ (%) | $S_{CO_x}$ (%) | By-products  | Ref.  |
|--------------|---------|--|---------------------------------|-------------------|-------------------------|--------------|----------------|--|-------|
| Benzene      | DBD     | TiO <sub>2</sub> /MnO <sub>x</sub> /SMF                              | Air                             | 0.5               | 1000                    | 70           | 30             | -  | [164] |
|              | DBD     | MnO <sub>x</sub>   | Air                             | 0.1               | 200                     | 100          | 50             | -  | [165] |
|              | Corona  | CuO/AC   | Humid air (50%)                 | 16.7              | 200                     | 90           | -              | C <sub>6</sub> H <sub>5</sub> OH, C <sub>6</sub> H <sub>6</sub> O <sub>2</sub> , C <sub>6</sub> H <sub>5</sub> NO <sub>3</sub> | [166] |
| Toluene      | HSPBD   | Ag-Ce/ $\gamma$ -Al <sub>2</sub> O <sub>3</sub>                      | Air                             | 0.5               | 400                     | 80           | 60             | O <sub>3</sub> , NO <sub>2</sub>   | [167] |
|              | DBD     | Nb <sub>2</sub> O <sub>5</sub>                                       | Air                             | 0.067             | 800                     | 96           | -              | NO <sub>x</sub>  | [118] |
|              |         | 1w% Au/Al <sub>2</sub> O <sub>3</sub>                                |                                 |                   |                         |              |                |  |       |
|              | DBD     | Au/CeO/Al <sub>2</sub> O <sub>3</sub>                                | Air                             | 0.2               | 100                     | 100          | 90             | O <sub>3</sub> , N <sub>2</sub> O, N <sub>2</sub> O <sub>5</sub>   | [168] |
|              | DBD     | NiO-TiO <sub>2</sub>   | Dry air                         | 0.1               | 40                      | 96           | 70             | -  | [169] |
|              |         |  | Humid air (5 vol%)              |                   |                         | 47.6         | -              |  |       |
|              | DBD     | Ca-Ni/ZSM-5  | Air                             | 0.1               | 100                     | 90           | 70             | N <sub>2</sub> O, O <sub>3</sub> , HCOOH   | [170] |
|              | DBD     | CeO <sub>2</sub> / $\gamma$ -Al <sub>2</sub> O <sub>3</sub> @ 200 °C | Humid air (1 vol%)              | 0.5               | 0.87 g/m <sup>3</sup>   | 80           | > 60           | C <sub>6</sub> H <sub>5</sub> CHO, C <sub>6</sub> H <sub>5</sub> OH, C <sub>7</sub> H <sub>8</sub> O                           | [171] |
|              | DBD     | 5% Ni/ $\gamma$ -Al <sub>2</sub> O <sub>3</sub>                      | Air                             | 0.1               | 160                     | 89           | -              | -  | [172] |
|              | DBD     | CeO <sub>2</sub> -MnO <sub>2</sub>                                   | Air                             | 0.25              | 1500                    | 96           | 91             | Organic compound   | [173] |
| Xylene       | DBD     | Ag/ZSM-5   | Air                             | 1                 | 150                     | 96           | 100            | O <sub>3</sub> , N <sub>2</sub> O  | [174] |
|              | DBD     | 60Co/MCM-41  | Air                             | 0.2               | 100                     | 100          | 80             | O <sub>3</sub>   | [175] |
|              | DBD     | Mn/ $\gamma$ -Al <sub>2</sub> O <sub>3</sub>                         | Air                             | 2                 | 500                     | 82           | 41             | -  | [176] |
|              | DBD     | Pd-OMS-2/ $\gamma$ -Al <sub>2</sub> O <sub>3</sub>                   | Air                             | 6                 | 9                       | 100          | 60             | HCOOH, CH <sub>3</sub> CHO   | [177] |
|              | DBD     | Mn/Al <sub>2</sub> O <sub>3</sub>                                    | Air                             | -                 | 200                     | 95           | 13             | C <sub>8</sub> H <sub>8</sub> O, C <sub>8</sub> H <sub>10</sub> O, O <sub>3</sub>  | [178] |
| Formaldehyde | DBD     | CuI-CeI  | Air                             | 1                 | 57.7                    | 95           | > 95           | -  | [179] |
|              | DBD     | 8000 ppm NaNO <sub>2</sub> /RR                                       | Air                             | 8.5               | 50 mg/m <sup>3</sup>    | 90           | -              | CH <sub>3</sub> OH   | [180] |
|              |         | Ag/CeO <sub>2</sub>  | Humid air (1% H <sub>2</sub> O) | 0.6               | 276                     | 99           | 86             | -  | [181] |
| Acetaldehyde | DBD     | Au NP/TiO <sub>2</sub> /SiO <sub>2</sub>                             | Air                             | 0.1               | 1000                    | 70           | -              | -  | [182] |
|              | DBD     | Ag/TiO <sub>2</sub> /SiO <sub>2</sub>                                | Air                             | 0.1               | 1000                    | 98           | -              | CH <sub>4</sub> COO, CH <sub>3</sub> NO <sub>2</sub> , CH <sub>3</sub> OH, C <sub>2</sub> H <sub>6</sub> CO                    | [183] |

such as the dielectric constant, shape, and size, play an important role in determining the discharge characteristics of the packed bed dielectric barrier discharge (PBDBD) reactor.

There are many reviews focused on in-plasma catalytic removal of VOCs<sup>[188-193]</sup>. Recently, Li *et al.* wrote a comprehensive review on the use of DBD reactors for VOC abatement<sup>[194]</sup>. Therefore, this section only gives an account of work that has been carried out in the past five years.

#### Reactor structure

New configurations of discharge electrode materials such as iron oxide and metallic nanowire/multi-walled carbon nanotubes/sponge have been investigated for phenol degradation. The results show that this novel electrode configuration has high discharge efficiency and lower energy consumption<sup>[195]</sup>. The performance of the PBDBD reactors can be influenced by the thickness of the dielectric barrier. Mei *et al.* investigated the effect of dielectric barrier thickness (1.5, 2.0, and 2.5 mm) on CO<sub>2</sub> conversion and reported that the conversion and energy efficiency were reduced by ~15% for a fixed SIE (120 kJ/L)<sup>[196]</sup>. In this study, when the dielectric barrier thickness increased, the plasma volume and the residence time decreased, resulting in reduced conversion efficiency. Moreover, the charge transfer efficiency was decreased by 19% with the increase in thickness from 1.5 to 2.5 mm. Although AC power supply has been widely used for economic

reasons, in the past few years, some experimental works also focused on using bipolar pulse power supply to power DBD reactors. The discharge current and, thus, the power deposition is higher for the pulsed power supply when compared to AC power supply for similarly applied voltage<sup>[197]</sup>. In addition to the applied voltage and frequency, for the pulsed power supply, pulse rise time, pulse-forming capacitance, and pulsed modes also affect the discharge characteristics. Jiang *et al.* reported that toluene conversion efficiency and energy efficiency reduce with an increase in the pulse forming capacitance<sup>[198]</sup>. This is due to the fact that the charge transfer efficiency is closely related to the pulse forming capacitance. The systematic study on the effect of the pulse mode on toluene degradation revealed that the removal efficiency and energy yield increase in the following order: – pulse < + pulse < ± pulse<sup>[199]</sup>.

#### *Packing material*

Another interesting observation that has been made by researchers in the past few years is that higher specific surface area is not the only property of the packing material required for improving VOC removal efficiency and mineralization efficiency. Li *et al.* investigated the removal of toluene using ZSM-5 ( $S_{\text{BET}} = 306 \text{ m}^2/\text{g}$ ) and  $\gamma\text{-Al}_2\text{O}_3$  ( $S_{\text{BET}} = 175 \text{ m}^2/\text{g}$ ) and reported that the mineralization rate of  $\gamma\text{-Al}_2\text{O}_3$  PBDBD reactor is higher<sup>[200]</sup>. This is due to the better discharge characteristics of  $\gamma\text{-Al}_2\text{O}_3$  due to its higher dielectric constant. Wang *et al.* investigated different polymorphs of  $\text{MnO}_2$  (such as  $\alpha\text{-MnO}_2$ ,  $\beta\text{-MnO}_2$ ,  $\gamma\text{-MnO}_2$ , and  $\delta\text{-MnO}_2$ ) and reported that  $\alpha\text{-MnO}_2$  has better catalytic activity for toluene degradation, even though its specific surface area is lower than  $\gamma\text{-MnO}_2$ <sup>[201]</sup>. Among the four polymorphs under investigation,  $\alpha\text{-MnO}_2$  possesses a double-tunneled structure, the most stable crystal phase, the weakest Mn-O bond strength, and a larger content of surface-adsorbed oxygen. Thus, other surface and bulk properties of the packing material, such as dielectric constant and phase structure, are also important in addition to the large specific surface area for the plasma catalytic oxidation of VOCs.

#### *Removal of VOC mixtures*

Recently, Liu *et al.* investigated the simultaneous removal of co-existing VOCs in industrial exhaust (such as styrene and toluene) and reported that the presence of styrene inhibited the removal of toluene, whereas the removal of styrene was unaffected by the presence of toluene<sup>[202]</sup>. The effect of the co-existence on the removal efficiency was explained by the nature of the end group (single and double bond)<sup>[202]</sup>. Qin *et al.* investigated the mechanical mixing of two catalysts, Fe/13X and Mn/13X, for the simultaneous removal of toluene and ethyl acetate as the respective metal-loaded 13X has higher mineralization efficiency for the respective VOC<sup>[203]</sup>. As shown in Table 11, the number of works investigating the removal of a mixture of VOCs is limited.

#### *Novel approaches*

Recent works on double dielectric barrier discharge reactors (DDBD), where both electrodes are covered with the dielectric barrier, showed that the DDBD reactors have improved VOC removal efficiency and mineralization efficiency<sup>[204,206]</sup>. However, the research on the underlying mechanism which can explain the improved performance of the DDBD reactors is still in the nascent stage. Shang *et al.* investigated the decomposition of benzene using a novel approach by combining a DBD plasma catalysis reactor consisting of gas phase packed bed discharge ( $\text{Mn-Cu}/\text{Al}_2\text{O}_3$  as the catalyst) and gas-liquid phase discharge chamber ( $\text{Persulfate}/\text{H}_2\text{O}$ )<sup>[207]</sup>. It has been reported that the benzene decomposition efficiency and mineralization rate were improved due to the presence of  $\text{Mn-Cu}/\text{Al}_2\text{O}_3$  catalyst, the formation of by-products such as  $\text{O}_3$  and  $\text{NO}_2$  was suppressed due to the gas-liquid phase discharge and the addition of persulfate to  $\text{H}_2\text{O}$  further increased benzene removal efficiency (by the dissolution of  $\text{O}_3$  in water, enhancing the formation of active species such as OH and  $\text{H}_2\text{O}_2$ ).

**Table 11. Overview of published work on IPC for the abatement of VOC mixture**

| Reactor | Catalyst                                 | Carrier gas | Flow rate (L/min) | VOC <sub>in</sub> (ppm) | VOC     | $\eta_r$ (%) | $S_{CO_x}$ (%) | By-products   | Ref.  |
|---------|--|-------------|-------------------|-------------------------|---------|--------------|----------------|---------------|-------|
| DDBD    | Pt-Sn/Al <sub>2</sub> O <sub>3</sub>     | Air         | 1                 | 100                     | Toluene | 85           | -              | Solid deposit | [204] |
|         |  |             |                   |                         | TCE     | 71           |                |               |       |
|         |  |             |                   |                         | Benzene | 66           |                |               |       |
| DBD     | 10 wt% Mn/Al <sub>2</sub> O <sub>3</sub> | Air         | 0.2               | -                       | Benzene | 98           | -              | -             | [205] |
|         |  |             |                   |                         | Toluene | 99           |                |               |       |
|         |  |             |                   |                         | Xylene  | 74           |                |               |       |

### Adsorption plasma catalysis

Although plasma catalysis has been proven to be more efficient than the individual techniques for VOC abatement, the plasma discharge is continuously operating, resulting in reduced energy efficiency as most of the discharge energy will be utilized to excite the background gas (O<sub>2</sub> and N<sub>2</sub>)<sup>[208]</sup>. Thus, for the treatment of the large volume of exhaust gas containing very low concentrations of VOCs (< 100 ppm), the alternate approach of adsorption plasma catalysis (APC), also known as cycled “storage-discharge”, has been proposed and investigated<sup>[209,210]</sup>. Basically, APC involves two operating steps [Figure 14A]: (i) VOC in low concentration from exhaust or flue gas is trapped or adsorbed on the adsorbent and/or catalyst (storage stage-plasma off); and (ii) the trapped or adsorbed VOC is oxidized by NTP discharge (discharge stage-plasma on)<sup>[187]</sup>. Figure 14B shows the difference in the discharge power between continuous plasma catalysis and APC process. The energy cost (EC, in kWh/m<sup>3</sup>) to remedy 1 m<sup>3</sup> of exhaust gas using continuous plasma catalysis and APC is as follows:

$$EC_{cont} = \frac{P_{discharge}^{cont}}{F_1} \quad (1)$$

$$EC_{APC} = \frac{P_{discharge}^{APC} t_2}{F_1 t_1} \quad (2)$$

where  $F_1$  is the flow rate (in m<sup>3</sup>/h) during the storage stage of APC/during the continuous plasma catalysis process,  $P_{discharge}^{cont}$  is the discharge power of normal or continuous plasma catalysis (in kW),  $P_{discharge}^{APC}$  is the discharge power during the discharge stage of APC (in kW), and  $t_1$  and  $t_2$  are the storage and discharge periods, respectively.

For this approach of APC, one of the key factors is to find a suitable adsorbent and/or catalyst which has the following properties: (i) high capability of VOC adsorption, which reduces the energy cost of the APC process by increasing the adsorption time [according to Equation (2)]; (ii) the ability to completely oxidize the adsorbed VOC to avoid the formation of toxic and unwanted toxic by-products, which improves the product selectivity and carbon balance; (iii) the ability to be regenerated by the NTP exposure, to avoid the extra step of calcination to regenerate the adsorbent and/or catalyst; and (iv) the stability in the NTP exposure, to reduce the material cost. Other advantages of APC over the continuous plasma catalysis process are the possibility to choose a different discharge gas (other than air) in order to improve the product selectivity<sup>[120]</sup> and promote the regeneration of the adsorbent/catalyst and the ability to adapt to change in the flow rate and VOC concentration in the exhaust gas<sup>[188]</sup>.

*Effect of process parameters: adsorption stage*

Effect of surface and bulk properties of adsorbent/catalyst

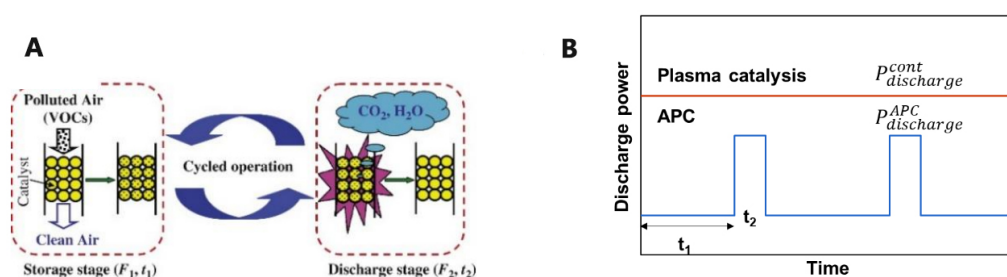


**Figure 14.** (A) The schematic representation of APC for VOC abatement and (B) the difference in discharge power for continuous plasma catalysis and APC. This figure is quoted with permission from Zhao *et al.*<sup>[120]</sup>. APC: Adsorption plasma catalysis; VOC: volatile organic compound.

The adsorption of VOCs on the adsorbent/catalyst plays an important role in determining the energy cost of APC process, and it depends on their surface and bulk properties, such as specific surface area, pore size, and pore volume. The choice of an adsorbent and/or catalyst with high  $S_{BET}$  and suitable pore size is crucial to enhance the adsorption time. Xu *et al.* investigated HZSM-5 with various  $S_{BET}$  (366–341 m<sup>2</sup>/g) and pore size (0.53–0.52 nm) for APC removal of toluene and xylene and reported that the VOC adsorption capacity decreased with the decrease in  $S_{BET}$ <sup>[211]</sup>. Yi *et al.* reported that the toluene adsorption capacity of MS-13X was far higher than MS-5A and Al<sub>2</sub>O<sub>3</sub><sup>[212]</sup>. Their  $S_{BET}$ , pore volume, and pore size are shown in Table 12. Although MS-5A has similar  $S_{BET}$  to that of MS-13X and higher pore volume, the microporous size of MS-5A is 0.55 nm, which is smaller than the kinetic diameter of toluene (0.67 nm), resulting in poor adsorption capacity.

#### Effect of metal loading

Xu *et al.* investigated various metal-loaded SBA-15 (pure, Mn/SBA-15, Ag/SBA-15, and AgMn/SBA-15) for APC removal of toluene<sup>[213]</sup>. The breakthrough curve showed that the adsorption capacity of Mn-loaded SBA is lower than that of pure SBA-15, which is due to the decrease in the  $S_{BET}$  of SBA-15 after Mn loading [Table 13]. However, with Ag loading (Ag/SBA-15 and AgMn/SBA-15), the toluene adsorption capacity was remarkably increased. The  $S_{BET}$  of Ag-loaded SBA-15 was lower than the pure SBA-15, showing that the increase in toluene adsorption was not because of physical adsorption. It was reported that the presence of metal which possesses empty s-orbital and electrons available in d-orbital forms  $\pi$ -complexation bonding, resulting in increased toluene adsorption<sup>[214,215]</sup>. A similar observation was made by other researchers for the adsorption of toluene on various metal-loaded adsorbents/catalysts which form  $\pi$ -complexation bonding, such as Co<sup>[212]</sup>.

The optimum amount of metal loading is crucial as this affects the  $S_{BET}$  and pore volume of the adsorbent. As shown in Figure 15, the toluene adsorption capacity increased with the increase in Co loading from 1% to 5% and then decreased with a further increase in Co loading. Yi *et al.* reported that, at the low value of Co loading, there was no formation of  $\pi$ -complexation bonding, whereas, at the higher value of Co loading, the pore volume and  $S_{BET}$  were decreased, resulting in reduced physical adsorption potential<sup>[212]</sup>.

#### Effect of humidity

In real-world applications, the presence of humidity in exhaust gas is inevitable, and the presence of humidity affects both the adsorption stage (competitive adsorption) and NTP discharge stage (a major source of OH and HO<sub>2</sub> radicals) of the APC process. Researchers have reported that the presence of

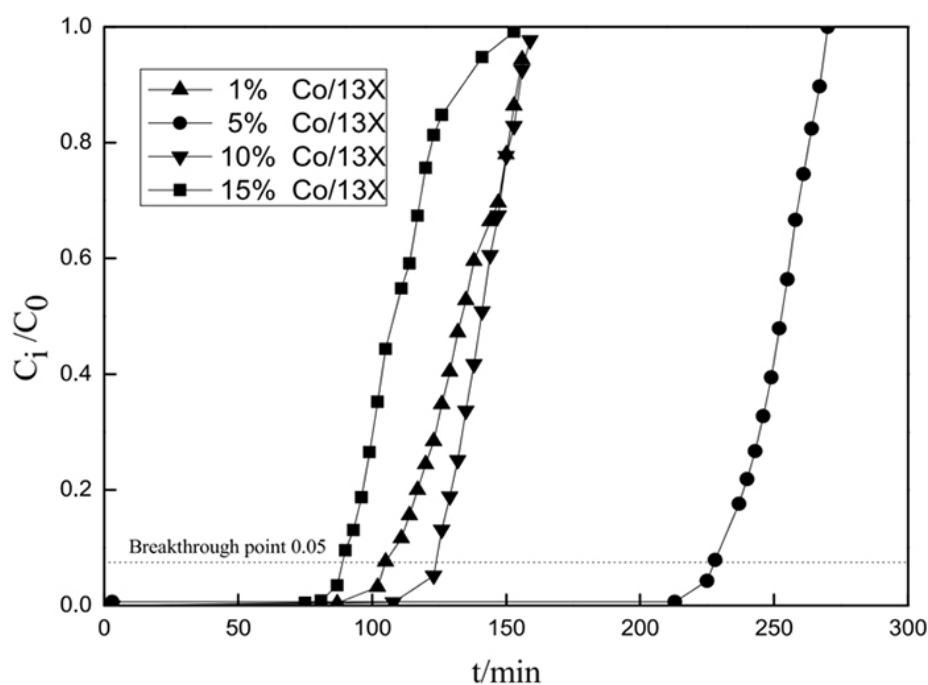


**Table 12.** Surface area, pore volume, and pore diameter of various adsorbents

| Catalyst                | $S_{\text{BET}}$ ( $\text{m}^2/\text{g}$ ) | Pore volume ( $\text{cm}^3/\text{g}$ ) | Pore size (nm) |         |
|-------------------------|--|--|----------------|---------|
|                         |  |  | Micro          | Average |
| MS-13X                  | 626.4                                      | 0.35                                   | 1.03           | 2.66    |
| MS-5A                   | 628.7                                      | 0.47                                   | 0.55           | 2.07    |
| $\text{Al}_2\text{O}_3$ | 264.9                                      | 0.37                                   | -              | 7.06    |

**Table 13.** Surface area, pore volume, and pore diameter of various metal-loaded SBA-15 catalysts<sup>[213]</sup>

| Catalyst    | $S_{\text{BET}}$ ( $\text{m}^2/\text{g}$ ) | Pore volume ( $\text{cm}^3/\text{g}$ ) | Pore size ( $\text{\AA}$ ) |
|-------------|--|--|----------------------------|
| SBA-15      | 499  | 0.90                                   | 68.0                       |
| Mn/SBA-15   | 425  | 0.83                                   | 71.7                       |
| Ag/SBA-15   | 446  | 0.85                                   | 69.4                       |
| AgMn/SBA-15 | 465  | 0.82                                   | 69.3                       |

**Figure 15.** Adsorption breakthrough curves of toluene on different Co-loaded 13X (cobalt loading = 1%, 5%, 10%, and 15%), with toluene initial concentration = 150 ppm and total flow rate = 0.4 L/min. Re-printed with permission from Yi *et al.*<sup>[212]</sup>.

humidity negatively impacts the removal of toluene<sup>[144,169]</sup>.

In the APC process, the choice of adsorbent/catalyst suitable for a wide range of humidity avoids the competitive adsorption during the adsorption stage, and the independence to choose the difference discharge gas during the discharge stage avoids the quenching of electrons. Zhao *et al.* investigated the adsorption of formaldehyde on AgCu/HZ for a wide range of humidity (RH = 20%-93%) and reported that the HCHO breakthrough capacity in humid gas stream was reduced slightly when compared to dry gas stream<sup>[120]</sup>. However, the HCHO breakthrough capacity was kept constant through the wide range of humidity, which was explained by the excellent humidity tolerance of hydrophobic high silica zeolite. Fan *et*

*al.* reported that the breakthrough of water on HZSM-5 and Ag/HZSM-5 was just a few minutes due to the hydrophobic nature of HZSM-5; thus, the adsorption of toluene in the presence of humidity (RH = 50%) was not affected<sup>[216]</sup>.

#### *Effect of process parameters: Discharge stage*

##### Effect of discharge gas

In the APC process, there is the possibility to choose a discharge gas other than the background exhaust gas. Although using O<sub>2</sub> as discharge gas avoids the formation of toxic by-products such as NO<sub>x</sub><sup>[217]</sup> and efficiently regenerates the adsorbent/catalyst, the use of O<sub>2</sub> increases the process cost and it is not readily available. On the other hand, air is readily available as a discharge gas. Zhao *et al.* compared the use of air and O<sub>2</sub> as discharge gas for APC removal of formaldehyde and reported that there was no difference in carbon balance and CO<sub>2</sub> selectivity<sup>[120]</sup>. However, while using air as discharge gas, the rate of CO<sub>2</sub> evolution was lower, resulting in extended “plasma on” time, which could negatively influence the energy cost of the APC process, and there was the formation of nitrogen oxides (such as N<sub>2</sub>O and NO<sub>2</sub>) as by-products. Dang *et al.* reported that the use of O<sub>2</sub> as discharge gas to oxidize toluene adsorbed on MnO<sub>x</sub>/γ-Al<sub>2</sub>O<sub>3</sub> and AgO<sub>x</sub>/γ-Al<sub>2</sub>O<sub>3</sub> effectively oxidized toluene to CO<sub>2</sub> within 60 min and suppressed the formation of N<sub>2</sub>O<sup>[218]</sup>.

##### Effect of gas flow

The gas flow rate plays an important role in determining the mineralization efficiency for plasma catalytic destruction of VOCs. When the gas flow rate increases, the residence time of VOCs in the plasma discharge region decreases and reduces the collision probability between the VOC molecules and plasma-generated active species<sup>[173]</sup>. In the APC process, the choice of discharge mode such as closed (inlet and outlet of the reactor are sealed), intermittent cycle (by alternating closed and ventilated discharge), or ventilated (with a flow of background gas such as N<sub>2</sub>, O<sub>2</sub>, or air) discharge depends mainly on the amount of adsorbed VOCs during the adsorption stage. Yi *et al.* investigated the closed and ventilated discharge for APC removal of toluene using MS-5A, MS-13X, and Al<sub>2</sub>O<sub>3</sub> as packing material<sup>[219]</sup>. As shown in Figure 16, although the toluene removal efficiency was not affected by the discharge mode, the carbon balance (B<sub>c</sub>) and CO<sub>x</sub> selectivity were dependent on the amount of toluene adsorbed (Tol<sub>ads</sub> for 13X, 5A, and Al<sub>2</sub>O<sub>3</sub> were 0.57, 0.021, and 0.05 mmol, respectively). In the closed discharge mode, the amount of oxygen was limited, and the oxidation of toluene was mainly dependent on the amount of active oxygen species generated, resulting in deep toluene oxidation in the presence of less toluene due to increased residence time. On the other hand, for 13X, the B<sub>c</sub> and CO<sub>x</sub> selectivity were increased in ventilated discharge, as the loss of oxygen was replenished by the continuous flow, whereas, for the low concentration of toluene (5A and Al<sub>2</sub>O<sub>3</sub>), the utilization of NTP generated active species was poor and the toluene was desorbed and released to the gas stream unconverted. Dang *et al.* compared the intermittent (closed = 5 min and ventilated = 10 min) and ventilated discharge for APC removal of toluene using MnO<sub>x</sub>/γ-Al<sub>2</sub>O<sub>3</sub> and reported that the continuous mode exhibited better and deep toluene oxidation<sup>[218]</sup>. This was because the amount of toluene adsorbed was high (0.88 mmol), and the continuous flow replenished the reactive species generation and removed the oxidative products (CO and CO<sub>2</sub>) produced, avoiding the active site blockage. The suitable gas flow rate during the discharge phase is dependent on the reactor configuration; thus, the optimization of the gas flow rate is important to obtain a better conversion, energy, and mineralization efficiency<sup>[220,221]</sup>.

##### Effect of humidity

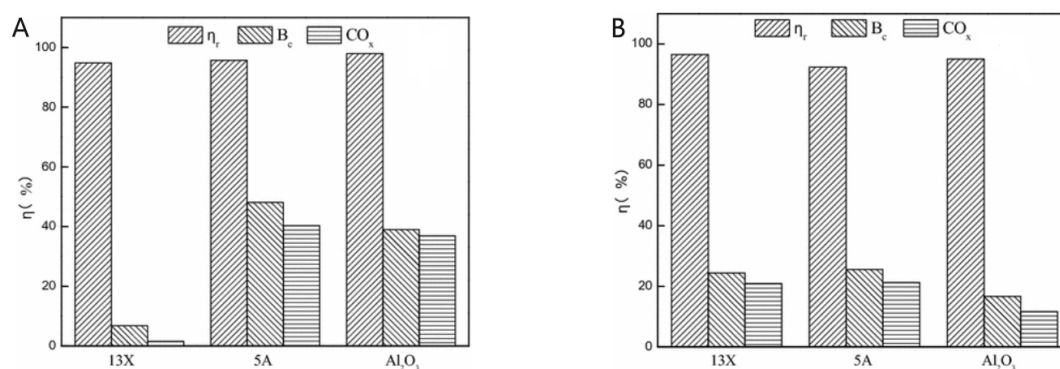


**Figure 16.** Degradation efficiency of toluene in APC process for (A) closed and (B) ventilated discharge mode. Re-printed with permission from Yi *et al.*<sup>[219]</sup>. APC: Adsorption plasma catalysis.

Xu *et al.* investigated APC removal of toluene using Ni-SBA in the presence of a wide range of humidity (RH = 20%-80%) and reported that the presence of humidity reduces the toluene mineralization rate<sup>[222]</sup>. This was explained by the quenching of energetic electrons due to the electronegative nature of water and the competitive adsorption of water vapor covers the active sites needed for  $O_3$  adsorption and decomposition. On the other hand, it was reported that the presence of humidity reduces  $CO$  yield, which was explained by the influence of humidity on the formation of intermediates favorable for  $CO_2$  formation.

#### Effect of metal loading

The mineralization efficiency and carbon balance of the APC process are important in order to reduce the formation of unwanted and more toxic by-products, and they depend on the catalytic activity of the adsorbent and/or catalyst. Noble metal-based catalysts such as Pt or Pd have been widely reported as highly active catalysts for VOC oxidation<sup>[223]</sup>. However, noble metal-based catalysts are expensive and susceptible to poisoning. Alternatively, transition metal oxide-based catalysts have been considered for the total oxidation of VOCs<sup>[224,225]</sup>. In the APC process, the decomposition of adsorbed VOC on adsorbent in NTP discharge proceeds via the reaction with the energetic electrons, ions, ozone, and atomic oxygen. It has been reported that the reaction rate of toluene with atomic oxygen ( $k = 7.6 \times 10^{-14} \text{ molecules}\cdot\text{cm}^{-3}\cdot\text{s}^{-1}$ ) is higher than that with ozone ( $k = 3.9 \times 10^{-22} \text{ molecules}\cdot\text{cm}^{-3}\cdot\text{s}^{-1}$ ), and the rate-determining step of toluene oxidation is the decomposition of ozone<sup>[213,226]</sup> according to Equations (3)-(5). Thus, to improve the  $CO_2$  yield and selectivity, the choice of the packing material (catalyst) suitable for the decomposition of ozone to produce atomic oxygen, oxidation of  $CO$ , and, thus, total oxidation of adsorbed toluene is important.



where \* represents the active catalyst site.

Xu *et al.* reported that loading SBA-15 with metals such as Ag and/or Mn showed improved  $CO_x$  yield and carbon balance when compared to pure SBA-15, which was mainly attributed to the ozone decomposition ability of the catalysts<sup>[213]</sup>. Yi *et al.* investigated various transition metal-loaded 13X (such as Cu/13X, Co/13X, Ce/13X, and Mg/13X) for the APC removal of toluene and reported that the  $CO$  and  $CO_2$  yield,

CO<sub>2</sub> selectivity ( $S_{CO_2}$ ), and carbon balance ( $B_c$ ) were the highest when using Co/13X [Figure 17]<sup>[212]</sup>. This is due to the presence of active sites (Co<sub>3</sub>O<sub>4</sub> in Co/13X) which has large oxygen adsorption capacity and converts them to O<sup>-</sup> and O<sup>2-</sup>, which are stabilized on the catalyst surface resulting in enhanced reactivity. Wang *et al.* reported that the mineralization rate of various metal-loaded HZSM-5 for APC removal of toluene from humid air (RH = 40%) occurred in the following order: Ag-Mn/HZSM-5 (~94%) > Ce-Mn/HZSM-5 ~ Mn/ HZSM-5 (~70%) > Ag/ HZSM-5 > Ce/ HZSM-5<sup>[215]</sup>. The better catalytic activity of Ce-Mn- and Mn-loaded HZSM-5 was attributed to the strong oxygen storage/release ability of Mn and ozone decomposition ability of Mn, whereas the addition of Ag in Ag-Mn/HZSM-5 changed the toluene adsorption site to Ag ( $\pi$ -complexation), thereby leaving the Mn active sites for O<sub>3</sub> decomposition.

In addition to the kind of metal loading, the amount of metal loading affects the catalytic performance by altering the oxidation state, crystal structure, aggregation, and redistribution. Yi *et al.* studied the effect of Co loading on APC removal of toluene (1%, 5%, 10%, and 15%) and observed that the optimum Co loading was 5% for better catalytic performance<sup>[212]</sup>. When 1% Co was loaded, there was not enough formation of active species for the complete toluene oxidation, whereas increasing the Co loading beyond 5% resulted in agglomeration of the active sites (observed in SEM).

#### Stability of adsorbent/catalyst

The stability of adsorbent/catalyst over multiple cycles is crucial for its applications in cyclic processes such as adsorption plasma catalysis. The activity of the adsorbent and/or catalyst used as packing material in PBDBD reactor for VOC abatement shows time-dependent deterioration. Deactivation can be due to either the accumulation of organic intermediates on the surface of the catalyst<sup>[227]</sup> or changes in the surface and bulk properties after exposure to NTP discharge<sup>[228]</sup>. Xu *et al.* investigated the stability of AgMn/SBA-15 for the APC removal of toluene and reported that the toluene conversion and CO<sub>x</sub> yield were not decreased during the five cycles of APC<sup>[213]</sup>. Zhao *et al.* investigated the stability of AgCu/HZ catalyst during APC removal of formaldehyde and reported that the carbon balance and CO<sub>2</sub> selectivity were maintained at ~100% for five cycles<sup>[120]</sup>. Fan *et al.* reported that the APC removal of benzene using Ag/HZSM-5 as a catalyst was very stable for five cycles<sup>[216]</sup>. Trinh *et al.* investigated the stability of Ag-loaded zeolite during APC removal of acetone for four cycles<sup>[229]</sup>. Although the catalytic performance was not degraded during these four cycles of APC, the temporal evolution curves of gaseous carbon-containing by-products (such as CO and CO<sub>2</sub>) tended to be broader, probably due to the oxidation of the low volatile organic deposits on the catalyst.

The above-mentioned works investigated the stability of adsorbent/catalyst under NTP exposure in the APC process by comparing the VOC removal efficiency, carbon balance, and CO<sub>2</sub> selectivity for a very limited number of cycles ( $\leq 5$ ). Wang *et al.* investigated the APC removal of toluene using Ag-Mn/HZSM-5 and reported that the toluene mineralization rate decreased from 93.5% to 68.6% during 10 cycles of APC<sup>[215]</sup>. They ascribed the deterioration of the catalyst performance to the accumulation of organic intermediates, and the catalytic activity was restored by calcination in air stream at 573 K for 2 h. It has also been reported that the surface and bulk properties of the adsorbent and/or catalyst can change, which leads to the deactivation of the catalysts<sup>[230]</sup>. Thus, it is crucial to investigate the bulk and surface properties of adsorbents and/or catalysts, such as phase, crystallinity, elemental composition, oxidation state of metal, morphology, *etc.*, which can be altered partially or completely by NTP exposure<sup>[187]</sup>. Qin *et al.* investigated the stability of  $\gamma$ -Al<sub>2</sub>O<sub>3</sub>-13X for APC removal of toluene by comparing both the mineralization rate (MR) and the physico-chemical properties of the fresh and used catalysts<sup>[231]</sup>. Although there was no significant change in the MR over the five cycles of APC, in FTIR spectra of the used catalysts, there were new peaks

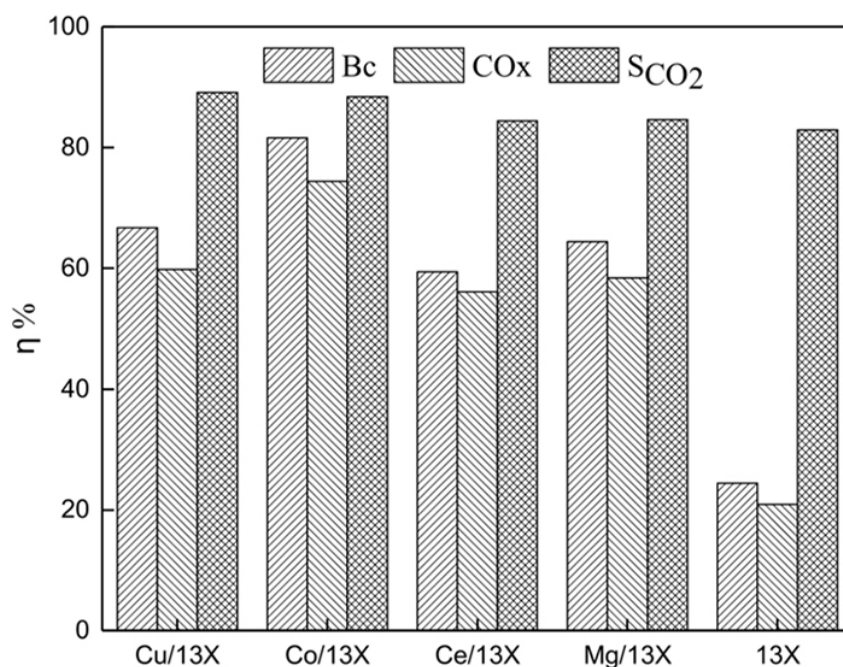


**Figure 17.** Carbon balance and CO<sub>x</sub> and CO<sub>2</sub> selectivity for various metal-loaded 13X catalysts (total air flow rate = 0.1 L/min; discharge power = 20 W). Re-printed with permission from Yi et al.<sup>[212]</sup>.

corresponding to C-O-H and methyl, indicating the presence of intermediate organic products on the surface of the catalyst. Other catalyst properties such as the crystal structure,  $S_{\text{BET}}$ , pore volume, and average pore size were not changed after the five cycles of APC. Although the deposition of organic products did not change the catalytic activity during five cycles of APC, the continuous accumulation of organic products might influence the catalytic activity and performance in the long run.

## COUPLING ADSORPTION AND PHOTOCATALYSIS FOR VOC REMOVAL

### Introduction

In addition to the above-discussed adsorption-catalysis coupling and plasma catalysis strategies for VOC removal, adsorption-photocatalysis coupling has also been exploited by researchers. Compared with the high temperature and pressure adopted during adsorption-catalysis and plasma catalysis processes, the adsorption-photocatalysis process gives rise to obvious advantages in VOC removal such as excellent elimination efficiency, low energy depletion, and environmentally friendliness<sup>[232-234]</sup>. As for the whole adsorption-photocatalysis process, the adsorption procedure ensures that the VOC molecules are transmitted from the gas phase to the solid phase to achieve the close contact between VOC molecules and photocatalysts. Moreover, the photocatalysis treatment is conducted at room temperature and decomposes VOCs into CO<sub>2</sub> and H<sub>2</sub>O and therefore guarantees the regeneration of the adsorbent for constant VOC elimination<sup>[235]</sup>. The above merits indicate adsorption-photocatalysis coupling technology is an efficient and promising method for VOC removal.

Generally, photocatalytic oxidation has been carried out during the photocatalysis treatment process, which endows a facile and effective pathway for completely decomposing VOC molecules by utilizing photoinduced oxidizing species [Figure 18]. For instance, titanium dioxide, a typical photocatalyst, has frequently been used in adsorption-photocatalysis coupling for VOC removal. Under UV light irradiation, TiO<sub>2</sub> gives rise to the generation of highly oxidizing radicals, such as ·OH radicals (·OH/H<sub>2</sub>O = +2.27 eV vs.



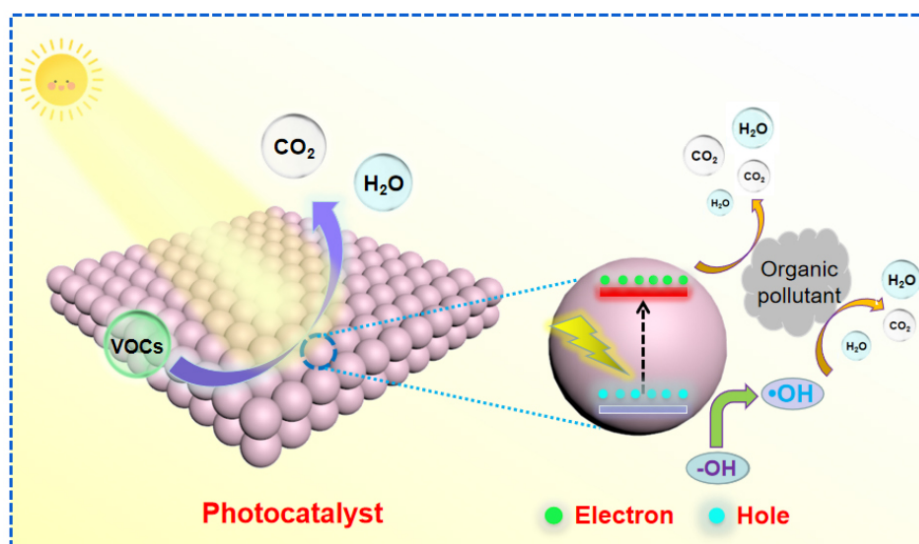


**Figure 18.** The schematic process of adsorption-photocatalysis coupling for VOC removal. VOC: Volatile organic compound.

SHE) and  $\cdot\text{O}_2^-$  (redox potential  $\text{O}_2/\cdot\text{O}_2^- = -0.28 \text{ eV vs. SHE}$ ), which lead to the decomposition of VOC molecules such as gaseous toluene and benzol in the atmosphere<sup>[232]</sup>. As for the strongly adsorbed VOC molecules on the surface of photocatalyst, they can be directly oxidized by the photogenerated hole on  $\text{TiO}_2$  photocatalyst.

### Mechanisms

Coupling adsorption and photocatalysis for VOC removal is composed of three predominant processes including mass transfer and transportation, surface photoredox reactions, and product desorption<sup>[236-240]</sup>. Here, we discuss the detailed mechanism of each process. (1) Mass transfer and transportation means that the VOC molecules are shifted from the gas phase to the surface of photocatalysts via an adsorption process due to the existence of interactions such as hydrogen bonds and van der Waals force between VOC molecules and photocatalysts. Thus, the modification of the surface chemistry of photocatalysts is of great importance for photocatalytic VOC elimination. (2) When the energy of excited light is greater than the band gap value of the photocatalyst, photogenerated electron-hole pairs are produced. The generated holes can directly oxidize organic molecules or oxidize water to produce hydroxyl radicals for the subsequent oxidation reaction. As to the electrons, they can combine with oxygen to create the oxidative superoxide radical to join in the oxidation degradation of organics. Finally, products such as  $\text{CO}_2$ ,  $\text{H}_2\text{O}$ , or other intermediates are generated on the surface of photocatalyst. (3) Product desorption is also a crucial part of photocatalytic VOC elimination and sometimes will affect the activity and regeneration of photocatalyst. In particular, the undesired intermediates such as hydrocarbons and oxygen related species often adhere to the surface of photocatalyst, which may lead to the deactivation by the saturation and poison the catalyst surface, and thus bring out decreased catalytic performance<sup>[235]</sup>. Therefore, fast desorption of the produced products from the surface of the catalyst is significant for photocatalytic VOC elimination.

### The state-of-art photocatalysts

Up to now, a series of semiconductors such as metal oxides and metal hydroxides have been developed for various photocatalytic applications<sup>[234-238]</sup>. Metal oxides are major candidates for VOC elimination via adsorption-photocatalysis coupling. Here, we present the state-of-the-art materials for VOC removal via adsorption-photocatalysis coupling technology. Meanwhile, the modification methods, operational parameters, and the mechanism for VOC removal are also thoroughly discussed.



## TiO<sub>2</sub>

As a well-studied photocatalyst, TiO<sub>2</sub> displays tremendous potential for photocatalytic VOC elimination under UV light illumination. Two forms of TiO<sub>2</sub>, anatase and rutile, with band gaps of around 3.2 and 3.1 eV, respectively, are often obtained during chemical synthesis<sup>[241-243]</sup>. In comparison with rutile, anatase always gives rise to much higher photocatalytic VOC elimination activity because its conduction band level is more likely to produce stable surface ·OH radicals<sup>[241]</sup>. In practical applications, TiO<sub>2</sub> photocatalysts are prone to agglomeration and inactivation during a long-term reaction, which reduces their VOC elimination performance. Therefore, various strategies such as substrate fixing, ions doping, surface modification coupling with other metal oxides, and noble metal loading have been explored to enhance the VOC removal activity.

### Structure and morphology modulation

The structure and morphology of TiO<sub>2</sub> have a great influence on its final photocatalytic performance. TiO<sub>2</sub> nanotubes have recently attracted much attention owing to their unique structure and morphology. For example, Xu *et al.* reported powder-type TiO<sub>2</sub> nanotubes for the enhanced photocatalytic gaseous acetaldehyde degradation ability in comparison with that of commercial P25 photocatalyst<sup>[241]</sup>. A TiO<sub>2</sub> nanotube array can be formed by loading uniform TiO<sub>2</sub> nanotubes on a titanium substrate, which shows an ordered structure and porous surface. Such a unique architecture favors reactant diffusion and transfer, thus being beneficial for the improved photocatalytic ability. Therefore, immobilization of TiO<sub>2</sub> nanotubes on a substrate is available from the view of practical air purification. Typically, highly ordered TiO<sub>2</sub> nanotube arrays on titanium foils with different lengths are fabricated by an electrochemical anodization strategy for photocatalytic degradation of gaseous acetaldehyde [Figure 19A and B]<sup>[242]</sup>. It has been revealed that enhancing the lengths of nanotube arrays to a certain degree leads to increased photocatalytic acetaldehyde molecule elimination. Moreover, the as-fabricated TiO<sub>2</sub> nanotube arrays give rise to higher photocatalytic activity than that of a commercial P25-based film with the same thickness and geometric area. This enhancement can be attributed to the unique infrastructure and morphology of the nanotube array, which was profitable for the facile mass diffusion and the prohibited deactivation of TiO<sub>2</sub> nanotube during photocatalytic degradation.

### Carbon substrate fixing

Carbon materials with abundant porous and large surface areas have been considered as promising substrates to support the distribution and fixation of TiO<sub>2</sub> photocatalysts<sup>[244,245,248-250]</sup>. Moreover, the stronger adsorption capacity, black color, and rapid electron shift on the interface of the carbon-TiO<sub>2</sub> hybrid can guarantee the adequate absorption of pollutant molecules on the active sites of photocatalyst, promote visible light harvesting, facilitate the production of active radicals, and prohibit the formation of by-products and the inactivation of photocatalysts.

For example, Li's team reported that TiO<sub>2</sub> particles are uniformly dispersed on activated carbon fibers (TiO<sub>2</sub>-ACF) [Figure 19C] through an acid treatment method for efficient formaldehyde removal<sup>[244]</sup>. The C-Ti bond and surface hydroxyl groups are formed in the TiO<sub>2</sub>-ACF composite. By changing the acid treatment time, the amounts of surface hydroxyl groups can be well tuned. Significantly, the created C-Ti bond on the interface between TiO<sub>2</sub> and ACF can promote the electron migration in the photocatalyst, and the abundant ·OH species give rise to the increased adsorption of water and formaldehyde molecules, thus bringing out more ·OH radicals. Moreover, the rich pore structures in ACFs are also beneficial for reactant molecules' transfer and transportation. The synergistic effects of the enhanced light adsorption, facile mass diffusion,

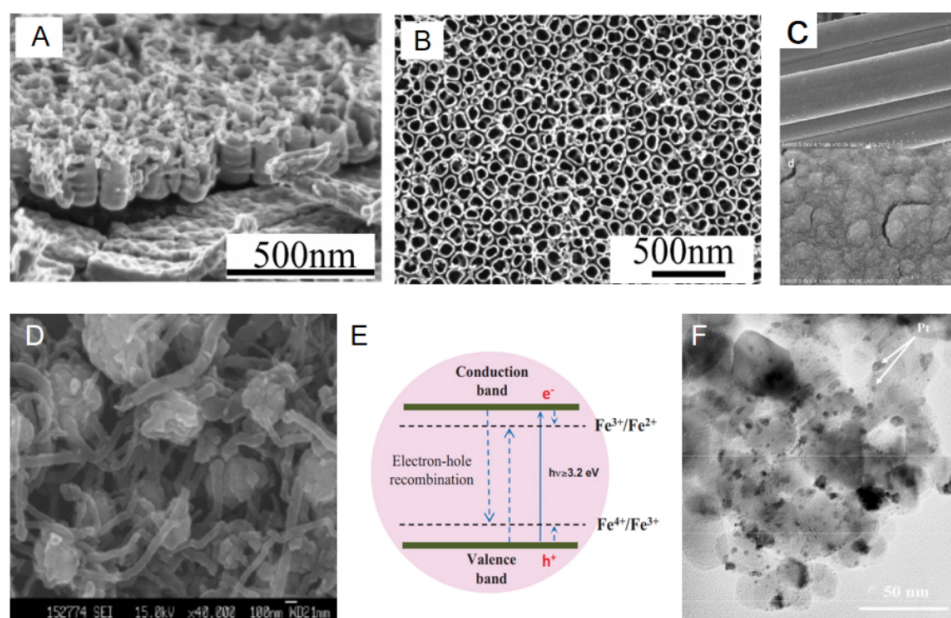


**Figure 19.** (A and B) SEM images of the  $\text{TiO}_2$  nanotube arrays<sup>[242]</sup>. This figure is used with permission from the American Physical Society. (C) SEM image of the  $\text{TiO}_2$ -ACF photocatalyst<sup>[244]</sup>. This figure is used with permission from the Elsevier. (D) SEM image of the MWCNT- $\text{TiO}_2$  composite<sup>[245]</sup>. (E) Schematic Energy diagram of  $\text{Fe}^{3+}$  doped  $\text{TiO}_2$ <sup>[246]</sup>. This figure is used with permission from the Elsevier. (F) TEM image of the Pt-loaded  $\text{TiO}_2$  photocatalyst<sup>[247]</sup>.

and improved adsorption of water molecules result in increased photocatalytic formaldehyde elimination. Specifically, the  $\text{TiO}_2$ -ACF composite exhibited 20 times higher formaldehyde removal rate than that of pure  $\text{TiO}_2$  powder.

Different from ACF discussed above, carbon nanotubes (CNTs) with a specific 1D cylinder configuration endow the unique hollow structure, which is profitable for better fixation of  $\text{TiO}_2$  particles and prolongs the residence time of VOC molecules in photocatalysts, thus making CNTs an ideal co-adsorbent and matrix for photocatalytic VOC molecule removal<sup>[245,248]</sup>.  $\text{TiO}_2$  nanosphere-loaded carbon nanotubes (MWCNT- $\text{TiO}_2$ ) were fabricated using a hydrothermal strategy by An *et al.*<sup>[245]</sup>. SEM images show that the  $\text{TiO}_2$  nanospheres with tunable crystal facets are wrapped around CNTs with sphere sizes from 200 to 600 nm [Figure 19D]. As expected, the MWCNT- $\text{TiO}_2$  composite exhibited higher activity for the photocatalytic degradation of styrene gas than that of single anatase  $\text{TiO}_2$ . The improved styrene gas degradation performance for composite is attributed to the synergistic effects of nanostructured  $\text{TiO}_2$  spheres and the positive function of CNTs. Specifically, by modulating the reaction conditions such as the ratios of CNTs/ $\text{TiO}_2$  and temperature of hydrothermal preparation,  $\text{TiO}_2$  spheres with various crystal facets can be obtained. Moreover, the merits of CNTs in promoting VOC molecule absorption and increasing contact between styrene and CNT- $\text{TiO}_2$  are involved. All the above facts are beneficial for the styrene molecule decomposition process.

Graphene possessing 2D layers of  $\text{sp}^2$  hybridized carbon atoms displays a variety of merits such as good electronic conductivity and thermal conductivity and has been widely used in catalytic fields<sup>[249]</sup>. However, a single layer of graphene is prone to be aggregated because of its great van der Waals force. Moreover, the hydrophobic surface of graphene is not suitable to load and disperse oxides and attract VOC molecules. In this regard, some methods such as oxidation and acid treatment have been exploited to modify graphene. Up to today, graphene derivatives including graphene oxide (GO) and reduced graphene oxide (rGO),

endowed with abundant oxygen related groups such as hydroxyl, carboxylic, and carbonyl species on their surface, bring out both anchor dispersibility and favorable adsorption sites for oxide particles to facilitate VOC molecule removal.

For instance, Roso *et al.* synthesized a series of graphene-based  $\text{TiO}_2$  hybrids and studied the effects of various co-catalysts (graphene, GO, and rGO) on the photocatalytic methanol vapor elimination ability<sup>[250]</sup>. They found that the morphologies of as-prepared composites depend on the type of graphene used. Graphene and GO are prone to be located inside the final composites, leaving  $\text{TiO}_2$  on the outer surface of composites to contact with VOC molecules. As to the rGO/ $\text{TiO}_2$  hybrid, the  $\text{TiO}_2$  nanoparticles are uniformly dispersed between nanofibers due to the partial affinity of the composite with the polymer matrix. The configuration of rGO/ $\text{TiO}_2$  is favorable for VOC molecule degradation because of the imitate contact with the photocatalyst and lower mass-transfer restrictions. Therefore, the functional groups on rGO surface exert significant function in affecting the adsorption–photocatalytic process during VOC molecule removal. Finally, the rGO/ $\text{TiO}_2$  hybrid brings out the best activity for photocatalytic gas-phase methanol degradation.

As discussed above,  $\text{TiO}_2$  immobilization on various carbon substrates is useful for improved adsorption-photocatalysis VOC removal. Adopting an available coating method and type of carbon substrate, two important facts in  $\text{TiO}_2$  fixing should be considered. The used carbon substrate must have extraordinary physical and chemical stability in long-term photocatalysis VOC removal. Moreover, a carbon substrate with a large surface area or abundant porous structure for the  $\text{TiO}_2$  fixing is necessary. Other fundamental characteristics of the carbon substrate are also required, such as strong attraction of  $\text{TiO}_2$  nanoparticles, resistance against high calcination temperatures, and efficient absorbance ability for VOC molecules.

### Metal ion doping

Transition metal ions are frequently doped into the lattice of  $\text{TiO}_2$  for efficient photocatalysis VOC removal<sup>[246,251,252]</sup>. The new energy level can be created in the band gap of  $\text{TiO}_2$ , thus promoting visible light absorption. When the metal dopants substitute the sites of  $\text{Ti}^{4+}$ , the new energy level is formed near the CB of  $\text{TiO}_2$ , which can significantly promote photoinduced electron-hole pairs separation for the improved photocatalytic ability. In fact, the photocatalytic activity of metal ion-doped  $\text{TiO}_2$  depends on several factors such as the amounts of dopants, the chemical properties of dopants, and the preparing conditions. Next, we outline several common metal ion dopants and discuss their photocatalytic VOC removal activity and limitations.

Transition metals such as Fe, Cu, and Ni can also be doped into  $\text{TiO}_2$  for enhanced photocatalytic VOC removal activity due to the enhanced carrier separation and the reduced band gap<sup>[246,251-254]</sup>. More importantly, the lower cost of transition metals in comparison with noble metals is expected to lead to widespread utilization in large-scale industrial applications. Besides, the category and concentration of transition metal dopants are major factors in determining the photocatalytic VOC removal ability. The optimal amount of transition metal dopant is of great significance. When the amount is over the optimal value, the photocatalytic ability will decrease because more dopants will crash the lattice of  $\text{TiO}_2$  and serve as a recombination site. Moreover, the change of chemical valence states (such as  $\text{Fe}^{3+}/\text{Fe}^{2+}$  and  $\text{Ni}^{2+}/\text{Ni}^{+}$ ) of transition metal ions [Figure 19E] can also promote photoinduced electron-hole pair separation and facilitate photoelectrons transfer to oxygen to produce  $\cdot\text{O}_2^-$  radicals<sup>[246]</sup>. Hence, many studies are dedicated to investigating the optimal category and amount of dopant for the best photocatalytic VOC removal activity. For example, Yang *et al.* reported that iron-doped  $\text{TiO}_2$  was prepared on flexible glass fibers by a sol-gel

strategy for the improved photocatalytic elimination of benzene, toluene, ethylbenzene, and o-xylene<sup>[252]</sup>. Tieng *et al.* found that Fe<sup>3+</sup> dopant in TiO<sub>2</sub> serving as trapping sites can effectively trap both photoinduced electrons and holes and maintain a long lifetime of photo-charges, thus giving rise to the higher photocatalytic ethylene degradation than that of pure TiO<sub>2</sub> photocatalyst.

Although metal ion doping leads to efficient photocatalytic VOC removal, some disadvantages still exist. For example, doping TiO<sub>2</sub> with Fe ions will lead to partial blockage on TiO<sub>2</sub> porous surface sites and cause the growth of particles, thus resulting in a reduced specific surface area and decreased photocatalytic activity. Therefore, the design of low-cost and efficient transition metals doped into TiO<sub>2</sub> is worthy of further study in the future.

### Nonmetal ion doping

Nonmetal ion doping in TiO<sub>2</sub> materials has been considered an effective way to improve adsorption-photocatalysis VOC removal by enhancing the photo-response and modulating the energy configuration. Generally, the nonmetal ions replace the oxygen in the TiO<sub>2</sub> matrix and result in a reduced band gap for more visible light absorption. For TiO<sub>2</sub> photocatalyst, nonmetal ions such as C and N are frequently adopted into the TiO<sub>2</sub> lattice for enhanced photocatalytic VOC elimination<sup>[255-257]</sup>.

C-doped TiO<sub>2</sub> with mesoporous structure was fabricated via a hydrothermal method with Ti (SO<sub>4</sub>)<sub>2</sub> and glucose as precursors by Dong *et al.*<sup>[255]</sup>. A series of characterizations demonstrated that the oxygen atoms in the TiO<sub>2</sub> were replaced by carbon atoms, and a new O-Ti-C bond was created. Meanwhile, a new mid-gap state was produced in the band gap of TiO<sub>2</sub>, thus promoting visible light absorption and prohibiting photoinduced carrier recombination. Based on these advantages, the as-synthesized C-doped TiO<sub>2</sub> photocatalyst showed higher activity in photocatalytic toluene vapor elimination than that of commercial P25 and C-doped TiO<sub>2</sub> synthesized by the solid-state route. Soon after, the post-thermal treatment of the obtained C-doped TiO<sub>2</sub> for further improved photocatalytic VOC elimination was also developed by this team<sup>[256]</sup>. The improvement of gaseous toluene elimination was found by the post-thermal treatment of the C-doped TiO<sub>2</sub> between 100 and 300 °C, and the optimal thermal treatment temperature was 200 °C. The enhancement can be attributed to the changes in the surface chemistry and optical properties of C-doped TiO<sub>2</sub>. Specifically, thermal treatment repairs the surface defects and thus restricts the recombination of photoinduced carrier pairs. Moreover, the visible light absorption was further increased after post-thermal treatment.

Although nonmetal ion doping exerts an efficient function in promoting photocatalytic VOC elimination, some drawbacks still exist. For example, doping nonmetal ions into the TiO<sub>2</sub> lattice leads to the generation of oxygen vacancies, which may serve as an active site to facilitate photoinduced charge carrier recombination and thus are detrimental to the enhanced photocatalytic VOC removal. Thus, optimizing the synthesis route and precisely controlling the location and amount of oxygen vacancies in the TiO<sub>2</sub> lattice are of great importance for acquiring better photocatalytic VOC removal activity. Moreover, the synthesis route and cost for the photocatalyst should also be considered for large-scale VOC treatment. In general, the doping of nonmetal ions into the TiO<sub>2</sub> lattice needs high thermal treatment temperatures (> 500 °C) and a long synthesis time; hence, tremendous energy consumption is inevitable. Meanwhile, the utilization of detrimental, expensive, or unstable raw materials is often involved during the synthesis process. Therefore, finding a green, facile, low-cost, and sustainable preparation process is necessary for large-scale photocatalyst production.

## Noble metal loading

Noble metals such as Pd, Pt, and Ag can expand the visible light absorption of  $\text{TiO}_2$  photocatalysts<sup>[247,258,259]</sup>. Meanwhile, a Schottky barrier can be created at the noble metal- $\text{TiO}_2$  interface, which can retard the carrier recombination and thus increase photocatalysis activity. More importantly, noble metals possess extraordinary resistance to oxidation and corrosion in a humid atmosphere. For example, silver-doped  $\text{TiO}_2$  photocatalysts with various silver amounts were prepared by Mogal *et al.*<sup>[258]</sup>. The obtained silver-doped  $\text{TiO}_2$  photocatalysts presented improved photocatalytic phthalic acid degradation under UV light excitation due to the fast carrier separation and low-energy band gap. Similarly, enhanced ethanol partial oxidation degradation was also achieved over the Pt doped  $\text{TiO}_2$  catalyst [Figure 19F]<sup>[247]</sup>.

## Coupling with other metal oxides

Coupling with other metal oxides such as  $\text{SiO}_2$  and  $\text{WO}_3$  has been developed for enhanced photocatalytic VOC molecule removal<sup>[260-262]</sup>. Thus far, much research has focused on  $\text{TiO}_2/\text{SiO}_2$  composites. Although  $\text{SiO}_2$  is a total insulator and has no photocatalytic ability, the introduction of  $\text{SiO}_2$  components in the composites can change the structure and surface functional group, such as pore volume and hydrophilic properties, thus influencing the final VOC molecule removal ability.

For example, Guan *et al.* found that the surface of  $\text{TiO}_2/\text{SiO}_2$  shows stronger hydrophilic properties than that of pure  $\text{TiO}_2$ <sup>[260]</sup>. Specifically, the introduction of  $\text{SiO}_2$  improves the acidity and leads to the enhancement of the hydroxyl amount in the composite films, thus favoring VOC molecules absorption and leading to promoted VOCs degradation (Figure 20A). Yu *et al.* confirmed that the grain size of  $\text{TiO}_2/\text{SiO}_2$  hybrid was reduced when increasing the ratio of  $\text{SiO}_2$ <sup>[262]</sup>. Meanwhile, the rich hydroxyl species adhered to the surface of  $\text{TiO}_2/\text{SiO}_2$  hybrid. The reduced size of  $\text{TiO}_2$  may lead to a stronger driving force for photocarriers migration existing in quantum-sized  $\text{TiO}_2$  in the  $\text{TiO}_2/\text{SiO}_2$  hybrid. Meanwhile, the increased surface area brings out an enhanced adsorption ability of VOC molecules. More importantly, the abundant -OH species on the surface can trap photoinduced holes and thus restrict the recombination of electron-hole pairs. All these factors are favorable for the enhanced photocatalytic VOC elimination. As a result, hybrid  $\text{TiO}_2/\text{SiO}_2$  photocatalytic activities of the composite thin films are still higher than that of pure  $\text{TiO}_2$ .

Zou *et al.* prepared the  $\text{TiO}_2\text{-SiO}_2$  pellets using the sol-gel method<sup>[261]</sup>. The  $\text{TiO}_2\text{-SiO}_2$  pellets presented high surface areas and abundant porous structure [Figure 20B], therefore giving rise to the strong adsorption capacity of VOCs. A series of characterizations suggested that the  $\text{TiO}_2\text{-SiO}_2$  pellets exerted two functions as a photocatalyst and as an adsorbent in the adsorption-photocatalysis coupling system for gaseous toluene elimination. It is noteworthy that the catalyst can be self-regenerated by photocatalytic oxidation of the adsorbed toluene molecules. Thus, the  $\text{TiO}_2\text{-SiO}_2$  pellets can be used for continuous VOC removal in a fixed-bed reactor under UV light illumination.

## Surface modification

Surface modification has been developed to increase the photocatalytic activity of  $\text{TiO}_2$ <sup>[262,263]</sup>. Sumitsawan *et al.* adopted a plasma discharge method to treat  $\text{TiO}_2$  nanoparticles adhering to a glass substrate<sup>[263]</sup>. It is found that the  $\text{TiO}_2$  nanoparticles can be fluorinated (Ti-F) or covered with perfluorocarbon film (C-F) by controlling the plasma discharge conditions. Both modified  $\text{TiO}_2$  photocatalysts showed higher photocatalytic m-xylene elimination than that of pristine  $\text{TiO}_2$  nanoparticles. The water contact angle test suggested that plasma surface treatment can convert  $\text{TiO}_2$  nanoparticles from hydrophilic to hydrophobic [Figure 20C and D]. Pristine  $\text{TiO}_2$  presents as completely wettable at the contact angle of the water droplet.



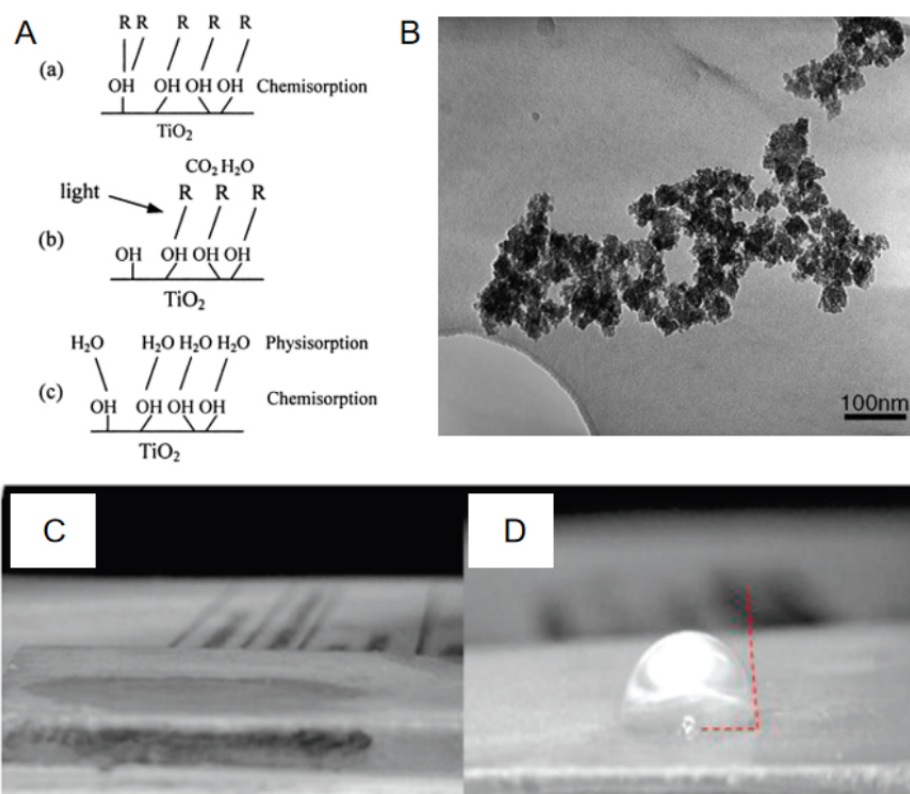


**Figure 20.** (A) Schematic VOC molecule absorption and degradation on the hydrophilic TiO<sub>2</sub>-SiO<sub>2</sub> films<sup>[260]</sup>. (B) TEM image of the as-prepared TiO<sub>2</sub>-SiO<sub>2</sub> photocatalyst<sup>[261]</sup>. Water contact angle of untreated TiO<sub>2</sub> (C) and plasma treated TiO<sub>2</sub><sup>[263]</sup>. (D) This figure is used with permission from the American Physical Society.

In contrast, the plasma-treated TiO<sub>2</sub> shows a contact angle and is thus considered hydrophobic. The hydrophobic character of modified TiO<sub>2</sub> could enhance the adsorption of the xylene from the flowing air to the surface of the photocatalyst and thus favor the improved photocatalytic activity.

#### Other metal oxides

In addition to TiO<sub>2</sub>, other metal oxides such as WO<sub>3</sub> and Ga<sub>2</sub>O<sub>3</sub> have also been explored for photocatalytic VOC elimination<sup>[264-267]</sup>. WO<sub>3</sub>, as a typical semiconductor with a band gap value of about 2.5 eV, is widely used in photocatalytic oxidation reactions due to its positive VB potential (about 3.15 eV vs. NHE) and good chemical stability<sup>[264]</sup>. However, pure WO<sub>3</sub> photocatalyst usually displays insufficient photocatalysis oxidation ability because the lower CB edge (+0.3 - 0.5 eV vs. NHE) cannot afford enough reduction ability to reduce O<sub>2</sub> to produce strongly oxidizing radicals such as •O<sub>2</sub><sup>-</sup> and •HO<sub>2</sub>. The inability for O<sub>2</sub> reduction by photoinduced electrons on the CB of WO<sub>3</sub> may also cause the undesired recombination of electron-hole pairs and thus result in poor photocatalytic oxidation ability. It has been revealed that platinum nanoparticles loading can promote the multi-electron reduction of dioxygen to produce active oxygen related species on the CB of WO<sub>3</sub> at a relatively positive reduction potential and thus are favorable for high photocatalytic oxidation ability. Kim *et al.* reported that the Pt/WO<sub>3</sub> composite gives rise to higher activity for photocatalytic VOC [dichloroacetate (DCA), 4-chlorophenol (4-CP), tetramethylammonium (TMA), and arsenite] removal than that of pure WO<sub>3</sub><sup>[267]</sup>. Specifically, the loading of platinum nanoparticles led to concurrent oxidative reactions on the surface of WO<sub>3</sub>; meanwhile, the OH radicals were also produced by the reductive decomposition of H<sub>2</sub>O<sub>2</sub>, which was formed via the in situ reduction of O<sub>2</sub>. It is noteworthy that Pt/WO<sub>3</sub> presented a higher rate of H<sub>2</sub>O<sub>2</sub> generation than that of WO<sub>3</sub>, thus favoring the OH radical



formation and leading to the promoted photocatalytic oxidation performance [Figure 21A and B].

Hou *et al.* fabricated porous Ga<sub>2</sub>O<sub>3</sub> for efficient photocatalytic benzene decomposition<sup>[265]</sup>. Significantly, the photocatalytic elimination rate of gaseous benzene over Ga<sub>2</sub>O<sub>3</sub> was about two times greater than that of commercial P25. This enhancement can be attributed to that Ga<sub>2</sub>O<sub>3</sub> possesses stronger oxidative capability due to its more positive CB level [Figure 21C] and higher specific surface area in comparison with P25 photocatalyst.

#### *Metal hydroxide*

Apart from the above-mentioned metal oxides, metal hydroxide can also be used as a photocatalyst in adsorption-photocatalysis coupling for VOC removal<sup>[268-270]</sup>. For example, In (OH)<sub>3</sub> is a wide-gap semiconductor and can be used for UV light-driven photocatalytic reactions. Thus, using In (OH)<sub>3</sub> materials in adsorption-photocatalysis coupling has been conducted. Typically, In (OH)<sub>3</sub> nanocrystals with mesoporous structure have been fabricated by peptization of a colloidal precipitate with a post-heat treatment for acetone, benzene, and toluene degradation under UV light irradiation<sup>[268]</sup>. Specifically, the In (OH)<sub>3</sub> sample with a post-heat treatment temperature of 120 °C gives rise to the optimal photocatalytic performance for acetone degradation [Figure 21D], which can be ascribed to several major factors. Firstly, the In (OH)<sub>3</sub> sample post-treated at 120 °C exhibits the highest specific surface area. Therefore, more VOC molecules can be attracted on the surface of In (OH)<sub>3</sub>, favoring enhanced photocatalytic ability. In addition to the surface area, the porous character of In (OH)<sub>3</sub> sample can also lead to its enhanced activity. Specifically, the existence of abundant mesopores in the In (OH)<sub>3</sub> nanoparticles brings out the fast diffusion and transfer of organic molecules during the photocatalytic process and increases the VOC removal rate. Finally, the crystal phase should be considered during the photocatalytic process. When the post-heat treatment temperature is over 120 °C, the new phase of In<sub>2</sub>O<sub>3</sub> is formed due to the transformation from In (OH)<sub>3</sub>. The reduced ratio of In (OH)<sub>3</sub> in the photocatalyst results in low photocatalytic performance. Thus, the post-heat treatment temperature of 120 °C is the optimal condition for obtaining the In (OH)<sub>3</sub> with the best photocatalytic activity.

#### **Factors affecting PCO performance**

Generally, several factors such as humidity, airflow rate, light source, and the initial VOC concentration significantly influence adsorption-photocatalysis coupling for VOC removal. These factors are thoroughly outlined in this section.

#### *Humidity*

The relative humidity plays a great role during the photocatalytic oxidation process. In fact, the humidity can be both profitable and detrimental to VOC degradation<sup>[232,233]</sup>. Particularly, water molecules can take part in the photocatalytic removal process by serving as competitive adsorbents and resources of ·OH radicals. For the competitive adsorbents, water molecules absorbing on the surface active sites of photocatalysts will decrease the adsorption ability of VOC molecules and restrict the subsequent photocatalytic reactions<sup>[268]</sup>. As to the resources of ·OH radicals, the produced ·OH radicals from water molecules can accelerate the photocatalytic oxidation reaction, thus favoring photocatalytic VOC removal<sup>[271]</sup>. Hence, carefully modulating the relative humidity for efficient photocatalytic VOC removal is of great significance.

#### *Airflow rate*

Increasing the airflow rate can present two distinct effects for photocatalytic VOC removal<sup>[234,265,266,272]</sup>. On the one hand, a fast airflow rate will lead to the reduced residence time for photocatalytic VOC oxidation and thus decrease VOC degradation ability. On the other hand, the promoted mass migration between the VOC

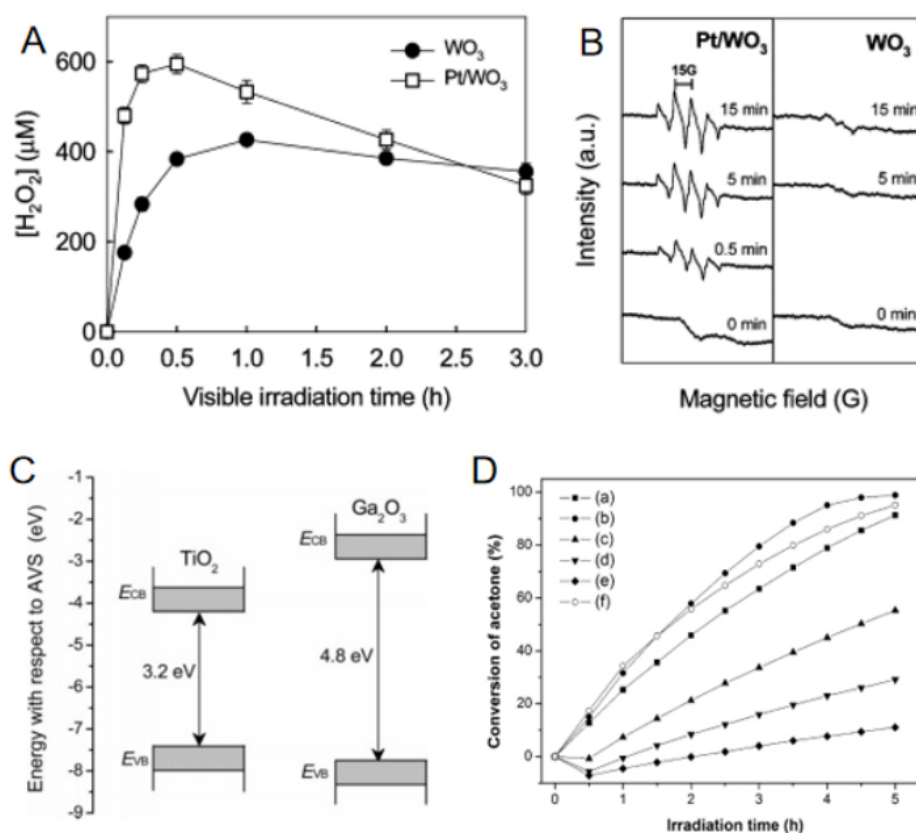


**Figure 21.** (A) Formation of  $\text{H}_2\text{O}_2$  over  $\text{WO}_3$  and  $\text{Pt}/\text{WO}_3$  under visible-light excitation. (B) ESR spectra of DMPO-OH• adducts in an aqueous dispersion of  $\text{Pt}/\text{WO}_3$  and  $\text{WO}_3$ . (C) Bandgap structure of  $\text{WO}_3$  and  $\text{Ga}_2\text{O}_3$ . (D) The photocatalytic acetone oxidation over  $\text{In}(\text{OH})_3\text{S}$  treated at various temperatures: (a) 60 °C; (b) 120 °C; (c) 160 °C; (d) 200 °C; and (e) 250 °C. (f) P25 was adopted as a reference. This figure is used with permission from the American Physical Society.

molecules and photocatalysts under a high airflow rate can improve the pollutant removal efficiency. Based on the above discussion, finding an optimum airflow rate to achieve maximum residence time of photocatalytic oxidation reaction and simultaneously optimal mass migration between the VOC molecules and photocatalysts is of significant importance to acquire the highest photocatalytic VOC molecule degradation efficiency.

Yang *et al.* studied the influence of various airflow rates on photocatalytic gaseous formaldehyde removal. It was revealed that enhancing airflow rate brings out a fast mass transfer and a low concentration gradient between the bulk and the photocatalyst surface in laminar regimes. The influence of airflow rate on pollutant elimination falls under three distinct regimes. In low airflow rates, improving airflow rate favors VOC molecule elimination, which suggests that mass transfer on the surface of photocatalyst restricts VOC removal. In intermediate airflow rates, flow rate variation has no considerable effect on VOC removal. This means that surface reaction kinetics is the controlling stage. Finally, in high airflow rates, an increased airflow rate decreases the residence time for transferring VOCs contaminants from the gas phase to the catalyst surface, thereby decreasing the VOC removal rate.

#### Light source

Photogenerated electron-hole pairs are the key factor during the photocatalytic VOC pollutant oxidation process. Frequently used catalysts such as  $\text{TiO}_2$  need a UV light equivalent energy source for the

illumination to produce photoinduced charge carriers. Among a series of reports, high-pressure mercury lamps, xenon lamps, and UV lights are major light sources for photocatalytic VOC removal<sup>[271-273]</sup>. Generally, the VOC elimination rate is proportional to the power of the light source. The photocatalytic VOC removal rate can be modulated by the first order of depletion rate of photogenerated carriers and a half order of their recombination speed. Therefore, the power of the light source has a direct influence on the removal rate. As UV light is deleterious to human beings and possibly results in forming secondary pollutants such as strong oxidizing species in the atmosphere<sup>[273]</sup>, visible-light-driven VOC removal should be further researched in detail.

#### *Deactivation and reactivation*

The chemical and physical stability of photocatalysts is very important for long-term VOC removal. In fact, deactivation, regeneration, and reactivation often occur during the photocatalytic VOC treatment process<sup>[234]</sup>. For the adsorption-photocatalysis coupling system, the photocatalytic rate usually decreases with extending reaction time and the surface active sites simultaneously reduce due to the deactivation of the photocatalyst. The accumulation of reaction intermediates on the surface of photocatalyst leads to deactivation because these intermediates occupy active sites. For example, reaction intermediates such as formic acid are often adhered to the surface of TiO<sub>2</sub> photocatalyst due to its strong affinity during photocatalytic acetaldehyde elimination<sup>[235]</sup>. Although a certain amount of formic acid can be emitted into the atmosphere, the occupation of the surface active site results in the deactivation of TiO<sub>2</sub> photocatalyst. In practical application, the photocatalyst will be totally deactivated after 20 consecutive photocatalytic acetaldehyde degradation reactions because all the active sites capture reaction intermediates<sup>[274]</sup>. Therefore, the recovery of photocatalyst is put on the agenda. Typically, the absorbed reaction intermediates, including benzaldehyde and benzoic acid, could be totally removed with a heat treatment over 653 K. Hence, the reactivation of the photocatalysts by post calcination is often adopted.

#### *Pollutant concentration*

The pollutant concentration has a non-negligible effect on photocatalytic VOC removal<sup>[275]</sup>. Many studies have suggested that the appropriately lower concentrations of VOC lead to the increased elimination ability of VOCs, which is ascribed to the active sites of photocatalysts possessing limited adsorption capacity<sup>[275-277]</sup>. Moreover, the produced reaction intermediates will prohibit the adsorption of VOC molecules, especially when the pollutant concentration is high in the reaction system. As a result, the adsorption-photocatalysis coupling reaction system is more likely to treat VOCs at a relatively low concentration. As to the high concentration VOC removal, the surface of the photocatalyst will become saturated because of the shielding effect of the pollutant molecules and is thus detrimental to the efficient VOC treatment<sup>[277]</sup>. Moreover, the saturation and competition of photocatalyst between adsorbed pollutants are higher when inlet VOCs are at a high concentration.

## **CONCLUSION AND OUTLOOK**

Human exposure to VOCs in the air is unavoidable in everyday life. Some VOCs are categorized as carcinogenic or reprotoxic by the European Union and the World Health Organization. Air-liquid interface exposure systems can be used to assess the toxicity of VOC emissions on respiratory symptoms. These techniques have the advantage of eliminating any direct interaction between the tested toxicants and the culture medium's components. Some experiments have used this technique to investigate the toxicity of single and mixed VOCs, as well as the compounds generated during the total catalytic oxidation of VOCs. By measuring the activation of XMEs, which are conventionally induced by polycyclic organic compounds, as well as the activation of AhR, in lung cells exposed to emissions from the catalytic degradation of toluene, the formation of high molecular weight compounds in total catalytic oxidation of VOCs can be deduced.

The toxicological study used to validate the system revealed the existence of by-products such as PAHs that were not discovered by the standard analytical method after the catalytic test. Therefore, adding an adsorption system seems to be a promising approach for thorough purification and validation of the catalytic processes. In this context, physico-chemical characterization of gaseous effluent is essential to implement an adapted and efficient VOC treatment technology. Data concerning the process, the chemicals used, and the effluent parameters (temperature, humidity, dust content, pressure, flow, *etc.*) must be collected first. Then, chemical analysis can be performed on a laboratory scale on the raw materials in order to prepare accurate on-site measurements. At last, continuous (e.g., THC analyzer) and semi-continuous (e.g., specific on-line analyzers, sampling on sorbent tubes, impingers, and containers) analytical techniques can be deployed on site for detailed evaluation. Continuous measurements give valuable information concerning the emission profile (cyclic or regular process) and the global concentration level, whereas semi-continuous techniques give detailed information about the specific VOCs involved. Depending on the industrial process studied, the VOC mixture to be treated can be quite complex and contain several chemical groups (e.g., aromatics, alcohol, esters, *etc.*), which may not react in the same way to the treatment technique.

In this review, three coupling techniques are presented, outlining their advantages and characteristics for effective removal of hazardous VOCs:

- Adsorption-catalytic oxidation:

Adsorption and catalytic oxidation are both efficient ways of environmental remediation of VOCs, whereas these techniques are sometimes not sufficient for some industrial applications, which produce low concentrated VOC emissions. Coupled, these systems become more adapted to treat diluted gaseous streams of VOCs (> 1%) since the adsorbent helps ensure a pre-concentration of VOCs before their elimination by catalytic oxidation. Adsorbents can act as solid catalysts, can be used as a support for a catalytic phase ensuring a high dispersion of the active species, and can be used prior to the catalytic set to eliminate organic or inorganic compounds (such as H<sub>2</sub>S). The most used adsorbents cited in the literature are activated carbon (AC), biochar, zeolites, *etc.* Experimental conditions are important to surpass some of the drawbacks these materials can present. Hybrid adsorption-catalytic technology exhibiting high adsorption capacity, catalytic activity, and selectivity is provided as a new practical, efficient, and economical alternative to the conventional VOC removal treatments for controlling small concentrations of VOCs in industrial emissions.

- Adsorption-plasma catalysis:

Although NTP has been proposed as an end-of-pipe technology for the removal of VOCs, the formation of toxic by-products is still the major hindrance to the commercialization of this technique. The main strength of plasma catalysis lies in the synergetic effect of the two individual technologies, which enhances the mineralization efficiency and reduces the formation of unwanted by-products by catalysis. For in-plasma catalysis (IPC), the catalytic material is placed either within the plasma discharge or in the downstream of the plasma discharge (post-plasma catalysis). Several points are important for a catalyst suitable for NTP environment: its stability in plasma and in situ regeneration by NTP exposure. Although plasma catalysis has been proven more efficient than the individual techniques for VOC abatement, the treatment of a large volume of exhaust gas containing a very low concentration of VOCs needs an alternative approach: adsorption-plasma catalysis (APC).

- Adsorption-photocatalysis:

The adsorption-photocatalysis coupling technology is also one of the effective and promising methods for VOC removal. Compared with the high temperature and pressure adopted during adsorption-catalysis and plasma catalysis processes, the adsorption-photocatalysis process gives rise to obvious advantages in VOC removal such as excellent elimination efficiency, low energy depletion, and being environmentally friendly. Metal oxides are major candidates for VOC elimination via adsorption-photocatalysis coupling. Generally, several factors such as humidity, airflow rate, light source, and the initial VOC concentration significantly influence adsorption-photocatalysis coupling for VOC removal. As a result, the adsorption-photocatalysis coupling reaction system is more likely to treat VOCs at a relatively low concentration.

Therefore, for any industrial emission, one of these coupling techniques should provide complete, low-energy VOC removal. On-site characterization is essential to making the choice, and a toxicological validation is recommended to determine if an additional coupling adsorbent is needed for the complete removal of VOCs.

## DECLARATIONS

### Acknowledgement

The authors want to acknowledge Karen Leus (Univ. Ghent, Research Unit Plasma Technology) for her contribution in obtaining the copyrights permissions of the figures and tables of the adsorption/plasma catalysis part in this review.

### Authors' contributions

This review is the result of a collaborative work between different teams and laboratories in the Interreg project:

- Toxicity of VOCs:

-Substantial contributions to conception, data curation and design of the study: Billet S, Landkocz Y, Méausoone C, Jaber N, Courcot D

-Writing-original draft preparation and review editing: Billet S

- Measurements of VOCs:

-Substantial contributions to conception, data curation and design of the study, writing-original draft preparation and review editing: Cazier F, Dewaele D, Genevray P

- Adsorption/catalysis of VOCs:

-Substantial contributions to conception, data curation and design of the study: El Khawaja R, Poupin C, Cousin R, Heymans N, De Weireld G, Siffert S

-Writing-original draft preparation and review editing: El Khawaja R, Siffert S

- Adsorption/plasma catalysis of VOCs:

-Substantial contributions to conception, data curation and design of the study: Veerapandian SKP, Bitar R, Abdallah G, Sonar S, Morent R, De Geyter N, Löfberg A, Lamonier JF, Giraudon JM

-Writing-original draft preparation: Veerapandian SKP, Bitar R

- Adsorption/photocatalysis of VOCs:

-Substantial contributions to conception, data curation and design of the study, writing-original draft preparation and review: Barakat T, Ding Y, Su BL

All authors contributed to the discussion and the revision of the paper. They have all read and agreed to the published version of the manuscript.

**Availability of data and materials**

Not applicable.

**Financial support and sponsorship**

The “DepollutAir” project (grant number 1.1.18) of the European Program INTERREG V France-Wallonie-Vlaanderen (FEDER), Région Wallone and Région Hauts-de-France are acknowledged for the funding and their support for this work.

**Conflicts of interest**

All authors declared that there are no conflicts of interest.

**Ethical approval and consent to participate**

Not applicable.

**Consent for publication**

Not applicable.

**Copyright**

© The Author (s) 2022.

**REFERENCES**

1. World Health Organization. Ambient air pollution: a global assessment of exposure and burden of disease; 2016. Available from: <https://apps.who.int/iris/handle/10665/250141> [Last accessed on 28 Jun 2022].
2. Dehghani M, Fazlzadeh M, Sorooshian A, et al. Characteristics and health effects of BTEX in a hot spot for urban pollution. *Ecotoxicol Environ Saf* 2018;155:133-43. DOI PubMed
3. Billionnet C, Gay E, Kirchner S, Leynaert B, Annesi-Maesano I. Quantitative assessments of indoor air pollution and respiratory health in a population-based sample of French dwellings. *Environ Res* 2011;111:425-34. DOI PubMed
4. Lim SK, Shin HS, Yoon KS, et al. Risk assessment of volatile organic compounds benzene, toluene, ethylbenzene, and xylene (BTEX) in consumer products. *J Toxicol Environ Health A* 2014;77:1502-21. DOI PubMed
5. Parra M, Elustondo D, Bermejo R, Santamaria J. Quantification of indoor and outdoor volatile organic compounds (VOCs) in pubs and cafés in Pamplona, Spain. *Atmospheric Environment* 2008;42:6647-54. DOI
6. Waring MS, Siegel JA. An evaluation of the indoor air quality in bars before and after a smoking ban in Austin, Texas. *J Expo Sci Environ Epidemiol* 2007;17:260-8. DOI PubMed
7. Lan Q, Zhang L, Li G, et al. Hematotoxicity in workers exposed to low levels of benzene. *Science* 2004;306:1774-6. DOI PubMed PMC
8. Baan R, Grosse Y, Straif K, et al. A review of human carcinogens - part F: chemical agents and related occupations. *The Lancet Oncology* 2009;10:1143-4. DOI PubMed
9. Guha N, Loomis D, Grosse Y, et al. Carcinogenicity of trichloroethylene, tetrachloroethylene, some other chlorinated solvents, and their metabolites. *The Lancet Oncology* 2012;13:1192-3. DOI PubMed
10. Marques MM, Beland FA, Lachenmeier DW, et al. Carcinogenicity of acrolein, crotonaldehyde, and arecoline. *The Lancet Oncology* 2021;22:19-20. DOI PubMed
11. Plenge-Bönig A, Karmaus W. Exposure to toluene in the printing industry is associated with subfecundity in women but not in men. *Occup Environ Med* 1999;56:443-8. DOI
12. Svensson BG, Nise G, Erfurth EM, Nilsson A, Skerfving S. Hormone status in occupational toluene exposure. *Am J Ind Med* 1992;22:99-107. DOI PubMed
13. Paterson CA, Sharpe RA, Taylor T, Morrissey K. Indoor PM2.5, VOCs and asthma outcomes: a systematic review in adults and their home environments. *Environ Res* 2021;202:111631. DOI PubMed
14. Monteil C. Acrolein toxicity: comparative in vitro study with lung slices and pneumocytes type II cell line from rats. *Toxicology* 1999;133:129-38. DOI PubMed
15. Win-Shwe TT, Fujimaki H. Neurotoxicity of toluene. *Toxicol Lett* 2010;198:93-9. DOI PubMed
16. Bolden AL, Kwiatkowski CF, Colborn T. New look at BTEX: are ambient levels a problem? *Environ Sci Technol* 2015;49:5261-76. DOI PubMed
17. Hirsch T, Weiland SK, von Mutius E, et al. Inner city air pollution and respiratory health and atopy in children. *Eur Respir J* 1999;14:669-77. DOI PubMed
18. Rumchev K, Spickett J, Bulsara M, Phillips M, Stick S. Association of domestic exposure to volatile organic compounds with asthma



- in young children. *Thorax* 2004;59:746-51. DOI PubMed PMC
19. Hulin M, Caillaud D, Annesi-Maesano I. Indoor air pollution and childhood asthma: variations between urban and rural areas. *Indoor Air* 2010;20:502-14. DOI PubMed
20. Ortega C, Hernandez-trujillo V. Exposure to indoor endocrine-disrupting chemicals and childhood asthma and obesity. *Pediatrics* 2019;144:S42-S42. DOI PubMed
21. Billionnet C, Sherrill D, Annesi-Maesano I; GERIE Study. Estimating the health effects of exposure to multi-pollutant mixture. *Ann Epidemiol* 2012;22:126-41. DOI PubMed
22. Arif AA, Shah SM. Association between personal exposure to volatile organic compounds and asthma among US adult population. *Int Arch Occup Environ Health* 2007;80:711-9. DOI PubMed
23. Ware JH, Spengler JD, Neas LM, et al. Respiratory and irritant health effects of ambient volatile organic compounds. The Kanawha County Health Study. *Am J Epidemiol* 1993;137:1287-301. DOI PubMed
24. Duong A, Steinmaus C, McHale CM, Vaughan CP, Zhang L. Reproductive and developmental toxicity of formaldehyde: a systematic review. *Mutat Res* 2011;728:118-38. DOI PubMed PMC
25. Huff JE, Eastin W, Roycroft J, Eustis SL, Haseman JK. Carcinogenesis studies of benzene, methyl benzene, and dimethyl benzenes. *Ann N Y Acad Sci* 1988;534:427-40. DOI PubMed
26. Kodavanti PR, Royland JE, Moore-Smith DA, et al. Acute and subchronic toxicity of inhaled toluene in male Long-Evans rats: oxidative stress markers in brain. *Neurotoxicology* 2015;51:10-9. DOI PubMed
27. Lash LH, Chiu WA, Guyton KZ, Rusyn I. Trichloroethylene biotransformation and its role in mutagenicity, carcinogenicity and target organ toxicity. *Mutat Res Rev Mutat Res* 2014;762:22-36. DOI PubMed PMC
28. Muralidhara S, Ramanathan R, Mehta SM, Lash LH, Acosta D, Bruckner JV. Acute, subacute, and subchronic oral toxicity studies of 1,1-dichloroethane in rats: application to risk evaluation. *Toxicol Sci* 2001;64:135-45. DOI PubMed
29. Zhang Y, Yang Y, He X, et al. The cellular function and molecular mechanism of formaldehyde in cardiovascular disease and heart development. *J Cell Mol Med* 2021;25:5358-71. DOI PubMed PMC
30. Toxicology Program. NTP toxicology and carcinogenesis studies of benzene (CAS No. 71-43-2) in F344/N rats and B6C3F1 mice (Gavage Studies). *Natl Toxicol Program Tech Rep Ser* 1986;289:1-277. DOI
31. Gałęzowska G, Chraniuk M, Wolska L. In vitro assays as a tool for determination of VOCs toxic effect on respiratory system: a critical review. *TrAC Trends in Analytical Chemistry* 2016;77:14-22. DOI
32. Norbäck D, Björnsson E, Janson C, Widström J, Boman G. Asthmatic symptoms and volatile organic compounds, formaldehyde, and carbon dioxide in dwellings. *Occup Environ Med* 1995;52:388-95. DOI PubMed PMC
33. Rasmussen RE. In vitro systems for exposure of lung cells to NO<sub>2</sub> and O<sub>3</sub>. *J Toxicol Environ Health* 1984;13:397-411. DOI PubMed
34. Aufderheide M, Knebel J, Ritter D. Novel approaches for studying pulmonary toxicity in vitro. *Toxicology Letters* 2003;140-141:205-11. DOI PubMed
35. Kim HR, Cho HS, Shin DY, Chung KH. Novel approach to study the cardiovascular effects and mechanism of action of urban particulate matter using lung epithelial-endothelial tetra-culture system. *Toxicol In Vitro* 2017;38:33-40. DOI PubMed
36. Thorne D, Kilford J, Payne R, et al. Development of a BALB/c 3T3 neutral red uptake cytotoxicity test using a mainstream cigarette smoke exposure system. *BMC Res Notes* 2014;7:367. DOI PubMed PMC
37. Al Zallouha M, Landkocz Y, Brunet J, et al. Usefulness of toxicological validation of VOCs catalytic degradation by air-liquid interface exposure system. *Environ Res* 2017;152:328-35. DOI PubMed
38. Brunet J, Genty E, Landkocz Y, et al. Identification of by-products issued from the catalytic oxidation of toluene by chemical and biological methods. *Comptes Rendus Chimie* 2015;18:1084-93. DOI
39. Livak KJ, Schmittgen TD. Analysis of relative gene expression data using real-time quantitative PCR and the 2<sup>-ΔΔC<sub>T</sub></sup> (T) Method. *Methods* 2001;25:402-8. DOI PubMed
40. Méausoone C, Landkocz Y, Cazier F, Seigneur M, Courcot D, Billet S. Toxicological responses of BEAS-2B cells to repeated exposures to benzene, toluene, m-xylene, and mesitylene using air-liquid interface method. *J Appl Toxicol* 2021;41:1262-74. DOI PubMed
41. Billet S, Garçon G, Dagher Z, et al. Ambient particulate matter (PM<sub>2.5</sub>): physicochemical characterization and metabolic activation of the organic fraction in human lung epithelial cells (A549). *Environ Res* 2007;105:212-23. DOI PubMed
42. Kim S, Lan Q, Waidyanatha S, et al. Genetic polymorphisms and benzene metabolism in humans exposed to a wide range of air concentrations. *Pharmacogenet Genomics* 2007;17:789-801. DOI PubMed
43. Gutierrez-Ruiz MC, Gomez Quiroz LE, Hernandez E, et al. Cytokine response and oxidative stress produced by ethanol, acetaldehyde and endotoxin treatment in HepG2 cells. *Isr Med Assoc J* 2001;3:131-6. PubMed
44. Méausoone C, El Khawaja R, Tremolet G, et al. In vitro toxicological evaluation of emissions from catalytic oxidation removal of industrial VOCs by air/liquid interface (ALI) exposure system in repeated mode. *Toxicol In Vitro* 2019;58:110-7. DOI PubMed
45. Cazier F, Dewaele D, Nouali H, Vasseur A. Improvement of the on site VOC measurement in industrial emissions, CEM 2006, Ademe 7ème Conférence Int. Sur La Mes. Polluants à l'émission, 31 Janvier - 2 Février 2006, Paris;2006.
46. Brown R, Purnell C. Collection and analysis of trace organic vapour pollutants in ambient atmospheres. *Journal of Chromatography A* 1979;178:79-90. DOI
47. Bishop RW, Valis RJ. A laboratory evaluation of sorbent tubes for use with a thermal desorption gas chromatography-mass selective

- detection technique. *Journal of Chromatographic Science* 1990;28:589-93. DOI
48. Bruner F, Crescentini G, Mangani F. Graphitized carbon black: a unique adsorbent for gas chromatography and related techniques. *Chromatographia* 1990;30:565-72. DOI
49. McCaffrey CA, MacLachlan J, Brookes BI. Adsorbent tube evaluation for the preconcentration of volatile organic compounds in air for analysis by gas chromatography-mass spectrometry. *Analyst* 1994;119:897-902. DOI
50. No CBPECCAS. Sampling method for volatile organic compounds (SMVOC); 1996. Available from: <https://wap.stanford.edu/20140413191218/http://www.epa.gov/epawaste/hazard/testmethods/sw846/pdfs/0031.pdf> [Last accessed on 28 Jun 2022].
51. British HSE method MDHS104: volatile organic compounds in air.
52. Thomas R, Marotta L, Provost R. A single-method approach for the analysis of volatile and semivolatile organic compounds in air using thermal desorption coupled with GC-MS. *LCGC Europe* 2014. Available from: <https://www.chromatographyonline.com/view/single> [Last accessed on 28 Jun 2022]
53. Kamal MS, Razzak SA, Hossain MM. Catalytic oxidation of volatile organic compounds (VOCs) - a review. *Atmospheric Environment* 2016;140:117-34. DOI PubMed
54. Liotta L. Catalytic oxidation of volatile organic compounds on supported noble metals. *Applied Catalysis B: Environmental* 2010;100:403-12. DOI
55. Jabłońska M, Król A, Kukulska-zajac E, et al. Zeolites Y modified with palladium as effective catalysts for low-temperature methanol incineration. *Applied Catalysis B: Environmental* 2015;166-167:353-65. DOI
56. Tidahy H, Siffert S, Wyrwalski F, Lamonier J, Aboukais A. Catalytic activity of copper and palladium based catalysts for toluene total oxidation. *Catalysis Today* 2007;119:317-20. DOI
57. Cecilia J, Arango-díaz A, Marrero-jerez J, et al. Catalytic behaviour of CuO-CeO<sub>2</sub> systems prepared by different synthetic methodologies in the CO-PROX reaction under CO<sub>2</sub>-H<sub>2</sub>O feed stream. *Catalysts* 2017;7:160. DOI
58. Romero D, Chlala D, Labaki M, et al. Removal of toluene over NaX zeolite exchanged with Cu<sup>2+</sup>. *Catalysts* 2015;5:1479-97. DOI
59. Castaño MH, Molina R, Moreno S. Mn-Co-Al-Mg mixed oxides by auto-combustion method and their use as catalysts in the total oxidation of toluene. *Journal of Molecular Catalysis A: Chemical* 2013;370:167-74. DOI
60. Zhang W, Qu Z, Li X, Wang Y, Ma D, Wu J. Comparison of dynamic adsorption/desorption characteristics of toluene on different porous materials. *Journal of Environmental Sciences* 2012;24:520-8. DOI PubMed
61. Wang Y, Su X, Xu Z, et al. Preparation of surface-functionalized porous clay heterostructures via carbonization of soft-template and their adsorption performance for toluene. *Applied Surface Science* 2016;363:113-21. DOI
62. Yang X, Yi H, Tang X, et al. Behaviors and kinetics of toluene adsorption-desorption on activated carbons with varying pore structure. *J Environ Sci (China)* 2018;67:104-14. DOI PubMed
63. Lillo-ródenas M, Cazorla-amorós D, Linares-solano A. Behaviour of activated carbons with different pore size distributions and surface oxygen groups for benzene and toluene adsorption at low concentrations. *Carbon* 2005;43:1758-67. DOI
64. Xie H, Shen Y, Zhou G, Chen S, Song Y, Ren J. Effect of preparation conditions on the hydrogen storage capacity of activated carbon adsorbents with super-high specific surface areas. *Materials Chemistry and Physics* 2013;141:203-7. DOI
65. Jain A, Balasubramanian R, Srinivasan M. Production of high surface area mesoporous activated carbons from waste biomass using hydrogen peroxide-mediated hydrothermal treatment for adsorption applications. *Chemical Engineering Journal* 2015;273:622-9. DOI
66. Zhang Z, Jiang C, Li D, et al. Micro-mesoporous activated carbon simultaneously possessing large surface area and ultra-high pore volume for efficiently adsorbing various VOCs. *Carbon* 2020;170:567-79. DOI
67. Srivastava I, Singh PK, Gupta T, Sankararamakrishnan N. Preparation of mesoporous carbon composites and its highly enhanced removal capacity of toxic pollutants from air. *Journal of Environmental Chemical Engineering* 2019;7:103271. DOI
68. Nasrullah A, Saad B, Bhat A, et al. Mangosteen peel waste as a sustainable precursor for high surface area mesoporous activated carbon: characterization and application for methylene blue removal. *Journal of Cleaner Production* 2019;211:1190-200. DOI
69. Wang J, Wu Z, Niu Q, et al. Highly efficient adsorptive removal of toluene using silicon-modified activated carbon with improved fire resistance. *J Hazard Mater* 2021;415:125753. DOI PubMed
70. Monneyron P, Manero M-, Manero S. A combined selective adsorption and ozonation process for VOCs removal from air. *Can J Chem Eng* 2007;85:326-32. DOI
71. Bläker C, Pasel C, Luckas M, Dreisbach F, Bathen D. Investigation of load-dependent heat of adsorption of alkanes and alkenes on zeolites and activated carbon. *Microporous and Mesoporous Materials* 2017;241:1-10. DOI
72. Zhang X, Gao B, Zheng Y, et al. Biochar for volatile organic compound (VOC) removal: Sorption performance and governing mechanisms. *Bioresour Technol* 2017;245:606-14. DOI PubMed
73. Kupryianchyk D, Hale S, Zimmerman AR, et al. Sorption of hydrophobic organic compounds to a diverse suite of carbonaceous materials with emphasis on biochar. *Chemosphere* 2016;144:879-87. DOI PubMed
74. Mohamed AR, Mohammadi M, Darzi GN. Preparation of carbon molecular sieve from lignocellulosic biomass: A review. *Renewable and Sustainable Energy Reviews* 2010;14:1591-9. DOI
75. Molina-sabio M, Gonzalez M, Rodriguez-reinoso F, Sepúlveda-escribano A. Effect of steam and carbon dioxide activation in the micropore size distribution of activated carbon. *Carbon* 1996;34:505-9. DOI
76. Feng D, Guo D, Zhang Y, et al. Functionalized construction of biochar with hierarchical pore structures and surface O-/N-containing

- groups for phenol adsorption. *Chemical Engineering Journal* 2021;410:127707. DOI
77. Han Y, Boateng AA, Qi PX, Lima IM, Chang J. Heavy metal and phenol adsorptive properties of biochars from pyrolyzed switchgrass and woody biomass in correlation with surface properties. *J Environ Manage* 2013;118:196-204. DOI PubMed
78. Dehkhoda AM, Gyenge E, Ellis N. A novel method to tailor the porous structure of KOH-activated biochar and its application in capacitive deionization and energy storage. *Biomass and Bioenergy* 2016;87:107-21. DOI
79. Lonappan L, Liu Y, Rouissi T, Brar SK, Surampalli RY. Development of biochar-based green functional materials using organic acids for environmental applications. *Journal of Cleaner Production* 2020;244:118841. DOI
80. Kumar A, Singh E, Khapre A, Bordoloi N, Kumar S. Sorption of volatile organic compounds on non-activated biochar. *Bioresour Technol* 2020;297:122469. DOI PubMed
81. Vikrant K, Na C, Younis SA, Kim K, Kumar S. Evidence for superiority of conventional adsorbents in the sorptive removal of gaseous benzene under real-world conditions: test of activated carbon against novel metal-organic frameworks. *Journal of Cleaner Production* 2019;235:1090-102. DOI
82. Rawal A, Joseph SD, Hook JM, et al. Mineral-biochar composites: molecular structure and porosity. *Environ Sci Technol* 2016;50:7706-14. DOI PubMed
83. Yang G, Chen H, Qin H, Feng Y. Amination of activated carbon for enhancing phenol adsorption: Effect of nitrogen-containing functional groups. *Applied Surface Science* 2014;293:299-305. DOI
84. Soscún H, Castellano O, Hernández J, Hinchliffe A. Acidity of the Brønsted acid sites of zeolites. *Int J Quantum Chem* 2001;82:143-50. DOI
85. Guisnet M, Pinard L. Zéolithes - De la synthèse aux applications. *Tech l'ingénieur* 2018. DOI
86. Brodu N, Sochard S, Andriantsiferana C, Pic JS, Manero MH. Fixed-bed adsorption of toluene on high silica zeolites: experiments and mathematical modelling using LDF approximation and a multisite model. *Environ Technol* 2015;36:1807-18. DOI PubMed
87. Kim K, Ahn H. The effect of pore structure of zeolite on the adsorption of VOCs and their desorption properties by microwave heating. *Microporous and Mesoporous Materials* 2012;152:78-83. DOI
88. Li X, Wang J, Guo Y, Zhu T, Xu W. Adsorption and desorption characteristics of hydrophobic hierarchical zeolites for the removal of volatile organic compounds. *Chemical Engineering Journal* 2021;411:128558. DOI
89. Yin T, Meng X, Jin L, Yang C, Liu N, Shi L. Prepared hydrophobic Y zeolite for adsorbing toluene in humid environment. *Microporous and Mesoporous Materials* 2020;305:110327. DOI
90. Lv Y, Sun J, Yu G, et al. Hydrophobic design of adsorbent for VOC removal in humid environment and quick regeneration by microwave. *Microporous and Mesoporous Materials* 2020;294:109869. DOI
91. Yang R. Gas separation by adsorption processes. *Chemical Engineering Science* 1988;43:985. DOI
92. Meier M, Turner M, Vallee S, Conner WC, Lee KH, Yngvesson KS. Microwave regeneration of zeolites in a 1 meter column. *AIChE Journal* 2009;55:1906-13. DOI
93. Cherbański R, Komorowska-durka M, Stefanidis GD, Stankiewicz AI. Microwave swing regeneration vs. temperature swing regeneration - comparison of desorption kinetics. *Ind Eng Chem Res* 2011;50:8632-44. DOI
94. Guillemot M, Mijoin J, Mignard S, Magnoux P. Volatile organic compounds (VOCs) removal over dual functional adsorbent/catalyst system. *Applied Catalysis B: Environmental* 2007;75:249-55. DOI
95. Urbutis A, Kitrys S. Dual function adsorbent-catalyst CuO-CeO<sub>2</sub>/NaX for temperature swing oxidation of benzene, toluene and xylene. *Open Chemistry* 2014;12:492-501. DOI
96. Wang Y, Yang D, Li S, Chen M, Guo L, Zhou J. Ru/hierarchical HZSM-5 zeolite as efficient bi-functional adsorbent/catalyst for bulky aromatic VOCs elimination. *Microporous and Mesoporous Materials* 2018;258:17-25. DOI
97. Nigar H, Julián I, Mallada R, Santamaria J. Microwave-assisted catalytic combustion for the efficient continuous cleaning of VOC-containing air streams. *Environ Sci Technol* 2018;52:5892-901. DOI PubMed
98. Roland U, Kraus M, Holzer F, Trommler U, Kopinke F. Selective dielectric heating for efficient adsorptive-catalytic cleaning of contaminated gas streams. *Applied Catalysis A: General* 2014;474:244-9. DOI
99. Joung H, Kim J, Oh J, You D, Park H, Jung K. Catalytic oxidation of VOCs over CNT-supported platinum nanoparticles. *Applied Surface Science* 2014;290:267-73. DOI
100. Kim K, Kang C, You Y, et al. Adsorption-desorption characteristics of VOCs over impregnated activated carbons. *Catalysis Today* 2006;111:223-8. DOI
101. Minh NT, Thanh LD, Trung BC, An NT, Long NQ. Dual functional adsorbent/catalyst of nano-gold/metal oxides supported on carbon grain for low-temperature removal of toluene in the presence of water vapor. *Clean Techn Environ Policy* 2018;20:1861-73. DOI
102. Zhang J, Rao C, Peng H, et al. Enhanced toluene combustion performance over Pt loaded hierarchical porous MOR zeolite. *Chemical Engineering Journal* 2018;334:10-8. DOI
103. Yao S, Fang W, Wang B, et al. Rh1Cu3/ZSM-5 as an efficient bifunctional catalyst/adsorbent for VOCs abatement. *Catal Lett* 2022;152:771-80. DOI
104. Aziz A, Sajjad M, Kim M, Kim KS. An efficient Co-ZSM-5 catalyst for the abatement of volatile organics in air: effect of the synthesis protocol. *Int J Environ Sci Technol* 2018;15:707-18. DOI
105. Beauchet R. Oxydation catalytique de divers composés organiques volatils (COV) à l'aide de catalyseurs zeolithiques; 2008. DOI
106. Baek S, Kim J, Ihm S. Design of dual functional adsorbent/catalyst system for the control of VOC's by using metal-loaded

- hydrophobic Y-zeolites. *Catalysis Today* 2004;93-95:575-81. DOI
107. Wu SM, Yang XY, Janiak C. Confinement effects in zeolite-confined noble metals. *Angew Chem Int Ed Engl* 2019;58:12340-54. DOI PubMed
108. Liu G, Tian Y, Zhang B, Wang L, Zhang X. Catalytic combustion of VOC on sandwich-structured Pt@ZSM-5 nanosheets prepared by controllable intercalation. *J Hazard Mater* 2019;367:568-76. DOI PubMed
109. Chai Y, Shang W, Li W, et al. Noble metal particles confined in zeolites: synthesis, characterization, and applications. *Adv Sci (Weinh)* 2019;6:1900299. DOI PubMed PMC
110. Chen C, Chen F, Zhang L, et al. Importance of platinum particle size for complete oxidation of toluene over Pt/ZSM-5 catalysts. *Chem Commun (Camb)* 2015;51:5936-8. DOI PubMed
111. Dong T, Liu W, Ma M, et al. Hierarchical zeolite enveloping Pd-CeO<sub>2</sub> nanowires: an efficient adsorption/catalysis bifunctional catalyst for low temperature propane total degradation. *Chemical Engineering Journal* 2020;393:124717. DOI
112. Soares OSGP, Fonseca AM, Parpot P, Órfão JJM, Pereira MFR, Neves IC. Oxidation of volatile organic compounds by highly efficient metal zeolite catalysts. *ChemCatChem* 2018;10:3754-60. DOI
113. Shi C, Chen B, Li X, Crocker M, Wang Y, Zhu A. Catalytic formaldehyde removal by "storage-oxidation" cycling process over supported silver catalysts. *Chemical Engineering Journal* 2012;200-202:729-37. DOI
114. Adebayo BO, Krishnamurthy A, Rownaghi AA, Rezaei F. Toluene abatement by simultaneous adsorption and oxidation over mixed-metal oxides. *Ind Eng Chem Res* 2020;59:13762-72. DOI
115. Kim H. Nonthermal plasma processing for air-pollution control: a historical review, current issues, and future prospects. *Plasma Process Polym* 2004;1:91-110. DOI
116. Fridman A. Plasma chemistry. New York: Cambridge University press; 2008. DOI
117. Vandenbroucke AM, Morent R, De Geyter N, Leys C. Non-thermal plasmas for non-catalytic and catalytic VOC abatement. *J Hazard Mater* 2011;195:30-54. DOI PubMed
118. An HT, Pham Huu T, Le Van T, Cormier J, Khacef A. Application of atmospheric non thermal plasma-catalysis hybrid system for air pollution control: toluene removal. *Catalysis Today* 2011;176:474-7. DOI
119. Holzer F, Kopinke FD, Roland U. Influence of ferroelectric materials and catalysts on the performance of non-thermal plasma (NTP) for the removal of air pollutants. *Plasma Chem Plasma Process* 2005;25:595-611. DOI
120. Zhao D, Li X, Shi C, Fan H, Zhu A. Low-concentration formaldehyde removal from air using a cycled storage-discharge (CSD) plasma catalytic process. *Chemical Engineering Science* 2011;66:3922-9. DOI
121. Urashima K, Jen-shih Chang. Removal of volatile organic compounds from air streams and industrial flue gases by non-thermal plasma technology. *IEEE Trans Dielect Electr Insul* 2000;7:602-14. DOI
122. Chen HL, Lee HM, Chen SH, Chang MB, Yu SJ, Li SN. Removal of volatile organic compounds by single-stage and two-stage plasma catalysis systems: a review of the performance enhancement mechanisms, current status, and suitable applications. *Environ Sci Technol* 2009;43:2216-27. DOI PubMed
123. Ollegott K, Wirth P, Oberstebeulmann C, Awakowicz P, Muhler M. Fundamental properties and applications of dielectric barrier discharges in plasma-catalytic processes at atmospheric pressure. *Chemie Ingenieur Technik* 2020;92:1542-58. DOI
124. Chang T, Shen Z, Huang Y, et al. Post-plasma-catalytic removal of toluene using MnO<sub>2</sub>-Co<sub>3</sub>O<sub>4</sub> catalysts and their synergistic mechanism. *Chemical Engineering Journal* 2018;348:15-25. DOI
125. Karuppiah J, Sivachandiran L, Karvembu R, Subrahmanyam C. Catalytic nonthermal plasma reactor for the abatement of low concentrations of isopropanol. *Chemical Engineering Journal* 2010;165:194-9. DOI
126. Tang X, Feng F, Ye L, et al. Removal of dilute VOCs in air by post-plasma catalysis over Ag-based composite oxide catalysts. *Catalysis Today* 2013;211:39-43. DOI
127. Sultana S, Vandenbroucke A, Mora M, et al. Post plasma-catalysis for trichloroethylene decomposition over CeO<sub>2</sub> catalyst: Synergistic effect and stability test. *Applied Catalysis B: Environmental* 2019;253:49-59. DOI
128. Yang S, Yang H, Yang J, et al. Three-dimensional hollow urchin  $\alpha$ -MnO<sub>2</sub> for enhanced catalytic activity towards toluene decomposition in post-plasma catalysis. *Chemical Engineering Journal* 2020;402:126154. DOI
129. Neyts EC, Bogaerts A. Understanding plasma catalysis through modelling and simulation - a review. *J Phys D: Appl Phys* 2014;47:224010. DOI
130. Mirzaei A, Kim J, Kim HW, Kim SS. Resistive-based gas sensors for detection of benzene, toluene and xylene (BTX) gases: a review. *J Mater Chem C* 2018;6:4342-70. DOI
131. Magureanu M, Mandache NB, Eloy P, Gaigneaux EM, Parvulescu VI. Plasma-assisted catalysis for volatile organic compounds abatement. *Applied Catalysis B: Environmental* 2005;61:12-20. DOI
132. Huang HB, Ye DQ, Leung DY. Removal of toluene using UV-irradiated and nonthermal plasma-driven photocatalyst system. *J Environ Eng* 2010;136:1231-6. DOI
133. Subrahmanyam C, Renken A, Kiwi-minsker L. Catalytic non-thermal plasma reactor for abatement of toluene. *Chemical Engineering Journal* 2010;160:677-82. DOI
134. Durme J, Dewulf J, Demeestere K, Leys C, Van Langenhove H. Post-plasma catalytic technology for the removal of toluene from indoor air: effect of humidity. *Applied Catalysis B: Environmental* 2009;87:78-83. DOI
135. Hayashi K, Yasui H, Tanaka M, Futamura S, Kurita S, Aoyagi K. Temperature dependence of toluene decomposition behavior in the discharge-catalyst hybrid reactor. *IEEE Trans on Ind Appl* 2009;45:1553-8. DOI



136. Ban J, Son Y, Kang M, Choung S. Highly concentrated toluene decomposition on the dielectric barrier discharge (DBD) plasma-photocatalytic hybrid system with Mn-Ti-incorporated mesoporous silicate photocatalyst (Mn-Ti-MPS). *Applied Surface Science* 2006;253:535-42. DOI
137. Huang H, Ye D. Combination of photocatalysis downstream the non-thermal plasma reactor for oxidation of gas-phase toluene. *J Hazard Mater* 2009;171:535-41. DOI PubMed
138. Harling AM, Glover DJ, Whitehead JC, Zhang K. The role of ozone in the plasma-catalytic destruction of environmental pollutants. *Applied Catalysis B: Environmental* 2009;90:157-61. DOI
139. Delagrangé S, Pinard L, Tatibouet J. Combination of a non-thermal plasma and a catalyst for toluene removal from air: Manganese based oxide catalysts. *Applied Catalysis B: Environmental* 2006;68:92-8. DOI
140. Demidyuk V, Whitehead JC. Influence of temperature on gas-phase toluene decomposition in plasma-catalytic system. *Plasma Chem Plasma Process* 2007;27:85-94. DOI
141. Harling AM, Demidyuk V, Fischer SJ, Whitehead JC. Plasma-catalysis destruction of aromatics for environmental clean-up: effect of temperature and configuration. *Applied Catalysis B: Environmental* 2008;82:180-9. DOI
142. Demidiouk V, Jae Ou Chae. Decomposition of volatile organic compounds in plasma-catalytic system. *IEEE Trans Plasma Sci* 2005;33:157-61. DOI
143. Li D, Yakushiji D, Kanazawa S, Ohkubo T, Nomoto Y. Decomposition of toluene by streamer corona discharge with catalyst. *Journal of Electrostatics* 2002;55:311-9. DOI
144. Durme J, Dewulf J, Sysmans W, Leys C, Van Langenhove H. Efficient toluene abatement in indoor air by a plasma catalytic hybrid system. *Applied Catalysis B: Environmental* 2007;74:161-9. DOI
145. Ge H, Hu D, Li X, Tian Y, Chen Z, Zhu Y. Removal of low-concentration benzene in indoor air with plasma-MnO<sub>2</sub> catalysis system. *Journal of Electrostatics* 2015;76:216-21. DOI
146. Jiang N, Qiu C, Guo L, et al. Post plasma-catalysis of low concentration VOC over alumina-supported silver catalysts in a surface/packed-bed hybrid discharge reactor. *Water Air Soil Pollut* 2017:228. DOI
147. Hu J, Jiang N, Li J, Shang K, Lu N, Wu Y. Degradation of benzene by bipolar pulsed series surface/packed-bed discharge reactor over MnO<sub>2</sub>-TiO<sub>2</sub>/zeolite catalyst. *Chemical Engineering Journal* 2016;293:216-24. DOI
148. Zhang S, Shen X, Liang J. Atmospheric pressure oxidation of dilute xylene using plasma-assisted MnOX catalysis system with different precursors. *Molecular Catalysis* 2019;467:87-94. DOI
149. Wang L, He H, Zhang C, Wang Y, Zhang B. Effects of precursors for manganese-loaded  $\gamma$ -Al<sub>2</sub>O<sub>3</sub> catalysts on plasma-catalytic removal of o-xylene. *Chemical Engineering Journal* 2016;288:406-13. DOI
150. Piroi D, Magureanu M, Mandache NB, Parvulescu VI. The decomposition of p-xylene in air by plasma-assisted catalysis. 2008 17th International Conference on Gas Discharges and Their Applications; 2008. p. 473-6. Available from: <https://ieeexplore.ieee.org/abstract/document/5379364> [Last accessed on 28 Jun 2022].
151. Fan X, Zhu TL, Wang MY, Li XM. Removal of low-concentration BTX in air using a combined plasma catalysis system. *Chemosphere* 2009;75:1301-6. DOI PubMed
152. Oda T, Takahashi T, Yamaji K. TCE decomposition by the nonthermal plasma process concerning ozone effect. *IEEE Trans on Ind Appl* 2004;40:1249-56. DOI
153. Han S, Oda T, Ono R. Improvement of the energy efficiency in the decomposition of dilute trichloroethylene by the barrier discharge plasma process. *IEEE Trans on Ind Appl* 2005;41:1343-9. DOI
154. Magureanu M, Mandache NB, Hu J, Richards R, Florea M, Parvulescu VI. Plasma-assisted catalysis total oxidation of trichloroethylene over gold nano-particles embedded in SBA-15 catalysts. *Appl Catal B* 2007;76:275-81. DOI
155. Vandenbroucke A, Morent R, De Geyter N, et al. Plasma-catalytic decomposition of TCE. *Int J Plasma Environ Sci Technol* 2010;4:135-8. Available from: <http://ijpest.com/Contents/04/2/PDF/04> [Last accessed on 28 Jun 2022]
156. Han S, Oda T. Decomposition mechanism of trichloroethylene based on by-product distribution in the hybrid barrier discharge plasma process. *Plasma Sources Sci Technol* 2007;16:413-21. DOI
157. Vandenbroucke A, Mora M, Jiménez-sanchidrián C, et al. TCE abatement with a plasma-catalytic combined system using MnO<sub>2</sub> as catalyst. *Appl Catal B* 2014;156-157:94-100. DOI
158. Dinh MN, Giraudon J, Lamonier J, et al. Plasma-catalysis of low TCE concentration in air using LaMnO<sub>3</sub>+ $\delta$  as catalyst. *Appl Catal B* 2014;147:904-11. DOI
159. Li Y, Fan Z, Shi J, Liu Z, Shangguan W. Post plasma-catalysis for VOCs degradation over different phase structure MnO<sub>2</sub> catalysts. *Chem Eng J* 2014;241:251-8. DOI
160. Li Y, Fan Z, Shi J, Liu Z, Zhou J, Shangguan W. Modified manganese oxide octahedral molecular sieves M'-OMS-2 (M' = Co,Ce,Cu) as catalysts in post plasma-catalysis for acetaldehyde degradation. *Catal Today* 2015;256:178-85. DOI
161. Chang T, Shen Z, Ma C, et al. Process optimization of plasma-catalytic formaldehyde removal using MnOx-Fe<sub>2</sub>O<sub>3</sub> catalysts by response surface methodology. *J. Environ Chem Eng* 2021;9:105773. DOI
162. Zhu X, Liu S, Cai Y, et al. Post-plasma catalytic removal of methanol over Mn-Ce catalysts in an atmospheric dielectric barrier discharge. *Appl Catal B* 2016;183:124-32. DOI
163. Norsic C, Tatibouët J, Batiot-dupeyrat C, Fourré E. Non thermal plasma assisted catalysis of methanol oxidation on Mn, Ce and Cu oxides supported on  $\gamma$ -Al<sub>2</sub>O<sub>3</sub>. *Chem Eng J* 2016;304:563-72. DOI
164. Karupiah J, Linga Reddy E, Manoj Kumar Reddy P, Ramaraju B, Subrahmanyam C. Catalytic nonthermal plasma reactor for the

- abatement of low concentrations of benzene. *Int J Environ Sci Technol* 2014;11:311-8. DOI
165. Guo H, Liu X, Hojo H, Yao X, Einaga H, Shangguan W. Removal of benzene by non-thermal plasma catalysis over manganese oxides through a facile synthesis method. *Environ Sci Pollut Res Int* 2019;26:8237-47. DOI PubMed
166. Xu N, Fu W, He C, et al. Benzene removal using non-thermal plasma with CuO/AC catalyst: reaction condition optimization and decomposition mechanism. *Plasma Chem Plasma Process* 2014;34:1387-402. DOI
167. Jiang N, Hu J, Li J, Shang K, Lu N, Wu Y. Plasma-catalytic degradation of benzene over Ag-Ce bimetallic oxide catalysts using hybrid surface/packed-bed discharge plasmas. *Appl Catal B* 2016;184:355-63. DOI
168. Zhu B, Zhang L, Li M, Yan Y, Zhang X, Zhu Y. High-performance of plasma-catalysis hybrid system for toluene removal in air using supported Au nanocatalysts. *Chem Eng J* 2020;381:122599. DOI
169. Wu J, Xia Q, Wang H, Li Z. Catalytic performance of plasma catalysis system with nickel oxide catalysts on different supports for toluene removal: effect of water vapor. *Appl Catal B* 2014;156-157:265-72. DOI
170. Xu W, Chen B, Jiang X, et al. Effect of calcium addition in plasma catalysis for toluene removal by Ni/ZSM-5 : acidity/basicity, catalytic activity and reaction mechanism. *J Hazard Mater* 2020;387:122004. DOI PubMed
171. Yao S, Chen Z, Xie H, et al. Highly efficient decomposition of toluene using a high-temperature plasma-catalysis reactor. *Chemosphere* 2020;247:125863. DOI PubMed
172. Wu J, Huang Y, Xia Q, Li Z. Decomposition of toluene in a plasma catalysis system with NiO, MnO<sub>2</sub>, CeO<sub>2</sub>, Fe<sub>2</sub>O<sub>3</sub>, and CuO catalysts. *Plasma Chem Plasma Process* 2013;33:1073-82. DOI
173. Wang B, Chi C, Xu M, Wang C, Meng D. Plasma-catalytic removal of toluene over CeO<sub>2</sub>-MnO<sub>x</sub> catalysts in an atmosphere dielectric barrier discharge. *Chem Eng J* 2017;322:679-92. DOI
174. Yu X, Dang X, Li S, Zhang J, Zhang Q, Cao L. A comparison of in- and post-plasma catalysis for toluene abatement through continuous and sequential processes in dielectric barrier discharge reactors. *J Clean Prod* 2020;276:124251. DOI
175. Xu X, Wu J, Xu W, et al. High-efficiency non-thermal plasma-catalysis of cobalt incorporated mesoporous MCM-41 for toluene removal. *Catal Today* 2017;281:527-33. DOI
176. Sudhakaran MSP, Trinh HQ, Karuppiiah J, Hossian MM, Mok YS. Plasma catalytic removal of p-Xylene from air stream using  $\gamma$ -Al<sub>2</sub>O<sub>3</sub> supported manganese catalyst. *Top Catal* 2017;60:944-54. DOI
177. Wang L, Zhang C, He H, Liu F, Wang C. Effect of doping metals on OMS-2/ $\gamma$ -Al<sub>2</sub>O<sub>3</sub> catalysts for plasma-catalytic removal of o-xylene. *Chem Eng J* 2020;381:122599. DOI
178. Wu Z, Zhou W, Zhu Z, Hao X, Zhang X. Enhanced oxidation of xylene using plasma activation of an Mn/Al<sub>2</sub>O<sub>3</sub> catalyst. *IEEE Trans Plasma Sci* 2020;48:163-72. DOI
179. Zhu X, Gao X, Qin R, et al. Plasma-catalytic removal of formaldehyde over Cu-Ce catalysts in a dielectric barrier discharge reactor. *Appl Catal B* 2015;170-171:293-300. DOI
180. Liang WJ, Li J, Li JX, Zhu T, Jin YQ. Formaldehyde removal from gas streams by means of NaNO<sub>2</sub> dielectric barrier discharge plasma. *J Hazard Mater* 2010;175:1090-5. DOI PubMed
181. Ding H, Zhu A, Lu F, Xu Y, Zhang J, Yang X. Low-temperature plasma-catalytic oxidation of formaldehyde in atmospheric pressure gas streams. *J Phys D: Appl Phys* 2006;39:3603-8. DOI
182. Jia Z, Ben Amar M, Yang D, et al. Plasma catalysis application of gold nanoparticles for acetaldehyde decomposition. *Chem Eng J* 2018;347:913-22. DOI
183. Vega-gonzález A, Dutén X, Sauce S. Plasma-catalysis for volatile organic compounds decomposition: complexity of the reaction pathways during acetaldehyde removal. *Catalysts* 2020;10:1146. DOI
184. Kostov K, Honda RY, Alves L, Kayama M. Characteristics of dielectric barrier discharge reactor for material treatment. *Braz J Phys* 2009;39:2. DOI
185. Chen HL, Lee HM, Chen SH, Chang MB. Review of packed-bed plasma reactor for ozone generation and air pollution control. *Ind Eng Chem Res* 2008;47:2122-30. DOI
186. Ye Z, Veerapandian SKP, Onyshchenko I, et al. An in-depth investigation of toluene decomposition with a glass beads-packed bed dielectric barrier discharge reactor. *Ind Eng Chem Res* 2017;56:10215-26. DOI
187. Kaliya Perumal Veerapandian S, Giraudon JM, De Geyter N, et al. Regeneration of hopcalite used for the adsorption plasma catalytic removal of toluene by non-thermal plasma. *J Hazard Mater* 2021;402:123877. DOI PubMed
188. Veerapandian S, Leys C, De Geyter N, Morent R. Abatement of VOCs Using packed bed non-thermal plasma reactors: a review. *Catalysts* 2017;7:113. DOI
189. Vandenbroucke AM, Morent R, Geyter ND, Leys C. Decomposition of toluene with plasma-catalysis: a review. *J Adv Oxid Technol* 2012;15:232-41. DOI
190. Feng X, Liu H, He C, Shen Z, Wang T. Synergistic effects and mechanism of a non-thermal plasma catalysis system in volatile organic compound removal: a review. *Catal Sci Technol* 2018;8:936-54. DOI
191. Durme J, Dewulf J, Leys C, Van Langenhove H. Combining non-thermal plasma with heterogeneous catalysis in waste gas treatment: a review. *Appl Catal B* 2008;78:324-33. DOI
192. Whitehead JC. Plasma-catalysis: the known knowns, the known unknowns and the unknown unknowns. *J Phys D: Appl Phys* 2016;49:243001. DOI
193. Neyts EC, Ostrikov KK, Sunkara MK, Bogaerts A. Plasma catalysis: synergistic effects at the nanoscale. *Chem Rev* 2015;115:13408-46. DOI PubMed



194. Li S, Dang X, Yu X, Abbas G, Zhang Q, Cao L. The application of dielectric barrier discharge non-thermal plasma in VOCs abatement: a review. *Chem Eng J* 2020;388:124275. DOI
195. Zhang Y, Nie J, Yuan C, et al. CuO@Cu/Ag/MWNTs/sponge electrode-enhanced pollutant removal in dielectric barrier discharge (DBD) reactor. *Chemosphere* 2019;229:273-83. DOI PubMed
196. Mei D, Tu X. Conversion of CO<sub>2</sub> in a cylindrical dielectric barrier discharge reactor: effects of plasma processing parameters and reactor design. *Journal of CO<sub>2</sub> Utilization* 2017;19:68-78. DOI
197. Yuan D, Tang S, Qi J, Li N, Gu J, Huang H. Comparison of hydroxyl radicals generation during granular activated carbon regeneration in DBD reactor driven by bipolar pulse power and alternating current power. *Vacuum* 2017;143:87-94. DOI
198. Jiang N, Qiu C, Guo L, et al. Improved performance for toluene abatement in a continuous-flow pulsed sliding discharge reactor based on three-electrode configuration. *Plasma Chem Plasma Process* 2019;39:227-40. DOI
199. Jiang N, Guo L, Qiu C, et al. Reactive species distribution characteristics and toluene destruction in the three-electrode DBD reactor energized by different pulsed modes. *Chem Eng J* 2018;350:12-9. DOI
200. Li S, Yu X, Dang X, Guo H, Liu P, Qin C. Using non-thermal plasma for decomposition of toluene adsorbed on  $\gamma$ -Al<sub>2</sub>O<sub>3</sub> and ZSM-5: Configuration and optimization of a double dielectric barrier discharge reactor. *Chem Eng J* 2019;375:122027. DOI
201. Wang T, Chen S, Wang H, Liu Z, Wu Z. In-plasma catalytic degradation of toluene over different MnO<sub>2</sub> polymorphs and study of reaction mechanism. *Chinese J Catal* 2017;38:793-803. DOI
202. Liu R, Song H, Li B, Li X, Zhu T. Simultaneous removal of toluene and styrene by non-thermal plasma-catalysis: effect of VOCs interaction and system configuration. *Chemosphere* 2021;263:127893. DOI PubMed
203. Qin C, Guo M, Jiang C, et al. Simultaneous oxidation of toluene and ethyl acetate by dielectric barrier discharge combined with Fe, Mn and Mo catalysts. *SSCI Total Environ* 2021;782:146931. DOI
204. Mustafa MF, Fu X, Liu Y, Abbas Y, Wang H, Lu W. Volatile organic compounds (VOCs) removal in non-thermal plasma double dielectric barrier discharge reactor. *J Hazard Mater* 2018;347:317-24. DOI PubMed
205. Hoseini S, Rahemi N, Allahyari S, Tasbihi M. Application of plasma technology in the removal of volatile organic compounds (BTX) using manganese oxide nano-catalysts synthesized from spent batteries. *J Clean Prod* 2019;232:1134-47. DOI
206. Mustafa MF, Fu X, Lu W, et al. Application of non-thermal plasma technology on fugitive methane destruction: configuration and optimization of double dielectric barrier discharge reactor. *J Clean Prod* 2018;174:670-7. DOI
207. Shang K, Ren J, Zhang Q, Lu N, Jiang N, Li J. Successive treatment of benzene and derived byproducts by a novel plasma catalysis-adsorption process. *J Environ Chem Eng* 2021;9:105767. DOI
208. Yamagata Y, Niho K, Inoue K, Okano H, Muraoka K. Decomposition of volatile organic compounds at low concentrations using combination of densification by zeolite adsorption and dielectric barrier discharge. *Jpn J Appl Phys* 2006;45:8251-4. DOI
209. Sivachandiran L, Thevenet F, Rousseau A. Non-thermal plasma assisted regeneration of acetone adsorbed TiO<sub>2</sub> surface. *Plasma Chem Plasma Process* 2013;33:855-71. DOI
210. Sultana S, Vandenbroucke A, Leys C, De Geyter N, Morent R. Abatement of VOCs with alternate adsorption and plasma-assisted regeneration: a review. *Catalysts* 2015;5:718-46. DOI
211. Xu W, Lin K, Ye D, Jiang X, Liu J, Chen Y. Performance of toluene removal in a nonthermal plasma catalysis system over flake-like HZSM-5 zeolite with tunable pore size and evaluation of its byproducts. *Nanomaterials (Basel)* 2019;9:290. DOI PubMed PMC
212. Yi H, Yang X, Tang X, et al. Removal of toluene from industrial gas over 13X zeolite supported catalysts by adsorption-plasma catalytic process: removal of toluene by adsorption plasma catalytic process. *J Chem Technol Biotechnol* 2017;92:2276-86. DOI
213. Xu X, Wang P, Xu W, et al. Plasma-catalysis of metal loaded SBA-15 for toluene removal: comparison of continuously introduced and adsorption-discharge plasma system. *Chem Eng J* 2016;283:276-84. DOI
214. Trinh QH, Lee SB, Mok YS. Removal of ethylene from air stream by adsorption and plasma-catalytic oxidation using silver-based bimetallic catalysts supported on zeolite. *J Hazard Mater* 2015;285:525-34. DOI PubMed
215. Wang W, Wang H, Zhu T, Fan X. Removal of gas phase low-concentration toluene over Mn, Ag and Ce modified HZSM-5 catalysts by periodical operation of adsorption and non-thermal plasma regeneration. *J Hazard Mater* 2015;292:70-8. DOI PubMed
216. Fan H, Shi C, Li X, Zhao D, Xu Y, Zhu A. High-efficiency plasma catalytic removal of dilute benzene from air. *J Phys D: Appl Phys* 2009;42:225105. DOI
217. Kim H, Ogata A, Futamura S. Oxygen partial pressure-dependent behavior of various catalysts for the total oxidation of VOCs using cyclic system of adsorption and oxygen plasma. *Appl Catal B* 2008;79:356-67. DOI
218. Dang X, Huang J, Cao L, Zhou Y. Plasma-catalytic oxidation of adsorbed toluene with gas circulation. *Catal Commun* 2013;40:116-9. DOI
219. Yi H, Yang X, Tang X, et al. Removal of toluene from industrial gas by adsorption-plasma catalytic process: comparison of closed discharge and ventilated discharge. *Plasma Chem Plasma Process* 2018;38:331-45. DOI
220. Hosseini MS, Asilian Mahabadi H, Yarahmadi R. Removal of toluene from air using a Cycled Storage-Discharge (CSD) plasma catalytic process. *Plasma Chem Plasma Process* 2019;39:125-42. DOI
221. Youn JS, Bae J, Park S, Park YK. Plasma-assisted oxidation of toluene over Fe/zeolite catalyst in DBD reactor using adsorption/desorption system. *Catal Commun* 2018;113:36-40. DOI
222. Xu W, Jiang X, Chen H, et al. Adsorption-discharge plasma system for toluene decomposition over Ni-SBA catalyst: in situ observation and humidity influence study. *Chem Eng J* 2020;382:122950. DOI
223. Abdelouahab-reddam Z, Mail RE, Coloma F, Sepúlveda-escribano A. Platinum supported on highly-dispersed ceria on activated

- carbon for the total oxidation of VOCs. *APPL CATAL A-GEN* 2015;494:87-94. DOI
224. Chen H, Yan Y, Shao Y, Zhang H. Catalytic activity and stability of porous Co–Cu–Mn mixed oxide modified microfibrillar-structured ZSM-5 membrane/PSSF catalyst for VOCs oxidation. *RSC Adv* 2014;4:55202-9. DOI
225. Liao Y, Zhang X, Peng R, Zhao M, Ye D. Catalytic properties of manganese oxide polyhedra with hollow and solid morphologies in toluene removal. *Appl Surf Sci* 2017;405:20-8. DOI
226. Durme J, Dewulf J, Sysmans W, Leys C, Van Langenhove H. Abatement and degradation pathways of toluene in indoor air by positive corona discharge. *Chemosphere* 2007;68:1821-9. DOI PubMed
227. Chao CY, Kwong CW, Hui KS. Potential use of a combined ozone and zeolite system for gaseous toluene elimination. *J Hazard Mater* 2007;143:118-27. DOI PubMed
228. Qin C, Huang X, Zhao J, Huang J, Kang Z, Dang X. Removal of toluene by sequential adsorption-plasma oxidation: mixed support and catalyst deactivation. *J Hazard Mater* 2017;334:29-38. DOI PubMed
229. Trinh QH, Gandhi MS, Mok YS. Adsorption and plasma-catalytic oxidation of acetone over zeolite-supported silver catalyst. *Jpn J Appl Phys* 2015;54:01AG04. DOI
230. Vepek S. Mechanism of the deactivation of Hopcalite catalysts studied by XPS, ISS, and other techniques. *J Catal* 1986;100:250-63. DOI
231. Qin C, Guo H, Bai W, et al. Kinetics study on non-thermal plasma mineralization of adsorbed toluene over  $\gamma$ -Al<sub>2</sub>O<sub>3</sub> hybrid with zeolite. *J Hazard Mater* 2019;369:430-8. DOI PubMed
232. Shayegan Z, Lee C, Haghighat F. TiO<sub>2</sub> photocatalyst for removal of volatile organic compounds in gas phase – a review. *Chem Eng J* 2018;334:2408-39. DOI
233. Tseng TK, Lin YS, Chen YJ, Chu H. A review of photocatalysts prepared by sol-gel method for VOCs removal. *Int J Mol Sci* 2010;11:2336-61. DOI PubMed PMC
234. Zou W, Gao B, Ok YS, Dong L. Integrated adsorption and photocatalytic degradation of volatile organic compounds (VOCs) using carbon-based nanocomposites: a critical review. *Chemosphere* 2019;218:845-59. DOI PubMed
235. Huang Y, Ho SS, Lu Y, et al. Removal of indoor volatile organic compounds via photocatalytic oxidation: a short review and prospect. *Molecules* 2016;21:56. DOI PubMed PMC
236. Li H, Jiang F, Drdova S, Shang H, Zhang L, Wang J. Dual-function surface hydrogen bonds enable robust O<sub>2</sub> activation for deep photocatalytic toluene oxidation. *Catal Sci Technol* 2021;11:319-31. DOI
237. Wang L, Xu X, Wu S, Cao F. Nonstoichiometric tungsten oxide residing in a 3D nitrogen doped carbon matrix, a composite photocatalyst for oxygen vacancy induced VOC degradation and H<sub>2</sub> production. *Catal Sci Technol* 2018;8:1366-74. DOI
238. Weon S, He F, Choi W. Status and challenges in photocatalytic nanotechnology for cleaning air polluted with volatile organic compounds: visible light utilization and catalyst deactivation. *Environ Sci : Nano* 2019;6:3185-214. DOI
239. Zhang W, Li G, Yin H, Zhao K, Zhao H, An T. Adsorption and desorption mechanism of aromatic VOCs onto porous carbon adsorbents for emission control and resource recovery: recent progress and challenges. *Environ Sci : Nano* 2022;9:81-104. DOI
240. Chen R, Li J, Wang H, et al. Photocatalytic reaction mechanisms at a gas–solid interface for typical air pollutant decomposition. *J Mater Chem A* 2021;9:20184-210. DOI
241. Xu H, Vanamu G, Nie Z, et al. Photocatalytic oxidation of a volatile organic component of acetaldehyde using titanium oxide nanotubes. *J Nanomater* 2006;2006:1-8. DOI
242. Liu Z, Zhang X, Nishimoto S, Murakami T, Fujishima A. Efficient photocatalytic degradation of gaseous acetaldehyde by highly ordered TiO<sub>2</sub> nanotube arrays. *Environ Sci Technol* 2008;42:8547-51. DOI PubMed
243. Wang M, Iocozia J, Sun L, Lin C, Lin Z. Inorganic-modified semiconductor TiO<sub>2</sub> nanotube arrays for photocatalysis. *Energy Environ Sci* 2014;7:2182. DOI
244. Liu R, Li W, Peng A. A facile preparation of TiO<sub>2</sub>/ACF with C Ti bond and abundant hydroxyls and its enhanced photocatalytic activity for formaldehyde removal. *Appl Surf Sci* 2018;427:608-16. DOI
245. An T, Chen J, Nie X, et al. Synthesis of carbon nanotube-anatase TiO<sub>2</sub> sub-micrometer-sized sphere composite photocatalyst for synergistic degradation of gaseous styrene. *ACS Appl Mater Interfaces* 2012;4:5988-96. DOI PubMed
246. Tieng S, Kanaev A, Chhor K. New homogeneously doped Fe (III)–TiO<sub>2</sub> photocatalyst for gaseous pollutant degradation. *APPL CATAL A-GEN* 2011;399:191-7. DOI
247. Murcia J, Hidalgo M, Navio J, Vaiano V, Ciambelli P, Sannino D. Ethanol partial photooxidation on Pt/TiO<sub>2</sub> catalysts as green route for acetaldehyde synthesis. *Catal Today* 2012;196:101-9. DOI
248. Shaban M, Ashraf AM, Abukhadra MR. TiO<sub>2</sub> nanoribbons/carbon nanotubes composite with enhanced photocatalytic activity; fabrication, characterization, and application. *Sci Rep* 2018;8:781. DOI PubMed PMC
249. Khan ME, Khan MM, Cho MH. Recent progress of metal-graphene nanostructures in photocatalysis. *Nanoscale* 2018;10:9427-40. DOI PubMed
250. Roso M, Boaretti C, Bonora R, Modesti M, Lorenzetti A. Nanostructured active media for volatile organic compounds abatement: the synergy of graphene oxide and semiconductor coupling. *Ind Eng Chem Res* 2018;57:16635-44. DOI
251. Colón G, Maicu M, Hidalgo M, Navio J. Cu-doped TiO<sub>2</sub> systems with improved photocatalytic activity. *Appl Catal B* 2006;67:41-51. DOI
252. Yang SB, Chun HH, Tayade RJ, Jo WK. Iron-functionalized titanium dioxide on flexible glass fibers for photocatalysis of benzene, toluene, ethylbenzene, and o-xylene (BTEX) under visible- or ultraviolet-light irradiation. *J Air Waste Manag Assoc* 2015;65:365-73.

[DOI PubMed](#)

253. Bensouici F, Bououdina M, Dakhel A, et al. Optical, structural and photocatalysis properties of Cu-doped TiO<sub>2</sub> thin films. *Appl Surf Sci* 2017;395:110-6. [DOI](#)
254. Shaban M, Ahmed AM, Shehata N, Betiha MA, Rabie AM. Ni-doped and Ni/Cr co-doped TiO<sub>2</sub> nanotubes for enhancement of photocatalytic degradation of methylene blue. *J Colloid Interface Sci* 2019;555:31-41. [DOI PubMed](#)
255. Dong F, Wang H, Wu Z. One-step “Green” synthetic approach for mesoporous C-doped titanium dioxide with efficient visible light photocatalytic activity. *J Phys Chem C* 2009;113:16717-23. [DOI](#)
256. Dong F, Guo S, Wang H, Li X, Wu Z. Enhancement of the visible light photocatalytic activity of c-doped TiO<sub>2</sub> nanomaterials prepared by a green synthetic approach. *J Phys Chem C* 2011;115:13285-92. [DOI](#)
257. Higashimoto S, Tanihata W, Nakagawa Y, Azuma M, Ohue H, Sakata Y. Effective photocatalytic decomposition of VOC under visible-light irradiation on N-doped TiO<sub>2</sub> modified by vanadium species. *APPL CATAL A-GEN* 2008;340:98-104. [DOI](#)
258. Mogal SI, Gandhi VG, Mishra M, et al. Single-step synthesis of silver-doped titanium dioxide: influence of silver on structural, textural, and photocatalytic properties. *Ind Eng Chem Res* 2014;53:5749-58. [DOI](#)
259. Nie L, Duan B, Lu A, Zhang L. Pd/TiO<sub>2</sub> @ carbon microspheres derived from chitin for highly efficient photocatalytic degradation of volatile organic compounds. *ACS Sustainable Chem Eng* 2019;7:1658-66. [DOI](#)
260. Guan K. Relationship between photocatalytic activity, hydrophilicity and self-cleaning effect of TiO<sub>2</sub>/SiO<sub>2</sub> films. *Surf Coat Technol* 2005;191:155-60. [DOI](#)
261. Zou L, Luo Y, Hooper M, Hu E. Removal of VOCs by photocatalysis process using adsorption enhanced TiO<sub>2</sub>-SiO<sub>2</sub> catalyst. *Chem Eng Process* 2006;45:959-64. [DOI](#)
262. Yu J, Yu JC, Zhao X. The effect of SiO<sub>2</sub> addition on the grain size and photocatalytic activity of TiO<sub>2</sub> thin films. *J Sol-Gel Sci Technol* 2002;24:95-103. [DOI](#)
263. Sumitsawan S, Cho J, Sattler ML, Timmons RB. Plasma surface modified TiO<sub>2</sub> nanoparticles: improved photocatalytic oxidation of gaseous m-xylene. *Environ Sci Technol* 2011;45:6970-7. [DOI PubMed](#)
264. Arai T, Horiguchi M, Yanagida M, Gunji T, Sugihara H, Sayama K. Complete oxidation of acetaldehyde and toluene over a Pd/WO<sub>3</sub> photocatalyst under fluorescent- or visible-light irradiation. *Chem Commun (Camb)* 2008;43:5565-7. [DOI PubMed](#)
265. Hou Y, Wang X, Wu L, Ding Z, Fu X. Efficient decomposition of benzene over a beta-Ga<sub>2</sub>O<sub>3</sub> photocatalyst under ambient conditions. *Environ Sci Technol* 2006;40:5799-803. [DOI PubMed](#)
266. Chen LC, Pan GT, Yang TC, Chung TW, Huang CM. In situ DRIFT and kinetic studies of photocatalytic degradation on benzene vapor with visible-light-driven silver vanadates. *J Hazard Mater* 2010;178:644-51. [DOI PubMed](#)
267. Kim J, Choi W. Response to comment on “Platinized WO<sub>3</sub> as an environmental photocatalyst that generates OH radicals under visible light”. *Environ Sci Technol* 2011;45:3183-4. [DOI](#)
268. Yan T, Long J, Shi X, Wang D, Li Z, Wang X. Efficient photocatalytic degradation of volatile organic compounds by porous indium hydroxide nanocrystals. *Environ Sci Technol* 2010;44:1380-5. [DOI PubMed](#)
269. Zhang W, Yang Z, Wang H, et al. Crystal facet-dependent frustrated Lewis pairs on dual-metal hydroxide for photocatalytic CO<sub>2</sub> reduction. *Appl Catal B Environ* 2022;300:120748. [DOI](#)
270. Lu KQ, Li YH, Zhang F, et al. Rationally designed transition metal hydroxide nanosheet arrays on graphene for artificial CO<sub>2</sub> reduction. *Nat Commun* 2020;11:5181. [DOI PubMed PMC](#)
271. Fresno F, Hernández-alonso MD, Tudela D, Coronado JM, Soria J. Photocatalytic degradation of toluene over doped and coupled (Ti,M)O<sub>2</sub> (M=Sn or Zr) nanocrystalline oxides: Influence of the heteroatom distribution on deactivation. *Appl Catal B* 2008;84:598-606. [DOI](#)
272. Han Z, Chang V, Wang X, Lim T, Hildemann L. Experimental study on visible-light induced photocatalytic oxidation of gaseous formaldehyde by polyester fiber supported photocatalysts. *Chem Eng J* 2013;218:9-18. [DOI](#)
273. Yang L, Liu Z, Shi J, Zhang Y, Hu H, Shangguan W. Degradation of indoor gaseous formaldehyde by hybrid VUV and TiO<sub>2</sub>/UV processes. *Sep Purif Technol* 2007;54:204-11. [DOI](#)
274. Ameen M, Raupp GB. Reversible catalyst deactivation in the photocatalytic oxidation of dilute-xylene in air. *J Catal* 1999;184:112-22. [DOI](#)
275. Mamaghani AH, Haghighat F, Lee C. Photocatalytic oxidation of MEK over hierarchical TiO<sub>2</sub> catalysts: effect of photocatalyst features and operating conditions. *Appl Catal B* 2019;251:1-16. [DOI](#)
276. Shayegan Z, Haghighat F, Lee C. Photocatalytic oxidation of volatile organic compounds for indoor environment applications: three different scaled setups. *Chem Eng J* 2019;357:533-46. [DOI](#)
277. Héquet V, Raillard C, Debono O, Thévenet F, Locoge N, Le Coq L. Photocatalytic oxidation of VOCs at ppb level using a closed-loop reactor: the mixture effect. *Appl Catal B* 2018;226:473-86. [DOI](#)

**Rebecca El Khawaja**

Rebecca El Khawaja obtained her M.Sc. in physical chemistry of materials from the Lebanese University in 2017. She worked with the Rennes School of Chemistry on her final project to study the hydrogenation of aromatic compounds in the presence of ordered mesoporous catalysts using various alumina precursors and organic surfactants. During her PhD at the University of the Littoral Opal Coast, Rebecca worked on the development of hybrid systems based on adsorption/catalysis coupling for the catalytic oxidation of oxygenated and cyclic VOCs from industrial sources. Her interests include hybrid material, catalysis, depollution and recently waste valorization as she joined EPIC research team at Polytechnique Montreal as a postdoctoral fellow.

**Savita Kaliya Perumal  
Veerapandian**

Savita Kaliya Perumal Veerapandian received her PhD degree in Engineering Physics from Ghent University, Belgium in 2021. She was working on the Sequential adsorption plasma catalysis for the abatement of toluene under the supervision of Prof. Rino Morent. Her research work was carried out within the framework of INTERREG project DepollutAir. The main aspects of her research include reducing process cost by sequential treatment, reducing material cost by plasma assisted regeneration of the catalysts and improving the product selectivity and yield. During her research career, she published 14 articles in peer-reviewed journals and she actively participated in 12 International conferences and workshops.

**Rino Morent**

Rino Morent obtained in 2004 his PhD in Engineering: Applied Physics at Ghent University. In 2012 he was appointed as professor in plasma technology at Ghent University, thanks to obtaining the ERC Starting Grant PLASMAPOR. At the moment he is Full Professor and leading the experimental Research Unit Plasma Technology (RUPT). RUPT focuses on the development of different atmospheric pressure plasma sources (including pulsed discharges, plasma jets & dielectric barrier discharges) and their applications in gas conversion, materials science, air cleaning, energy solutions, biomedical applications and plasma medicine.



**Guy De Weireld**

Guy De Weireld is full professor in chemical thermodynamics, environment, industrial processes, and sustainable development at the Faculty of Engineering, University of Mons (Belgium). His main research field is adsorption in porous materials and catalysis. He has experience in CO<sub>2</sub> capture, gas separation, gas purification (removing of acid compounds from natural gas, VOC from exhaust air) and CO<sub>2</sub> conversion to fuel as well as techno-economic and environmental assessments in carbon capture, utilization, and storage. Since 2019, he is the coordinator of the H2020-MOF4AIR project: Metal Organic Frameworks for carbon dioxide Adsorption processes in power production and energy Intensive industries.

**Yang Ding**

Yang Ding received his M.Sc. degree from College of Chemistry and Materials Science at Shanghai Normal University in 2018. He is currently a PhD student in the Laboratory of Inorganic Materials Chemistry (CMI) of University of Namur under the supervision of Prof. Bao-Lian Su. His research interests include porous materials synthesis and characterization, photocatalytic pollutants elimination and sustainable energy production.

**Renaud Cousin**

Renaud Cousin received his PhD degree in Spectroscopy and Chemistry from Littoral Côte d'Opale University in Dunkirk, France, in 2000 on the topic "Soot Oxidation". After a postdoctoral position at the University of Strasbourg sponsored by Daimler, he worked as Assistant Professor at the Littoral Côte d'Opale University, France, from 2003 to 2016. In 2014 he obtained the accreditation to Supervise Research (Habilitation Thesis). Since 2016 he was promoted to Full Professor. Currently his research focuses on the development and characterization of heterogeneous catalysts for application to the elimination of environmental pollutants (Soot, CO, VOCs, ...). He has co-authored over 80 peer reviewed scientific papers and 1 patent.

**Fabrice Cazier**

Fabrice Cazier obtained his PhD in Chemical Sciences at Lille University (France) in 1990 with works dealing with “Development of analytical methods for organic and nitrated pollutants in the atmosphere”. He worked then as a searcher for the Air Quality monitoring network on VOC and nitrogen oxides monitoring. In 1993, he managed the creation of an analytical laboratory dedicated to risk evaluation and environmental analysis. He became the Director of this unit in 1995. Since then, as Director of the Common Centre of Measurements (CCM) of the Université du Littoral Côte d’Opale (ULCO), he has developed a large expertise in chemical analysis applied to the environment and manages a highly equipped laboratory available as well for research teams as for industrial partners. He is notably specialized in gaseous compounds and particulate matter measurements.

**Sylvain Billet**

Sylvain Billet has been an associate professor in industrial and environmental toxicology at the Environmental Chemistry and Interactions with the Living Organisms at the University of the Opal Coast (UCEIV, ULCO), France since 2009. He is general secretary of the French Cellular and Molecular Toxicology Society (STCM). His PhD in toxicology focused on the biotransformation and genotoxicity of organic pollutants adsorbed on the surface of fine atmospheric particles. He has since set up a method of exposure of complex cultures of human respiratory cells in order to characterize the toxicity of gaseous air pollutants alone or in mixtures.

**Jean-François Lamonier**

Jean-François Lamonier is a full Professor in Department of Chemistry and Deputy Director of the Chevreul Institute, Lille University (France). Jean-François Lamonier leads the team “Catalytic Remediation” of the « Unité de Catalyse et Chimie du Solide » laboratory. His research addresses the catalytic oxidation technologies for Volatile Organic Compounds emissions removal and the catalytic pyrolysis of plastic waste. His research comprises (i) the development of transition metal oxide nanomaterials with emphasis in the elucidation of the structure-chemical properties and catalytic activity relationship and (ii) the coupling of abatement technologies such as non-thermal plasma and heterogeneous catalysis. For this last-mentioned topic Jean-François Lamonier heads the International Associated Laboratory “Plasma & Catalysis” between Lille University and Ghent University (Belgium).



**Bao-Lian Su**

Bao-Lian Su created the Laboratory of Inorganic Materials Chemistry (CMI) at the University of Namur, Belgium in 1995. He is Full Professor, Member of the European Academy of Sciences, Member of the Royal Academy of Belgium, Fellow of the Royal Society of Chemistry, UK and Life Member of Clare Hall College, University of Cambridge. He is also a strategy scientist at Wuhan University of Technology, China. His research fields include the synthesis, the property study and the molecular engineering of organized, hierarchically porous and bio-organisms for artificial photosynthesis, (photo) Catalysis, Energy Conversion and Storage, Biotechnology, Cell therapy and Biomedical applications.

**Stéphane Siffert**

Stéphane Siffert is a full Professor in Department of Chemistry and Director of Unit of Environmental Chemistry and Interactions with leaving organisms (UCEIV, UR 4492, FR CNRS 3417), Dunkerque (France). He was coordinator of three European Interreg projects till 2022 on Volatile Organic Compounds (VOC) removal. His main research is on catalytic treatment of pollutants, especially the oxidation of VOC, and also purification and valorisation of CO<sub>2</sub>. He works on oxides synthesized by "classic" and "hydrotalcite" way, zeolites and highly structured meso and macroporous compounds and noble metals catalysts.